

In presenting the dissertation as a partial fulfillment of the requirements for an advanced degree from the Georgia Institute of Technology, I agree that the Library of the Institute shall make it available for inspection and circulation in accordance with its regulations governing materials of this type. I agree that permission to copy from, or to publish from, this dissertation may be granted by the professor under whose direction it was written, or, in his absence, by the Dean of the Graduate Division when such copying or publication is solely for scholarly purposes and does not involve potential financial gain. It is understood that any copying from, or publication of, this dissertation which involves potential financial gain will not be allowed without written permission.

A handwritten signature in dark ink, consisting of a series of loops and a long horizontal stroke, positioned above a horizontal line.

7/25/68

AN EXPERIMENTAL STUDY OF CERTAIN NEUTRAL
COSMIC RAY INTERACTIONS

A THESIS

Presented to

The Faculty of the Division of Graduate
Studies and Research

By

Charles Thomas Brown

In Partial Fulfillment

of the Requirements for the Degree

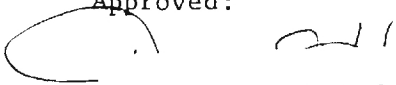
Doctor of Philosophy in the School of Physics

Georgia Institute of Technology

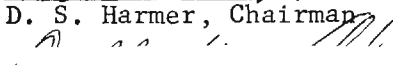
November, 1972

AN EXPERIMENTAL STUDY OF CERTAIN NEUTRAL
COSMIC RAY INTERACTIONS

Approved:



D. S. Harmer, Chairman



R. M. Ahrens

J. M. Wampler

Date approved by Chairman: 10 Nov. 1972

ACKNOWLEDGMENTS

The interests and efforts of many people have made this work possible and even enjoyable. It is with pleasure that I attempt to acknowledge the many contributions made by this rather large group of people.

I am deeply indebted to T. P. Lang, Jr. for his numerous contributions to this thesis. He not only suggested these studies, but through his position as Director of Research for Advanced Research Corporation was able to supply the necessary materials, manpower, and equipment for this experiment. His constant interest, helpful discussions, and expert professional guidance have been overshadowed only by his personal friendship.

I would also like to express my appreciation to my thesis advisor, Dr. Don S. Harmer, for his guidance and excellent advice. I would further like to express my gratitude to Dr. R. M. Ahrens and Dr. J. M. Wampler for their contributions as members of the reading committee.

This project could not have been undertaken without the support of Advanced Research Corporation, Atlanta. The use of their facilities was greatly appreciated. Additionally, the efforts of Bill Jeter, Steve Johnson, Jack Cook, Ray Champion, and Gay Jolly during the construction phase of this experiment were greatly valued. A special thanks is due Jack Cook who designed and constructed much of the special electronics necessary for this study.

I would also like to express my gratitude to Dr. C. L. Cowan of

Catholic University of America and to Dr. Robert N. Shelby of the United States Naval Academy for their discussions and encouragement. I am also indebted to Dr. Cowan and Dr. Shelby for the loan of the large sheets of plastic scintillator that were used as part of the anticoincidence system of the detector. The neutron cross sections supplied by Dr. Hugo W. Bertini were invaluable in interpreting the results of this experiment.

A special thanks is due Mrs. Lydia S. Geeslin for her attention and care in typing the thesis.

Last, but not least, I wish to acknowledge the patience and understanding of my wife, Donna, and our two daughters, Yvonne and Michele. They have received the neglect so common to the family of a graduate student. For their interest and encouragement in this project, they have received only lonely evenings and weekends. It is with a great sense of gratitude and love that I thank them for their contribution.

In order that this dissertation could be published separately as a report of sponsored research, special permission was received from the Graduate Division to depart from its regulations governing figure captions.

TABLE OF CONTENTS

	Page
ACKNOWLEDGMENTS.	ii
LIST OF TABLES	vi
LIST OF ILLUSTRATIONS	vii
SUMMARY	x
Chapter	
I. INTRODUCTION	1
Our Radiation Environment	1
Historical Background	5
Georgia Tech Program	11
II. THE FACILITY	13
The Detector	13
Module Construction	
Development of Scintillator	25
Solvent	
Solutes and Secondary Solvent	
Scintillator Preparation	
Effects of Dissolved Oxygen	
Scintillator Pulse Shape	
Electronics	30
Testing and Calibration of Equipment	35
Response as a Function of Position in Cell A	
Calibration of Target Cells	
Determination of the Muon Decay Electron Energy	
Distribution	40
Calibration of TAC-Multichannel Analyzer System	
Effectiveness of Anticoincidence System	50
Determination of Muon Lifetime	54
III. COLLECTION OF DATA	56

TABLE OF CONTENTS (Concluded)

Chapter	Page
IV. ANALYSIS OF DATA.	61
Analysis of Lifetime.	61
Observed Experimental Rate Due to Incident Neutral Particles	66
Determination of Expected Muon Decay Rate From Incident Neutrons	69
The Neutron Energy Spectrum	
Pion Production Cross Sections	
Pion Production in Target	
Detection Efficiency for Pion Pulse	
Determination of the μ -e Decay Electron Detection Efficiency	
Observed Rate Expected from Neutron Production of Pions	
V. CONCLUSIONS AND RECOMMENDATIONS	87
Conclusions	87
The Facility	
The Neutral Particle Experiment	
Recommendations	90
APPENDICES	
A. ELECTRONICS	94
300 MHz Low Gain Mixer.	94
150 MHz, X20 Mixer.	96
15 Microsecond Updating Oneshot (AR-10)	98
Electronic Instrument Inventory	98
B. PION PRODUCTION CROSS SECTIONS FOR PROTONS AND NEUTRONS ONTO CARBON.	103
Cross Section Bibliography.	106
LITERATURE CITED	108
VITA	112

LIST OF TABLES

Table	Page
1. Cell Dimensions and Volumes of Cosmic Ray Detector . . .	22
2. Composition of Liquid Scintillator	28
3. Summary of Data Collected August 19 to November 27, 1971	59
4. Composition of Raw Data	68
5. Summary of Data Used to Determine Pion Production in Target Volume	80
6. Pion Detection Efficiency as a Function of Target and Anticoincidence Threshold Energy	82
7. μ -e Decay Electron Detection Efficiency as a Function of Anticoincidence Threshold	85
8. Individual and Product Detection Efficiencies for the μ -e Decay Electron	85
9. Data for Determination of Observed Rate Due to Neutrons	86
10. Inventory of Electronic Nuclear Instruments	100
11. Summary of Available Experimental Cross Section Data for $\begin{Bmatrix} n \\ p \end{Bmatrix} + C \rightarrow \pi^{\pm}$. . . Reactions from Threshold to 1.1 GeV.	104

LIST OF ILLUSTRATIONS

Figure	Page
1. Production of the Secondary Components of the Cosmic Radiation. After Sandstrom ⁴	3
2. The Direct Production of a Muon by a Neutral Component of the Cosmic Rays	8
3. A π - μ -e Event Initiated by a Cosmic Ray Neutron	8
4. Target Region of Cosmic Ray Detector	15
5. Cosmic Ray Detector's Anticoincidence System	16
6.- 13. Cosmic Ray Detector During Various Stages of Construction	18-21
14. Technique for Bonding Acrylic Plastics	24
15. Relative Light Output of Mineral Oil Based Scintillator as a Function of PPO Concentration	27
16. Telescope Arrangement for Calibration of Target Cells . .	36
17. Detector Response as a Function of Position in Cell A . .	37
18. Muon Thru-Peak and Energy Calibration of Cells A and C	39
19. Location of 10.5 MeV Threshold with Respect to Target Background Energy Distribution	41
20. Discriminator Count Rate Versus Threshold Energy for Target Cell A	42
21. Electron Energy Distribution from μ -e Decay	43

LIST OF ILLUSTRATIONS (Continued)

Figure	Page
22. Electronics Configuration for Determining Decay	
Electron Energy Distribution	45
23. μ -e Decay Electron Energy Distribution with and Without	
Anticoincidence on Second Pulse. Muon Thru-Peak	
Shown for Reference. All Scales Linear	46
24. Comparison of Experimental μ -e Decay Electron Energy	
Distribution with Computer Generated Distribution . . .	48
25. Calibration of the Time to Amplitude Converter	49
26. Muon Telescope	52
27. Summary of Anticoincidence System Charged Particle	
Rejection Ratios	52
28. Muon Life Time Curve Before and After Correction for	
Background	55
29. System Logic for Collection of Neutral Particle Induced	
Data	57
30. Raw Lifetime Data from Neutral Particle Induced Events .	63
31. Muon Lifetime from Neutral Particle Induced Data	65
32. The Differential Neutron Energy Spectrum at Sea Level	
as Given by Hess and Modified by Hughes and Marsden.	
After Hughes and Marsden ²⁸	71
33. Differential Cross Sections for $n + C^{12} \rightarrow \pi^{\pm} + \dots$	74
34. Pion Energy Distribution in Center-of-Mass System of	
Colliding Nucleons. Protons onto Carbon Target	76
35. Pion Angular Distributions in Center-of-Mass System of	
Colliding Nucleons. Neutrons onto Carbon Target . . .	76

LIST OF ILLUSTRATIONS (Concluded)

Figure	Page
36. Flux-Cross Section Product for $n + C \rightarrow \pi^{\pm} + \dots$ with Cosmic Ray Neutron	78
37. 300 MHz Mixer Schematic and Test Point Board	95
38. Schematic of X20 Anticoincidence Mixer	97
39. Schematic of 15 Microsecond Updating Oneshot	99

SUMMARY

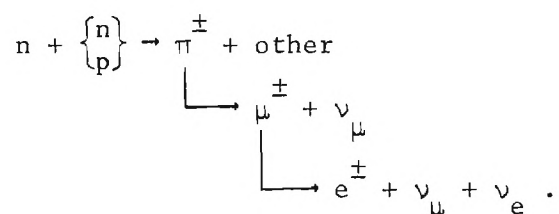
During the past ten years, experiments performed by others have yielded results that indicate an anomalously large rate of production of muons in large volume detectors by neutral components of the cosmic radiation. Equally important is the fact that the event rate associated with this phenomenon is sidereal-time dependent, yielding several significant source regions on the celestial sphere. It is worth noting that the right ascension coordinate of the inner arm of our galaxy coincides with one of these source regions. These results raise the very interesting possibility that the detection of events having a particular signature might yield additional information about the structure and composition of our galaxy.

A further study of this phenomenon was undertaken at Georgia Institute of Technology with particular emphasis placed on an independent confirmation of the existence of an anomaly in the rate of production of muons by neutral components of the cosmic radiation. To satisfy this objective a versatile cosmic ray facility was designed and constructed to allow not only the confirmation of the phenomenon, but also to serve as a base for a broad range of other experiments in this area. This facility consists of a large volume, modular, liquid scintillation detection system, appropriate electronics for the collection and preliminary reduction of desired data, and liquid scintillation development and preparation apparatus.

Prior to the collection of neutral-particle-induced muon data, much effort was expended in the checkout and calibration of the detection system. A determination of the mean muon lifetime in mineral oil served as a final check on the system. A value of $\tau = 2.13 \pm 0.05$ microseconds was obtained.

Neutral-particle-induced muon data were collected for 1,802.63 hours between August 19, 1971 and November 27, 1971. The signature for an interesting event consisted of the production of an energetic charged particle by an incident neutral cosmic ray, followed by the characteristic decay of the muon. After correction for the chance rate and for leaking muons, an average rate of 0.82 ± 0.15 events/hour was obtained.

The production of pions within the detector by cosmic ray neutrons was assumed to be a likely candidate to explain the observed neutral-particle-induced event rate. The proposed event would be the following:



Due to the short lifetime of the pion (~ 25 nanoseconds) and the low energy of the emitted muon (~ 4 MeV), this event is in general indistinguishable from direct muon production processes. Such was the case in this experiment and in all previous neutral-particle-induced muon experiments conducted by others.

Using available cosmic-ray neutron flux data and pertinent pion

production cross section data, an absolute event rate for the neutron initiated π - μ -e event was established for the detector. The efficiency for the detection of the π - μ -e decay event was determined with the aid of a computer model of the detector. A FORTRAN program modeling pertinent aspects of the incident neutron flux, the pion production cross sections, the pion energy and angular distributions, the muon energy distributions, and the detector's geometry was written for the Georgia Tech Univac 1108 computer. Using Monte Carlo techniques it was possible to integrate the incident neutron flux over the detector volume, and thus simulate the π - μ -e process. The resulting expected event rate due to incident neutrons was determined to be 1.31 ± 0.59 events/hour.

The available evidence indicated that the near sea level cosmic ray neutron intensity is sufficient to account for the observed neutral-particle-induced muon event rate in the detector. It is pointed out, however, that the data are not inconsistent with the hypothesis that up to 25 percent of the events may be due to processes other than pion production by incident neutrons. In conclusion, no obvious anomaly in the rate of production of muons by neutral components of the cosmic radiation was observed.

CHAPTER I

INTRODUCTION

The purposes of this research program were twofold: (1) to design and construct a cosmic ray facility to allow continuing studies of the production of muons by neutral components of the cosmic radiation; and (2) to determine if an anomaly exists in the rate of production of single muons by neutral cosmic rays near sea level. As such this research is but a small part of the continuing effort of the scientific community to better understand our natural radiation environment.

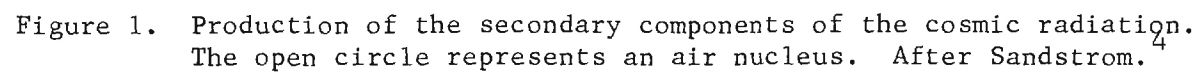
Our Radiation Environment

The cosmic rays were discovered at the turn of the century as a result of measurements on the conductivity of gases. At that time dry air ionization chambers were being used to study various natural and man-made radiations. The dry air was assumed to be a near perfect insulator, and the presence of a persistent "dark current" in the chambers was of great concern. Initial efforts to shield the chambers from the earth's natural radioactivity reduced the background somewhat, but even great quantities of shielding failed to eliminate the effect. Likewise, meticulous cleaning and decontamination of the chambers produced disappointing results. In an attempt to escape the effects of the earth's natural radioactivity, experiments measuring the residual background were conducted with the aid of balloons at various altitudes above the earth's surface. These experiments indicated that the background

initially decreased with altitude but by the time the instruments reached 5000 meters the "dark current" was several times its sea level value. The results of such studies, notably by Hess¹ and later by Kolhörster,² provided clear evidence for the existence of an extra-terrestrial source of radiation.

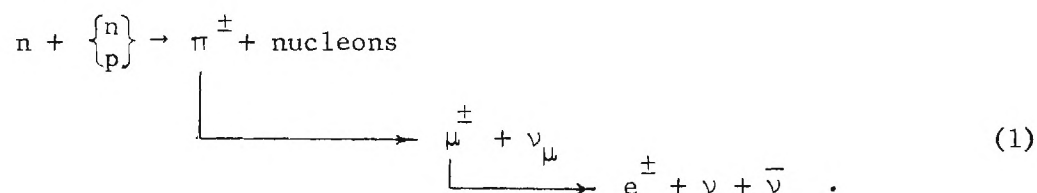
The primary cosmic radiation consists of energetic protons, helium nuclei, heavier nuclei, electrons, electromagnetic radiations such as gamma rays and X-rays, and probably neutrinos. The electromagnetic radiation and the electrons are completely absorbed by the earth's upper atmosphere and will not be discussed further. The primary neutrino flux, if it exists, is probably several orders of magnitude smaller than the secondary neutrino flux created within the earth's atmosphere, and for the purposes of this dissertation the two will be treated together. Of the primary nuclear component approximately 90 percent of the flux consists of protons, 10 percent helium nuclei, and 1 or 2 percent nuclei with $Z \geq 3$. To this component of the primary radiation the earth's atmosphere acts as a thick absorber of approximately 10 mean free paths and thus a negligible fraction of the primary flux reaches the earth's surface. Many of these particles are however quite energetic (up to at least 10^{20} eV³), and their interactions with nuclei in the upper atmosphere produce secondary particles and radiations which are ultimately detected at ground level.

The secondary cosmic radiation consists of nucleons, electrons, photons, pions, muons, and to a lesser extent most if not all of the other "elementary" particles. Figure 1 illustrates in a schematic way the generation of these secondaries.



Near sea level the bulk of the cosmic radiation is generally divided into a "hard" component which has great penetrating power and a "soft" component which is relatively easily absorbed. The hard component is known to consist mainly of energetic muons while the soft component consists of electrons, photons, and low energy muons. The remaining components of the sea level radiation have rates that are quite small (\lesssim five percent of the muon flux) when compared to those mentioned above. Yet, it is these particles and their interactions that are often the subject of investigation and many techniques have been devised to study such particles under these less than ideal conditions.

One class of event occurring near sea level is the production of single muons by neutral components of the cosmic radiation. This process can be accomplished in two ways: directly, in which one of the products of the interaction is a muon, and indirectly, in which the muon is a decay product of a short lived particle produced in the interaction. The majority of indirectly produced muons by neutral components of the cosmic radiation involves the neutron as the incident neutral particle. High energy neutrons colliding with other nucleons produce, via strong interaction, short lived pions which decay rapidly into muons. This process is summarized as follows:



The only known processes for the direct production of a single

muon by an incident neutral particle are the neutrino reactions:

$$\bar{\nu}_{\mu} + p \rightarrow n + \mu^{+} \quad (2)$$

and

$$\nu_{\mu} + n \rightarrow p + \mu^{-}. \quad (3)$$

Cross sections for these reactions are believed to be extremely small—of the order of 10^{-39} cm^2 .

An anomaly in the rate of production of single muons by neutral components of the cosmic radiation would imply one of the following:

(1) The cosmic ray neutron flux near sea level is larger than has been reported;

(2) The pion production cross sections for neutrons on nuclei are larger than presently believed;

(3) The muon neutrino flux near sea level is much larger than presently believed;

(4) The muon neutrino cross sections are much larger than expected, possibly the result of a resonance phenomenon; or

(5) A heretofore unknown particle is producing muons via its interaction with matter.

Historical Background

In the fall of 1960 Cowan and Ryan⁶ placed in operation a detector designed to look for the direct production of muons by incident neutral cosmic rays. It was intended to build a rather small modular detector, understand all events occurring within it, and then enlarge the detector. This process was to be repeated until they ultimately achieved a detector

capable of observing the neutrino reactions:

$$\bar{\nu}_{\mu} + p \rightarrow n + \mu^{+} \quad (4)$$

and

$$\nu_{\mu} + n \rightarrow p + \mu^{-}. \quad (5)$$

The signature for such an event would consist of the production of an energetic charged particle by an incident neutral cosmic ray, followed by the characteristic decay of the muon. A typical event is shown in Figure 2.

The detector was operated at ground level and at 200 meters water equivalent underground for a total of four years. During this period events were observed having the above described signature but at a rate then believed to be an order of magnitude above that which could be explained based on a current knowledge of the cosmic rays.⁷ Furthermore, the event rate was shown to occur in diurnal cycles fixed in sidereal time, suggesting the neutral flux to be of a cosmic origin external to the solar system.

The primary source of background events in this experiment was that due to incident neutrons initiating the π - μ -e decay chain within the detector. That is,

$$\begin{array}{lcl}
 n + \left\{ \begin{smallmatrix} n \\ p \end{smallmatrix} \right\} \rightarrow \pi^{\pm} + \text{nucleons} & & (6) \\
 \downarrow \begin{array}{l} \tau = 25 \text{ nsec} \\ E_{\mu} = 4 \text{ MeV} \end{array} & \rightarrow & \mu^{\pm} + \nu_{\mu} \\
 \downarrow \begin{array}{l} \tau = 2.2 \mu \text{ sec} \\ E_e = 0 \rightarrow 53 \text{ MeV} \end{array} & \rightarrow & e^{\pm} + \nu + \bar{\nu}.
 \end{array}$$

Such an event is shown in Figure 3. Note that, if the pion decay portion of this event is not detected, the signature of the event is identical to that for the direct production of a muon by an incident neutral particle. The fact that the pion decay portion of the event is of low energy and that it occurs on the tail of a much more energetic process made it impossible for Cowan-Ryan to distinguish neutron induced events from direct production events.

An estimate of the incident neutron flux was made by Cowan and Ryan by assuming that the neutral particle initiated singles rate in their detector was due solely to neutrons. This flux was then used to determine a pion production rate in the detector.

There were several possible explanations for the anomalously large neutral particle induced rate observed in this detector:

1. There was the remote possibility of a low energy resonance in one of the two neutrino cross sections mentioned above.
2. There was the possibility that the incident particles were muons which leaked through the anticoincidence system, stopped, and decayed.
3. There was the possibility that an error existed in the flux-cross section product used to calculate the event rate due to incident neutrons.
4. There was the possibility that a new elementary particle had been seen.
5. Finally, there was the possibility that the process was some combination of all four of the above.

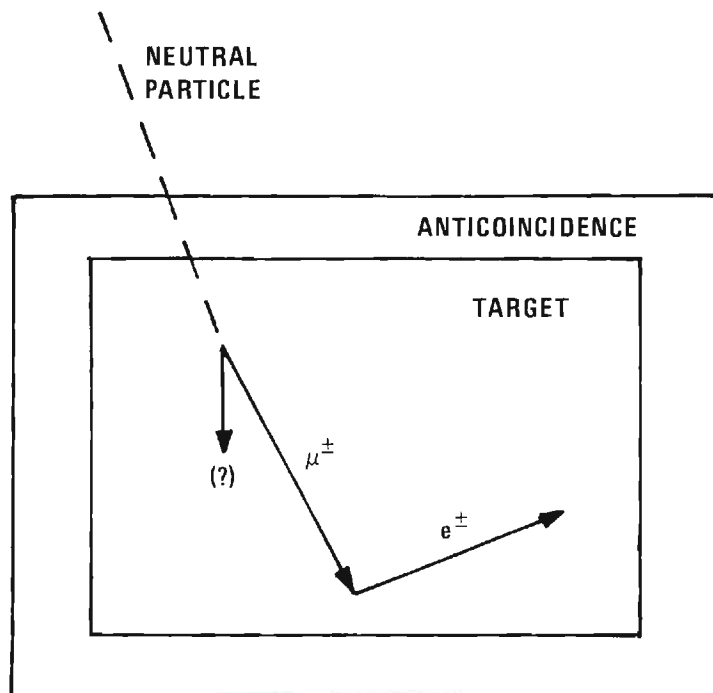


Figure 2. The direct production of a muon by a neutral component of the cosmic rays.

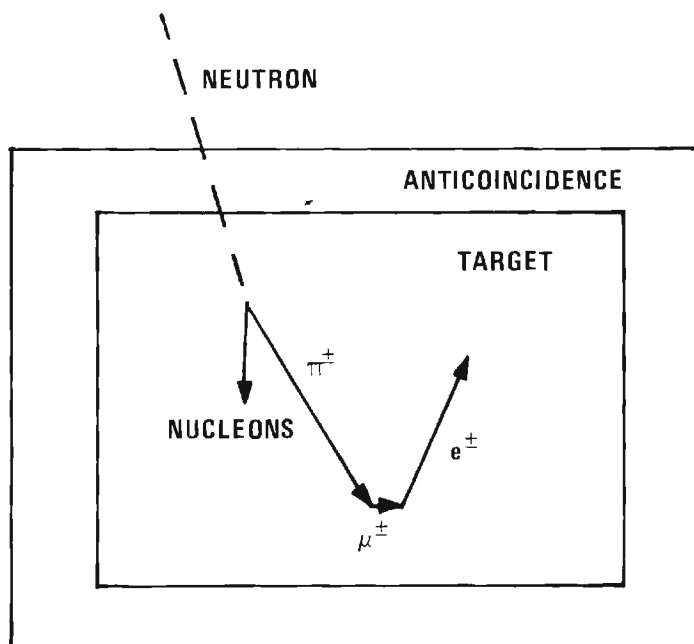


Figure 3. A π - μ - e event initiated by a cosmic ray neutron.

The sidereal time dependence of the event rate raised the very interesting possibility that a study of cosmic rays with a particular signature might yield information on the celestial positions of cosmic ray sources. The observed event rate also raised the possibility of a resonance perhaps associated with the postulated intermediate boson.

The first Cowan-Ryan detector had an anticoincidence rejection ratio of approximately 200:1. Their second detector⁷⁻⁹ consisted of a 2' x 4' x 1' slab of plastic scintillator surrounded on all sides by an anticoincidence system constructed of 3/4-inch plastic scintillator. This system had an anticoincidence rejection ratio estimated to be 1200:1. It was operated at ground level during 1965-66 and collected approximately $13\frac{1}{2}$ events per hour. At most, only 11 events/hour could be accounted for without assuming an anomaly.⁷

This detector was believed to have good time resolution and was used to search for the presence of a pion as an intermediate particle in the process by determining the muon decay curve at times near zero (less than 50 nanoseconds). The decay curve of a directly produced muon would be a simple exponential with a 2.2 microsecond lifetime. The decay curve of a pion produced muon would exhibit the characteristic mother-daughter relationship of a multiple decay process and would, at short times, deviate from the simple exponential and would intersect the origin at time zero. The results of the lifetime studies indicated that the muons were being produced directly, but the statistics were rather poor. The sidereal time dependence of the event rate was still present; one two-hour-time bin standing 4.8 standard deviations above the average rate.

The possibility of muon pair production by incident photons was also investigated with this detector. It was determined that "events representative of the production of two muons by neutrals are extremely rare in [their] data."⁸

Novey, 1965¹⁰ proposed that the phenomenon was due to cosmic ray neutrons from muon stars which are in equilibrium with the muon flux. These neutrons would create the μ -e decay chain via the indirect pion production process discussed earlier. To test this hypothesis Novey constructed a 2½-foot cube of liquid scintillator and surrounded it by plastic scintillator for an anticoincidence system. Eight feet of concrete was placed around the detector to yield a muon-neutron equilibrium environment. He observed a normalized event rate of approximately 1/4 that of the Cowan-Ryan work and consistent with the hypothesis of neutron production in the eight feet of concrete surrounding the detector.

Novey's work showed that at least one mechanism exists for the production of muons by energetic neutral cosmic rays. This is the normal indirect π - μ -e decay process discussed earlier. His work did not, however, rule out the possibility of the existence of other production mechanisms, both direct and indirect. Additionally, the presence of eight feet of concrete around the experiment makes it difficult to compare the results of Novey with those of Cowan-Ryan.

In 1965-66 Buckwalter, et al.,¹¹ using 650 Kgm of decalin-base liquid scintillator surrounded on all sides by 3/4-inch plastic scintillator, observed 16,495 events having the neutral-particle-produced muon signature. These data indicated a peak of 4.2 standard deviations above

mean background between 21 and 23 hours right ascension, consistent with the Cowan-Ryan data.

In 1967 Hesse, et al.¹² constructed a 4' x 4' x 4' internally triggered spark chamber complete with anticoincidence system to study the astrophysical implications of the neutral-particle-induced event. The results of a three-year program of mapping the neutral particle origins on the celestial sphere yielded a map containing several statistically significant regions, the most prominent being at approximately 21 hours right ascension by 25° N. declination.

In 1965 Standil and Bukata,¹³ using a pair of highly directional detectors, reported results which they interpreted as indicating a 15 percent anisotropy in the primary radiation above 40 BeV, with a preferred incident direction corresponding to a right ascension of 20.5 ± 1.0 hours. Malboux, et al.¹⁴ also reported a similar effect in a muon spectrometer experiment performed underground at 1300 meters water equivalent. In 1969 Buckwalter, et al.¹⁵ reported a strong sidereal time dependence in cosmic ray muons which stop and decay in a directional detector at sea level. Their data show a peak four standard deviations above background at about 21 hours right ascension.

O'Sullivan, 1969,¹⁶ and Shelby, 1970,¹⁷ improved the anticoincidence system of the Hesse spark chamber by adding four inches of liquid scintillator above the chamber and requiring that the first track project back through the liquid. Based on an analysis of 65 "events" in 1775 hours of operation in one case and 71 "events" in 2412.9 hours of operation in the other, they concluded that all of the spark chamber events could be neutron produced but that the data were also consistent with up

to 50 percent production by other processes. A major difficulty in the analysis of this experiment was the complicated overburden offered the detector by being in the basement of a two-storied concrete and brick building.

Georgia Tech Program

A further study of the production of single muons by neutral components of the cosmic radiation was undertaken at Georgia Institute of Technology with particular emphasis placed on an independent confirmation of the existence of the phenomenon. To satisfy this objective a versatile cosmic ray facility was designed and constructed to allow not only the confirmation of this phenomenon, but also to serve as a base for a broad range of other experiments in this area.

The facility consisted of a large volume, modular, liquid scintillation detection system, appropriate electronics for the collection, and preliminary reduction of desired data, and liquid scintillator development and preparation apparatus. Design criteria for the detector emphasized a reliable anticoincidence system and an uncomplicated overburden, two sources of problems in previous experiments. Prior to the collection of data on neutral-particle-induced events much emphasis was placed on an understanding of the characteristics of the detector.

The following chapter describes in some detail the design, construction, and checkout of the facility. Topics covered include a description of the detector and its electronics, the development of the liquid scintillator, and the results of numerous tests and calibrations. The collection and analysis of neutral-particle-induced muon data are described in Chapters III and IV, respectively. Conclusions and recommendations for future work are presented in Chapter V.

CHAPTER II

THE FACILITY

A versatile cosmic ray facility has been designed and constructed to allow continuing studies in the field of muon production by neutral components of the cosmic radiation. The elements of this facility are discussed in some detail with the hope that such a discussion might be of value to others interested in working in this field. Also included is a summary of the testing, calibration, and preliminary experimental studies undertaken before the start of collection of neutral-particle-induced data.

The Detector

Due to the nature of the signature involved in the proposed single-muon-production experiment, it was decided to construct a detector consisting of a central target region and a surrounding anticoincidence system. Considering the expected event rate per target nucleus and the range of produced particles, a rather large detector was envisioned. These criteria, along with those of economic feasibility and maximum versatility, prompted the design and construction of a large volume, modular, liquid scintillation detection system. This system was located near sea level in a single-storied building within the city limits of Atlanta, Georgia ($33^{\circ}48^{\text{m}}\text{N.}$, $84^{\circ}21^{\text{m}}\text{W.}$).

Ten large multi-region modules were constructed, arranged on a steel supporting frame, and filled with organic liquid scintillator.

These modules were constructed from one-half-inch-thick Plexiglas sheet. Two additional detectors, end anticoincidence units, were constructed from plastic scintillator to allow easy access to the target region of the detector.

The target region of the detector consisted of three Plexiglas modules arranged as shown in Figure 4. Each module was divided into a sensitive volume filled with a mineral oil base liquid scintillator, and two light pipe regions filled with pure mineral oil. The light pipes were included to improve the uniformity of response of the target region to scintillation light.

This detector was designed to perform several related experiments, only one of which is reported here. It was for these other experiments that the target volume was divided into the three regions described above. Although all three modules were present and filled with scintillator during the course of this experiment, only the two larger target modules were actually used. The effects associated with the presence of the small central module were, however, included in the analysis of the data.

The anticoincidence system consisted of nine modules arranged as shown in Figure 5. The two modules above the target region contained 5-1/2 inches of liquid scintillator and were each viewed by three five-inch-diameter photomultiplier tubes located at one end of each cell. The four side anticoincidence modules contained approximately four inches of liquid scintillator and were each viewed by two five-inch-diameter photomultiplier tubes located at each end. The end anticoincidence units were each constructed of two sheets of 3/4-inch

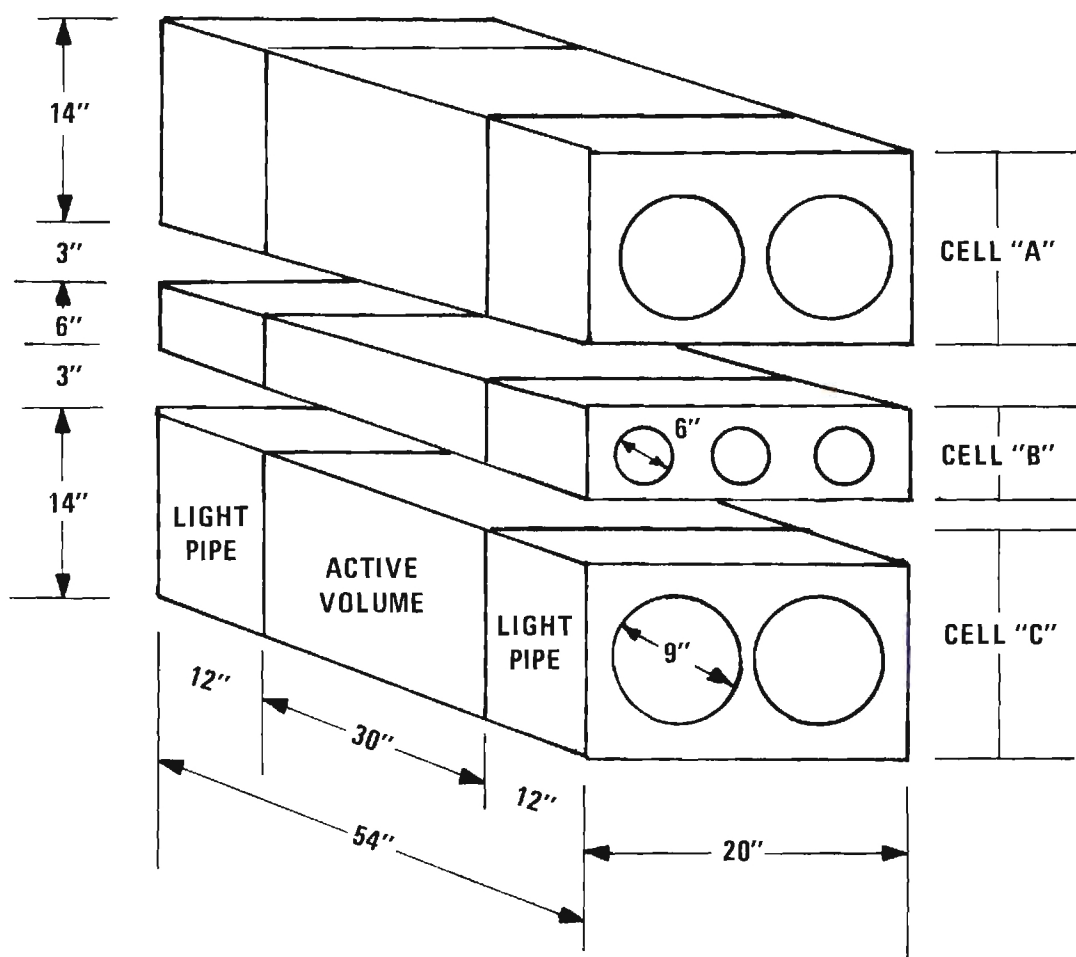


Figure 4. Target region of cosmic ray detector.

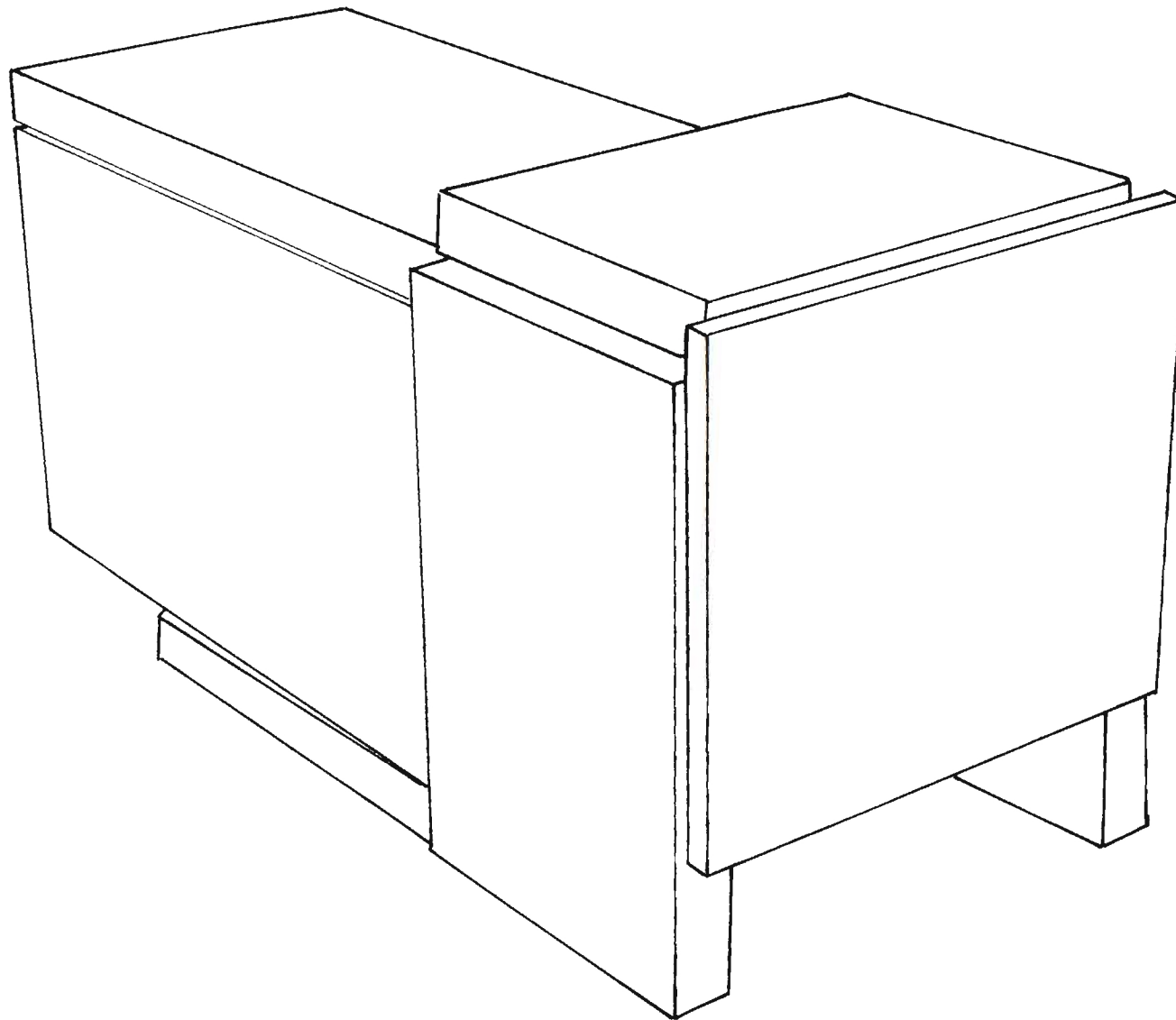


Figure 5. Cosmic ray detector anticoincidence system.

Pilot-B plastic scintillator which were optically isolated. This 1-1/2-inch-thick scintillator sandwich was viewed along the bottom edge by three two-inch diameter high gain photomultiplier tubes.

Each module of the detector was wrapped with loose-fitting aluminum foil to serve as a diffuse reflector to that portion of the scintillation light escaping the module. It has been shown by others¹⁸ that the addition of such a reflector can result in a non-negligible increase in the light output of most scintillation detectors employing internal reflection for the collection of the scintillation light. The foil also served the equally important purpose of optically isolating each module from the others.

Note that in the above application it was very important that the foil not be in optical contact with the modules. Such contact would destroy the internal reflection characteristics of a module and severely impair its performance.

To afford the accompanying photomultiplier tubes a satisfactory environment, the entire detector was enclosed in a light-tight box constructed of 5/8-inch particle board. This structure was painted inside and out with a flat black paint and sealed with a black silicone rubber.

Figures 6 through 13 show the detector during various stages of construction. A summary of the dimensions and volume of each module is given in Table 1.

Module Construction

Prior to the fabrication of the above described Plexiglas modules, much effort was placed on developing techniques to allow this construction to be done "in-house." The primary obstacle that had to



Figure 6.



Figure 7.

Cosmic ray detector during various stages of construction.

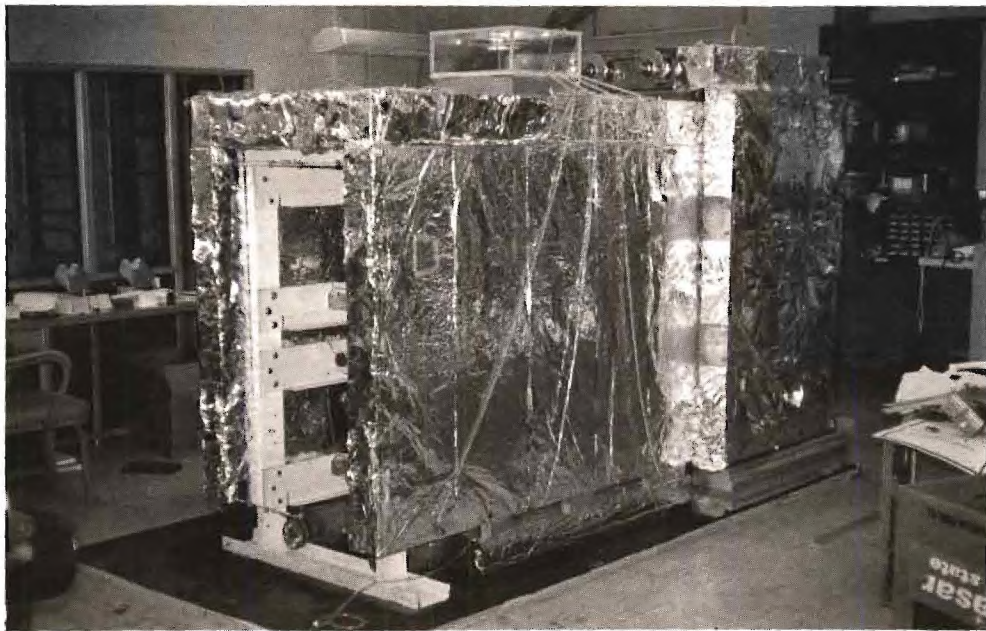


Figure 8.

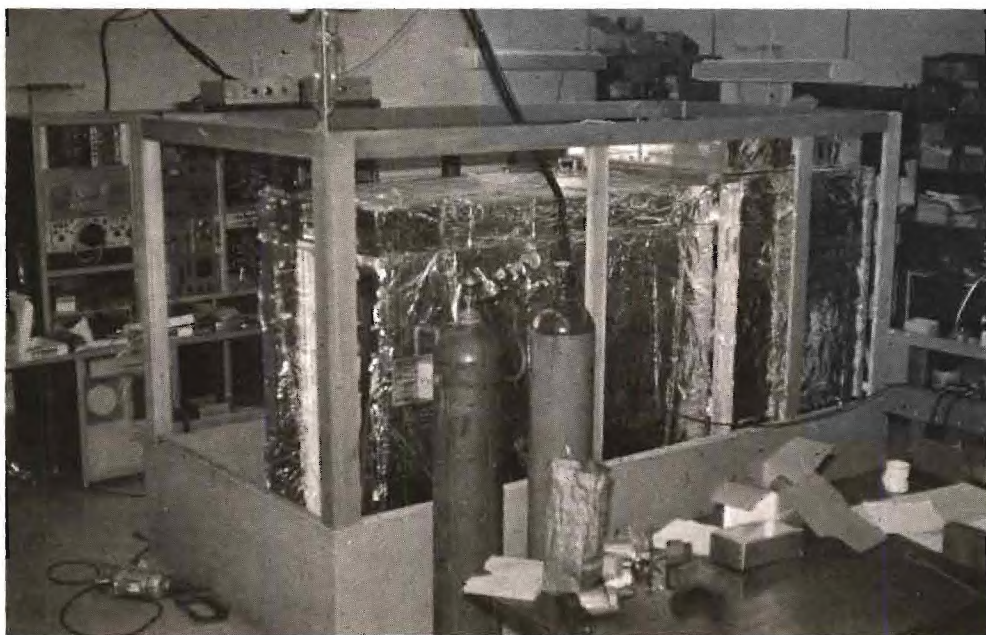


Figure 9.

Cosmic ray detector during various stages of construction.

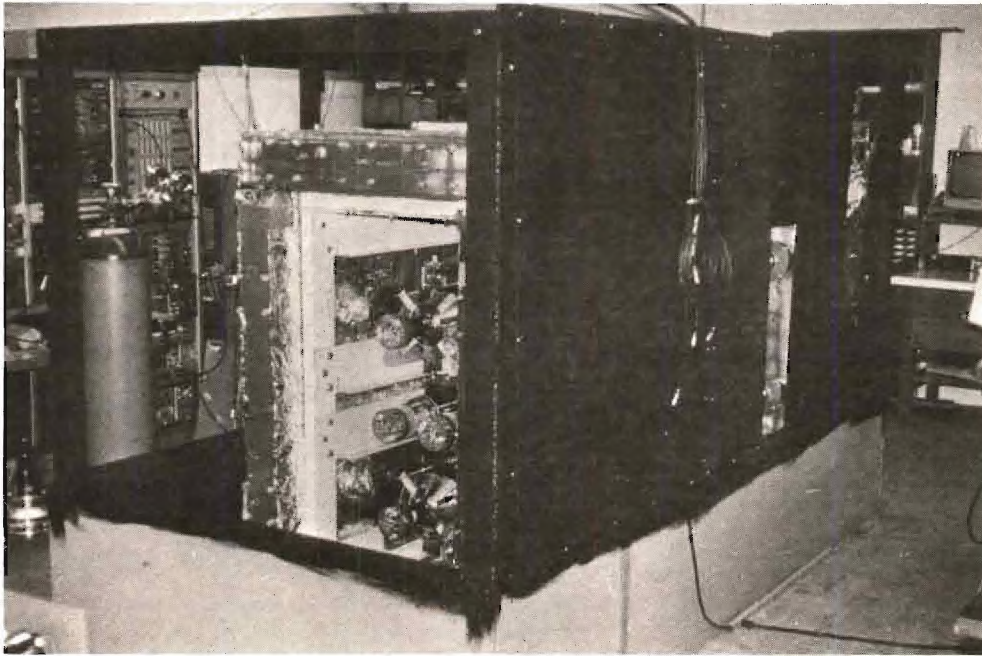


Figure 10.

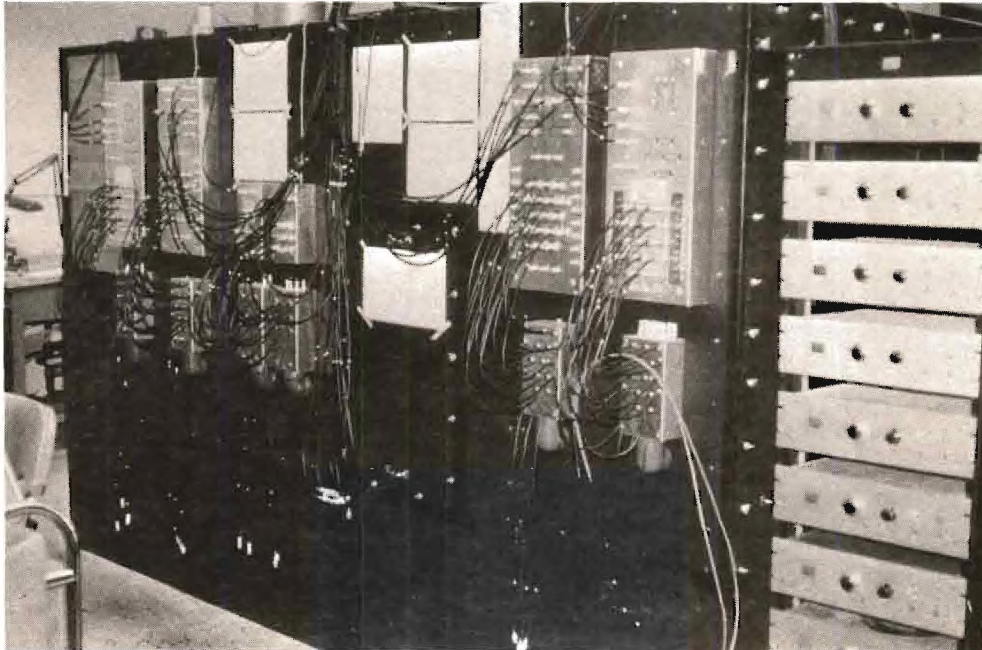


Figure 11.

Cosmic ray detector during various stages of construction.

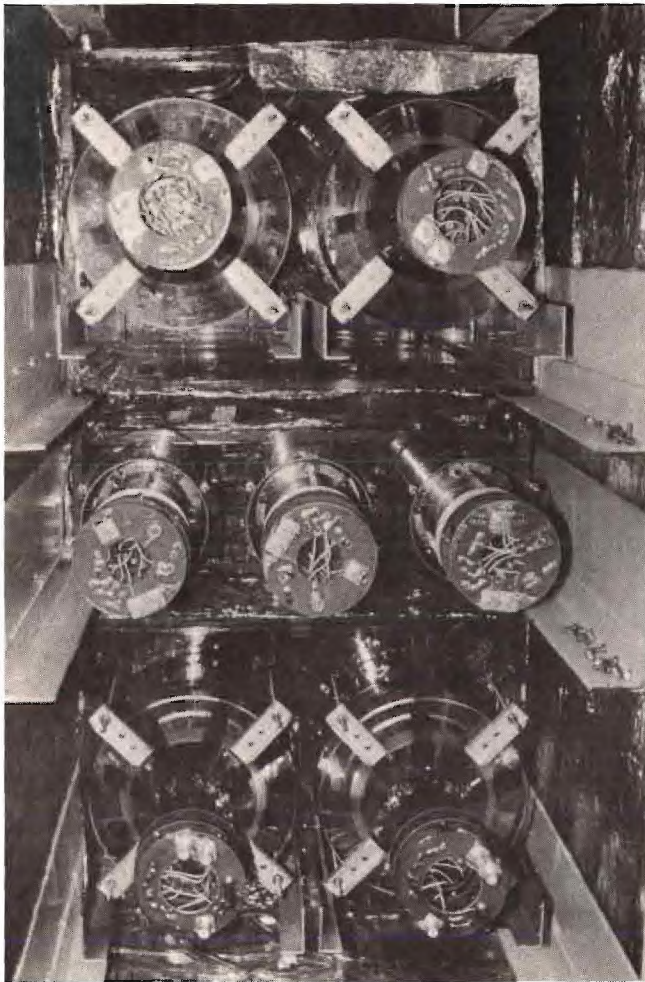


Figure 12.

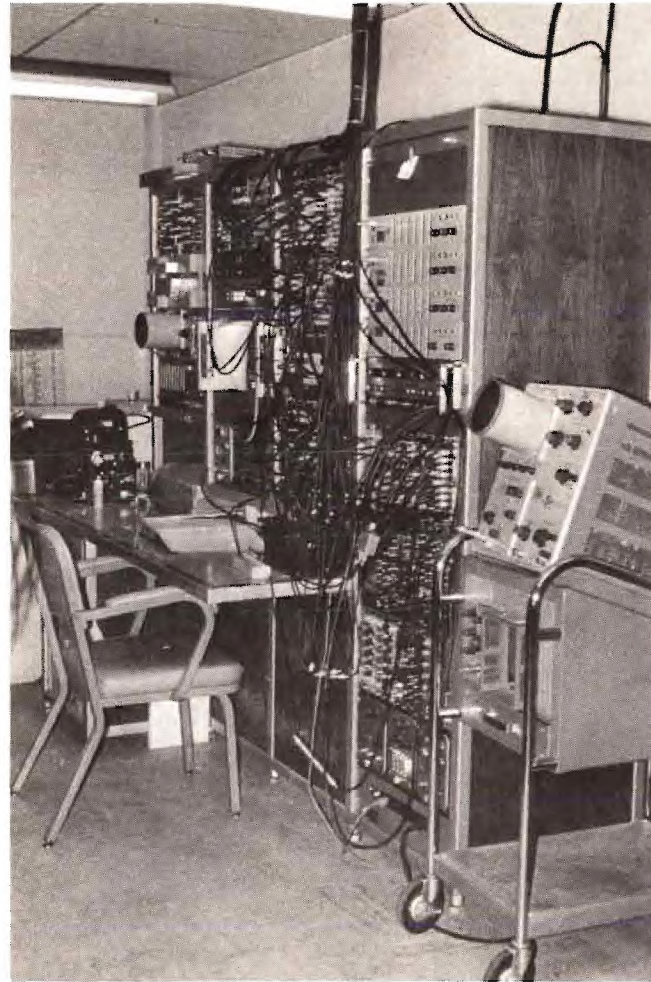


Figure 13.

Cosmic ray detector during various stages of construction.

Table 1. Cell Dimensions and Volumes of Cosmic Ray Detector

Module	Sensitive Volume		Light Pipe
	Dimensions (inches)	Volume (liters)	Dimensions (inches)
A	13.55 x 20 x 30	133.2	13.55 x 20 x 12
B	5.37 x 20 x 30	52.8	5.37 x 20 x 12
C	13.55 x 20 x 30	133.2	13.55 x 20 x 12
	Total Target Volume =	319.2	
D	5-1/2 x 35 x 71	224.0	
E	4 x 48-3/4 x 71	226.9	
F	4 x 48-3/4 x 71	226.9	
G	3-1/2 x 35 x 71	142.5	
H	5-1/2 x 35 x 41	129.3	
J	3-3/4 x 35 x 57-1/2	123.7	
K	3-3/4 x 35 x 57-1/2	123.7	
L	1-1/2 x 48 x 48	56.6	
M	1-1/2 x 48 x 48	56.6	
	Total Volume =	1,629.4	

Note: Cells L and M are sheets of Pilot-B plastic scintillator.

be overcome was that of size. The bonding of small pieces of plastic can be satisfactorily achieved via solvent bonding, but this requires that the two surfaces be in contact over the entire area to be bonded. When extrapolated to dimensions of the order of three to six feet, this requirement becomes almost impossible to satisfy. After several attempts involving extensive machining and elaborate jigs, the solvent bonding approach was abandoned as unworkable.

A product found to give very satisfactory results under these less than ideal conditions is PS-30, an acrylic adhesive manufactured by Cadillac Plastics.* It consists of a bulk component, which appears to be partially polymerized methyl methacrylate, and a catalyst. The primary advantage of this material is that it will fill the voids between two pieces of acrylic plastic which are being bonded, thus eliminating the need for extensive machining and elaborate fabrication facilities. Crude experimentation also indicated that a properly constructed joint was stronger than the material being bonded.

The technique used to bond two pieces of plastic at right angles is shown in Figure 14. The three-degree bevel insures that the adhesive reaches all parts of the surfaces to be bonded. With the aid of a rather large hypodermic needle to apply the adhesive, and capillary action to insure that the entire volume is filled, an optically clear joint can be achieved.

Although the adhesive comes as a two-part mixture, it was found that thinning with methyl methacrylate monomer was necessary to achieve

* Cadillac Plastic and Chemical Company, Atlanta, Georgia.

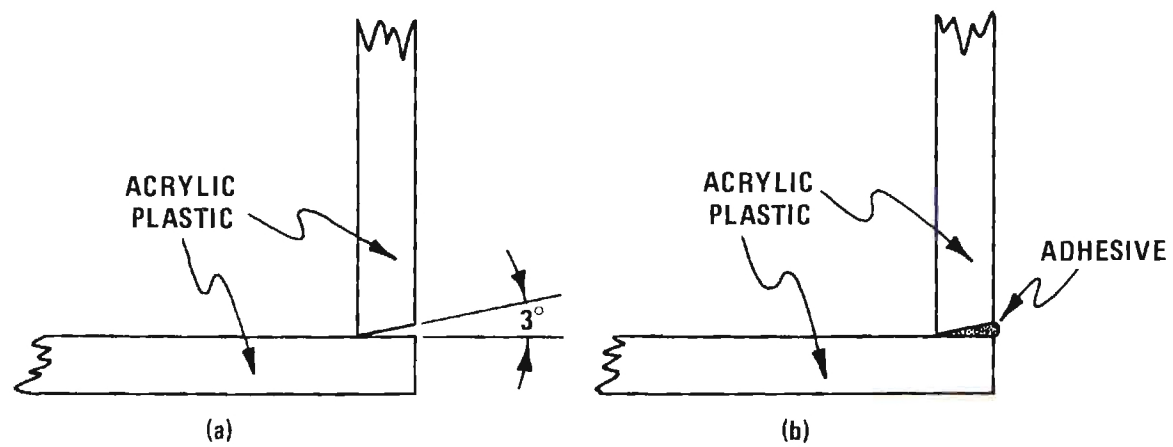


Figure 14. Technique for bonding acrylic plastic.

a workable viscosity. Satisfactory results were achieved using the following ratios of components: 45 grams adhesive, 15 grams methyl methacrylate monomer, and 3 grams catalyst. Following the thorough mixing of these components, it is necessary to remove trapped air by placing the sample under vacuum. The pot life of a prepared sample is approximately 10 minutes.

Development of Scintillator

Solvent

The choice of medicinal paraffin (mineral oil) as primary solvent for the liquid scintillator was based primarily on the following facts:

1. The mean free path of scintillation light in mineral oil is quite long (greater than two meters).¹⁹
2. The flash point of mineral oil is much higher than traditional scintillator solvents such as toluene, xylene, etc.
3. Mineral oil is relatively inexpensive.
4. The material requires no additional purification before use as a scintillator solvent.
5. The solvent is optically and chemically compatible with Plexiglas, the construction material of the modules.
6. Scintillator solutes are relatively easily dissolved in mineral oil.

Kaydol, a U.S.P. grade white mineral oil marketed by the Sonneborn Division of Witco Chemical Company, New York, was selected as the primary solvent. This material has an index of refraction of 1.482 and a specific gravity of 0.880/0.895 at 60°F.²⁰

Solutes and Secondary Solvent

The results of research conducted by Advanced Research Corporation, Atlanta, Georgia, in 1967²¹ indicated that appropriate quantities of mineral oil as solvent, PPO^{*} as scintillator, naphthalene as secondary solvent and Bis-MSB^{**} as wavelength shifter should result in a satisfactory liquid scintillator. The recent work of O'Sullivan¹⁵ with large mineral oil base scintillation detectors indicates that the optimum naphthalene concentration for such a scintillator is approximately 2-1/2 percent by weight.

Using 0.01 percent Bis-MSB and 2-1/2 percent naphthalene in heavy mineral oil data were collected on the relative light output of the scintillator as a function of the PPO concentration in a 12-inch-long cell. These data, when extrapolated to a 30-inch cell and a 72-inch cell, indicated the optimum PPO concentration to be approximately 0.35 percent by weight. Figure 15 shows the experimental arrangement and the data.

A summary of the scintillator components used in this experiment and their concentrations appears in Table 2.

Scintillator Preparation

The scintillator for the detector was mixed in 30 liter batches in a large Pyrex battery jar fitted with stirrer, heating tape, and cover. Following the addition of all components of the scintillator, the liquid was heated to approximately 50-55°C. and stirred for at

* PPO is an abbreviation for the organic compound 2,5-Diphenyloxazole.

** Bis-MSB is an abbreviation for the organic compound bis(0-Methylstyryl)-Benzene.

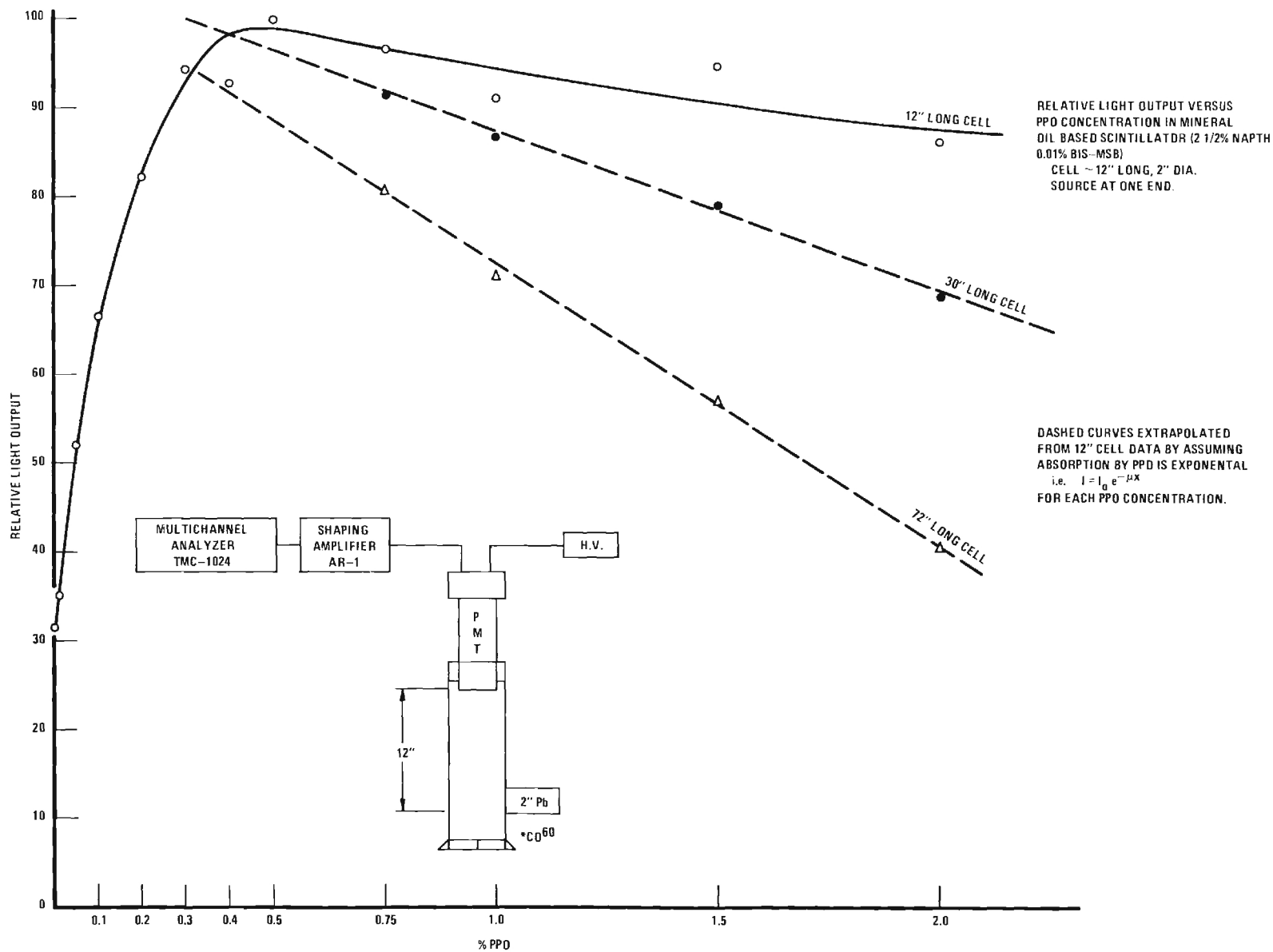


Figure 15. Relative light output of mineral oil based scintillator as a function of PPO concentration.

Table 2. Composition of Liquid Scintillator

Component	Percent by Weight
Heavy Mineral Oil (Kaydol)	97.14
Naphthalene	2.50
PPO	0.35
Bis-MSB	0.01

least three hours. Transfer of the scintillator to the detector was accomplished with the aid of a high speed stainless steel pump and Tygon tubing.

Effects of Dissolved Oxygen

It has been reported by many researchers²²⁻²⁴ that the removal of dissolved oxygen from a liquid scintillator may result in a substantial increase in the light output from that scintillator. Since the magnitude of this effect has been observed to vary considerably with the composition of the scintillator, it was felt that a determination of the quenching effects of dissolved oxygen in this mineral oil base scintillator was necessary. The relative light output from small (2-inch diameter x 1/2-inch-high) samples of the liquid scintillator was obtained before and after bubbling the samples with helium to remove dissolved oxygen. An improvement of more than 15 percent in the relative light output of the liquid was obtained by bubbling for five minutes. No additional improvement was gained by bubbling the liquid for longer periods of time.

Based on the above results, it was felt necessary to remove the dissolved oxygen from the scintillator in the large detector modules. Approximately 107 hours was spent bubbling 1000 cubic feet of helium gas through the 10 liquid-containing Plexiglas cells. At the conclusion of this bubbling an argon blanket was placed above the liquid in each cell.

Scintillator Pulse Shape

The decay time of the mineral oil base liquid scintillator was determined from oscilloscope photographs of pulses from small samples

of the liquid. The scintillator was viewed by a high gain, very fast Amperex^{*} 56AVP photomultiplier tube. The anode output of this tube was used to drive the 50-ohm terminated input of a 581A Tektronix^{**} oscilloscope containing a type 86 plug-in preamplifier. After correction for the finite rise time of the electronics, the decay time of the liquid scintillator was determined to be approximately 26 nanoseconds.

A determination of the light output of the scintillator was made by comparing it with Nuclear Enterprise's⁺ N.E. 213 liquid scintillator. Using identical test cells and the same electronics, Cobalt-60 spectra were collected and compared. The light output of the mineral oil base scintillator was determined to be 75 to 80 percent of that of the N.E. 213. Both samples were bubbled with helium to remove dissolved oxygen prior to the collection of data.

Electronics

The electronics system associated with this facility can be logically divided into four groups: (1) mounted photomultiplier tubes; (2) a mounted photomultiplier tube high voltage distribution system; (3) mixing networks to allow linear summing of photomultiplier outputs; and (4) extensive logic for the collection and preliminary analysis of data. A discussion of these groups and how they relate to one another is felt necessary for a complete understanding of the capabilities of this facility.

* Amperex Electronic Corporation, Hicksville, New York.

** Tektronix, Inc., Beaverton, Oregon.

⁺ Nuclear Enterprises Ltd., Winnipeg, Canada.

The choice of photomultiplier tubes for the detector was complicated by the wide variety of tubes available. Based on considerations such as physical size, availability, cost, allowable peak currents, timing characteristics, output dark current and cathode spectral response, four types of tubes were selected for use with the detector. It should be pointed out, however, that in some cases the choice of tube type was influenced by having a sufficient quantity of an acceptable tube "in-house."

The nine-inch diameter Amperex 57AVP photomultiplier tube was chosen for target cells A and C because it was the only large, fast photomultiplier tube which was economically feasible. This is not to berate the tube, for its characteristics were entirely satisfactory for the intended purpose.

Target cell B was designed to be a very "fast" cell to allow observation of the low energy muon associated with the decay of the short-lived pion. For that reason the cell was viewed by six very fast (two nanoseconds), high gain (10^8), five-inch-diameter Amperex XP1040 photomultiplier tubes. These tubes covered both ends of the cell in an attempt to collect a large fraction of the emitted light and thus minimize the statistical effects associated with summing a small number of photons. As mentioned previously, this cell was not actively involved in the present experiment.

The anticoincidence system photomultiplier tubes were divided into two groups according to scintillator thickness. The five-inch-diameter RCA^{*} 4525, a moderately high gain, low dark current, economically priced

* Radio Corporation of America, Harrison, New Jersey.

tube, was used with all liquid containing anticoincidence cells. This tube was found to be very satisfactory for situations requiring long term stability.

As mentioned earlier, the end anticoincidence detectors were each constructed from two pieces of 3/4-inch-thick Pilot-B^{*} plastic scintillator. Due to poor light transmission in this plastic and a less than ideal optical coupling between the plastic and the photomultiplier tubes, these sandwiches were each viewed by three two-inch-diameter Amperex 56AVP very high gain photomultiplier tubes. In an attempt to maximize the detection efficiency, these tubes were operated at near maximum rated high voltage and at a rather large anode current. As a result, some long term count rate stability problems existed, but were kept under control by frequent gain adjustments at the photomultiplier tube.

Each photomultiplier tube of the detector was supplied with a base consisting of a printed circuit board support structure, and a resistive divider chain for the application of appropriate voltage to the electrodes of the tube. The use of large supply currents and appropriate capacitive decoupling of the last several dynodes of the tubes insured that each tube remained stable under high count rate and large peak current conditions.

A suitable high voltage was applied to each tube base through a distribution system fed by nine highly regulated power supplies, each

* Pilot Chemicals, Inc., Watertown, Massachusetts.

supply furnishing power to from two to nine tubes. In an attempt to effect electrical isolation, especially among tubes being operated in coincidence, no power supply was allowed to furnish power to both ends of any module.

The gain of individual photomultiplier tubes were set by adjusting the voltage supplied to these tubes. These adjustments were accomplished with the aid of potentiometers operated in series with each tube base.

Additionally, the high voltage distribution system contained test points to allow precision determination of the voltage supplied to each tube.

Electrical signals from the detector were taken directly from the anode of each tube and brought to the outside of the light-tight enclosure via 50-ohm coaxial cable. Signal processing could begin at that point. This arrangement allowed access to the output of each photomultiplier tube without disturbing normal operating conditions.

The usual mode of data collection required that the outputs from all tubes at one end of each cell be linearly summed before further analysis. To accomplish this, several types of linear summing networks were designed and built for incorporation into the detector.

For the target region, two and three input, wide band, unity gain, dual output mixers were built. These units were designed to have a bandwidth of the order of 300 megahertz to allow work with very fast pulses. Additional features of these amplifiers include isolated test

points for each input, a high degree of isolation between inputs, a high degree of isolation between outputs, and NIM^{*} compatibility. Mixers of this type were also used to sum the three photomultiplier outputs of each end anticoincidence detector.

For the remainder of the anticoincidence region, two and three input, 150 megahertz, dual output mixers were designed and constructed. Due to the lower gain of the five-inch diameter anticoincidence photomultipliers and the need for a sensitive anticoincidence system, these mixers were designed with a gain of approximately 20. Additional features of this amplifier are similar to those of the unity gain mixer described above. A detailed description of these units can be found in Appendix A.

To minimize the cable lengths between the photomultiplier tubes and the mixers, all summing units were mounted on the outside surface of the light-tight housing. Additional lengths of cable were used as necessary to adjust signal delays to the mixers. Signals from the mixers to the electronics console were carried via 32-foot lengths of 50-ohm coaxial cable.

With the exception of the linear summing discussed above, all signal processing was done at the electronics console. This console contained an assortment of EG & G,^{**} ORTEC,⁺ and ARC⁺⁺ nuclear instrument modules (NIM), several scalars, a TMC-1024 multichannel analyzer and various input-output devices. A detailed listing of these instruments can be found in Appendix A.

^{*}In 1964 the AEC Committee on Nuclear Instrument Modules (NIM) was formed to draw up specifications for standard modules to assure mechanical and electrical interchange-ability within the industry. The program resulted in the issuance of module specifications in the form of government document TID-20893.

^{**}EG & G, Inc., Oak Ridge, Tennessee.

⁺ORTEC, Inc., Oak Ridge, Tennessee.

⁺⁺Advanced Research Corporation, Atlanta, Georgia.

Testing and Calibration of Equipment

Response as a Function of Position in Cell A

For a scintillation detection system to have the ultimate in energy resolution it is necessary that the detector respond identically to identical events occurring throughout the volume of the detector. For a given event this requires collecting a constant fraction of the scintillation light, independent of where the light was created within the volume. In reality self-absorption by the scintillator, reflection losses at interfaces, light trapping, optical flaws, and inefficient light piping may all contribute to a reduction in the uniformity of response of a detector.

The uniformity of response of target cell A was determined with the aid of the "muon telescope" arrangement shown in Figure 16. This arrangement defined a muon beam that passed vertically through the cell depositing approximately 57.6 MeV in the liquid. As shown in Figure 17, response data were collected at three cell positions and normalized to the center of the cell. Using these data and assuming that the scintillation light is attenuated exponentially with respect to the perpendicular distance from the light pipe-scintillator interface, it was determined that the effective attenuation of the scintillation light in the liquid could be expressed as

$$I = I_0 e^{-0.0061x} \quad (7)$$

where x is the perpendicular distance from an interface expressed in

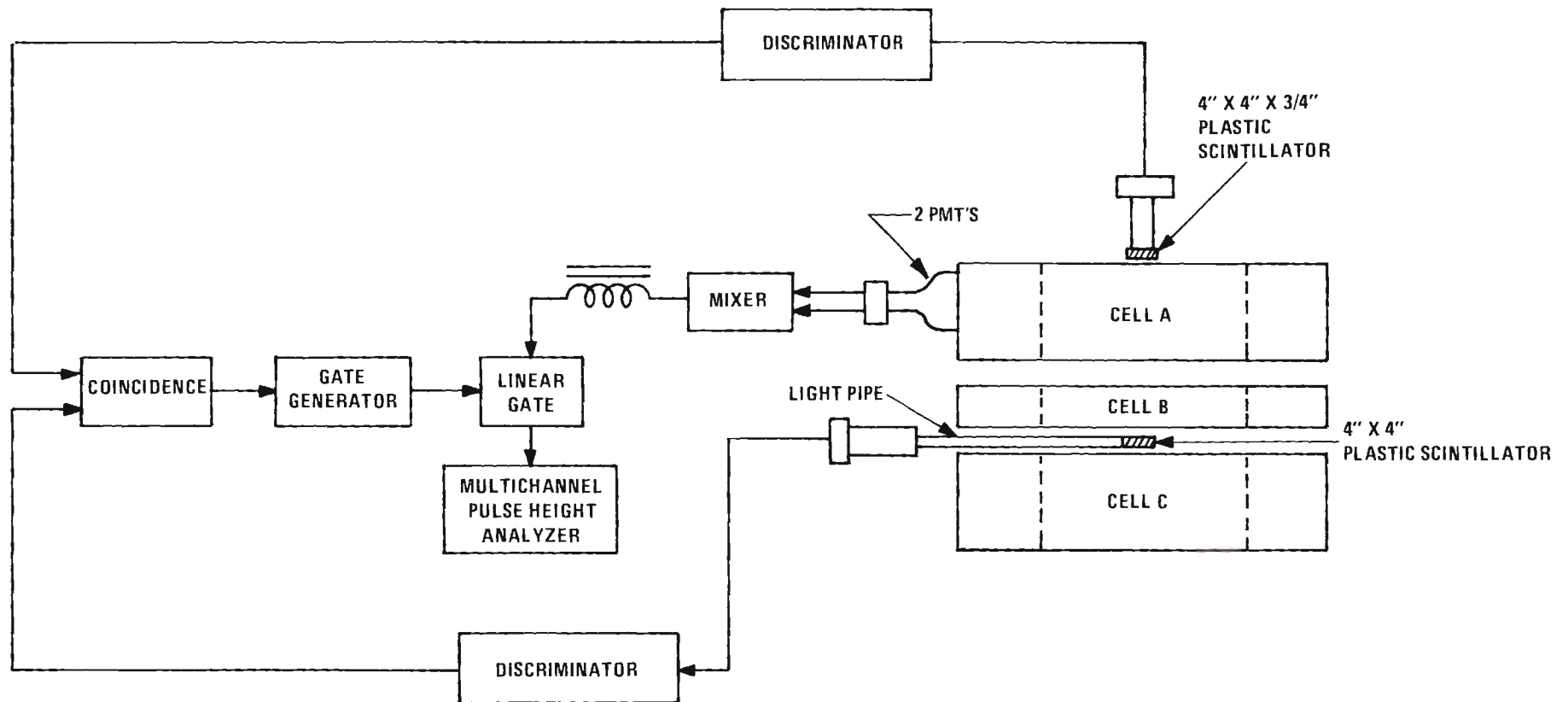


Figure 16. Telescope arrangement for calibration of target cells.

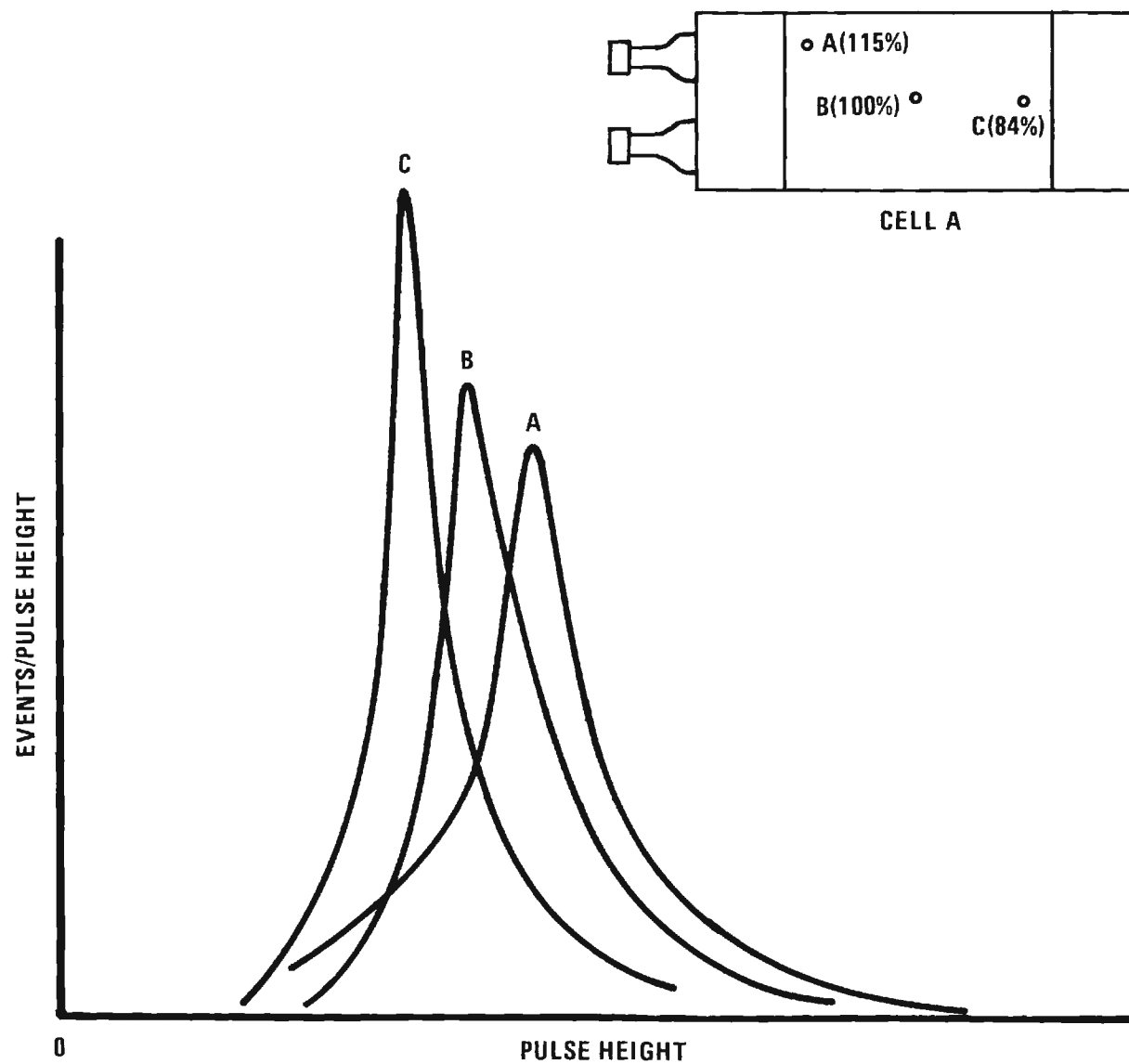


Figure 17. Detector response as a function of position in cell A.

centimeters. This expression yields an effective mean free path for the scintillation light of approximately 113 centimeters.

Calibration of Target Cells

The energy calibration of target cell A and thus its twin, cell C, was accomplished with the aid of the muon telescope arrangement described above. Figure 18 shows the "thru-peak" data collected with the telescope centered over the target region. It is estimated that the "thru-peak" energy corresponds to channel number^{*} 660 ± 30 .

The use of the muon "thru-peak" defined one energy point of a calibration curve. A second data point was chosen to be the multichannel analyzer's "zero of energy." If one verifies the linearity of a multichannel pulse height analysis system by plotting the charge delivered from an accurately calibrated pulser versus the corresponding channel number, the x-intercept is the system's "zero of energy." A mercury pulser of Advanced Research Corporation design (Model AR-Hg1) was used to supply pulses of known integrated charge. The linearity of the system was verified at two amplifier gains and from these data it was determined that the "zero of energy" corresponded to channel number $-(55 \pm 15)$. The error represents the maximum spread in the collected data.

Using the above two data points and their errors, a plot of energy versus channel number was made (Figure 18). As will be explained

*The determination of a pulse height distribution from a photomultiplier tube was accomplished in all cases with the aid of a multichannel pulse height analyzer. This device, consisting of an analog-to-digital converter and memory unit, determines the relative amplitude of input pulses and uses this information to build a histogram of pulse heights. The intervals of this histogram are often called channels and each channel is assigned a channel number. Channel numbers generally start at one and increase with increasing pulse height.

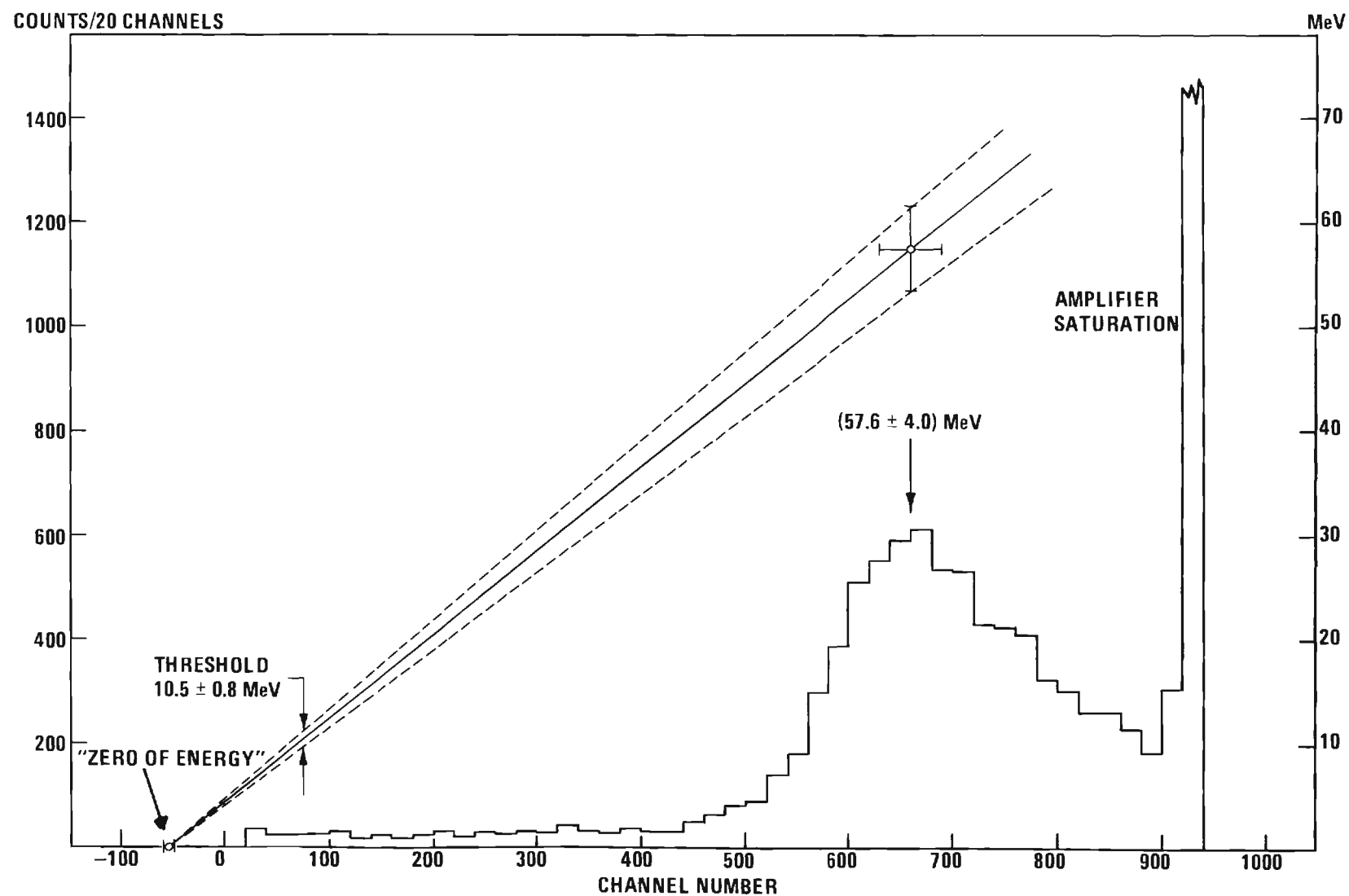


Figure 18. Muon "thru-peak" and energy calibration of cells A and C.

below, channel number 75 was chosen to represent the desired threshold setting for cells A and C. This setting corresponded to an energy of 10.5 ± 0.8 MeV referenced to the center of target cell A. Figure 19 shows the relationship of this threshold to the background spectrum collected by accepting all events occurring within cell A. The integrated background count rate above 10.5 MeV was determined to be 93.5 counts/second for cell A and 85.0 counts/second for cell C. The lower rate for cell C was a result of the additional overburden for that cell.

Using the numerical data of Figure 19, a plot of cell A count rate versus threshold energy was constructed. This plot, shown as Figure 20, indicates that to stay within 1.5 MeV of the desired 10.5 MeV threshold the cell A count rate must remain within approximately 4.0 percent of 93.5 counts/second. A similar determination was made for target cell C.

Determination of the Muon Decay Electron Energy Distribution

The energy distribution of the electron in μ -e decay is rather well known. In a sufficiently large detector, having excellent energy resolution, one would expect to see a distribution similar to that shown in Figure 21. In a realistic detector, however, this theoretical energy distribution will be altered by the nonuniformity of response and intrinsic resolution of the detector, and by the fact that some of the decay electrons will leave the detector volume before depositing all of their energy.

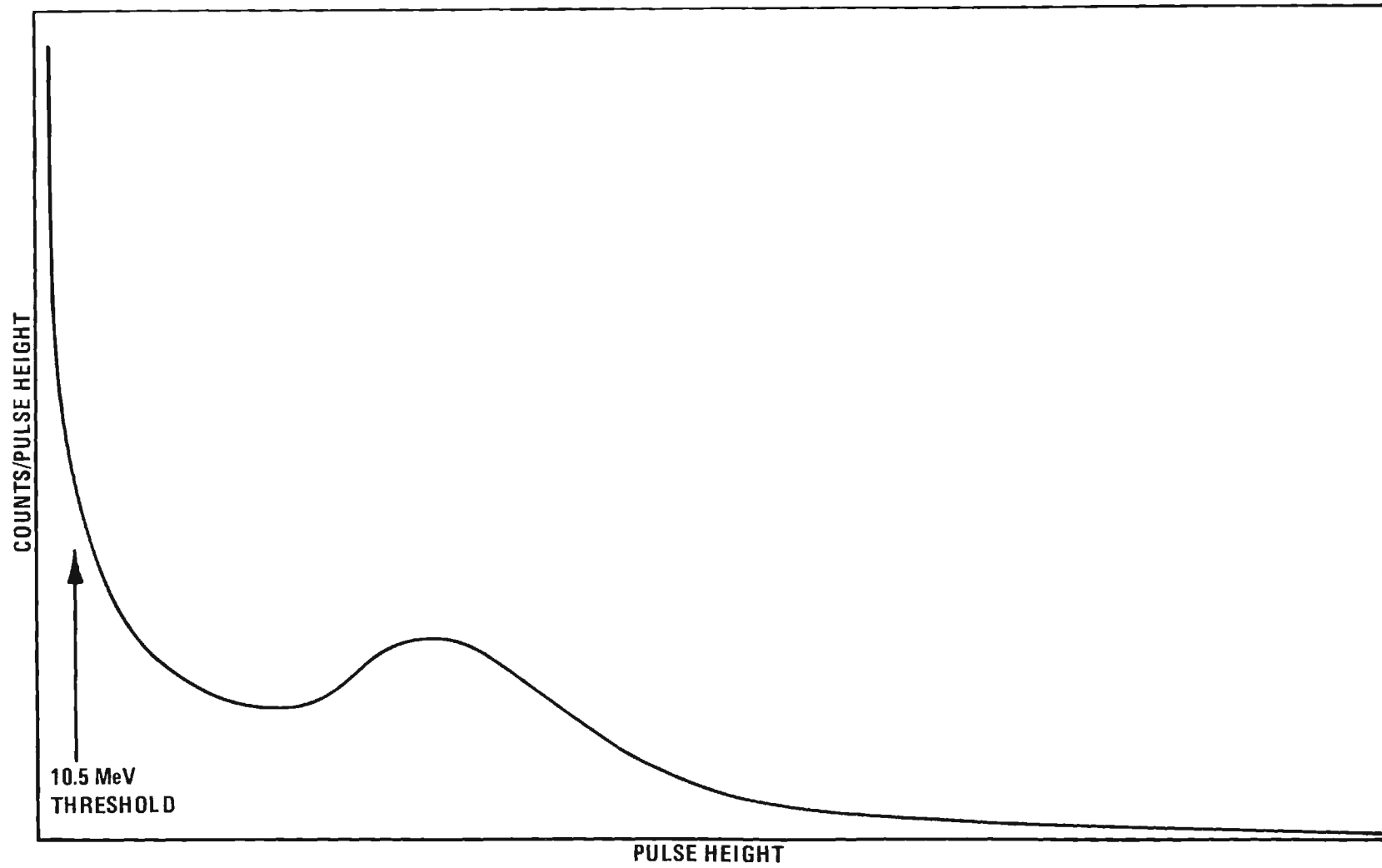


Figure 19. Location of 10.5 MeV threshold with respect to target background energy distribution.

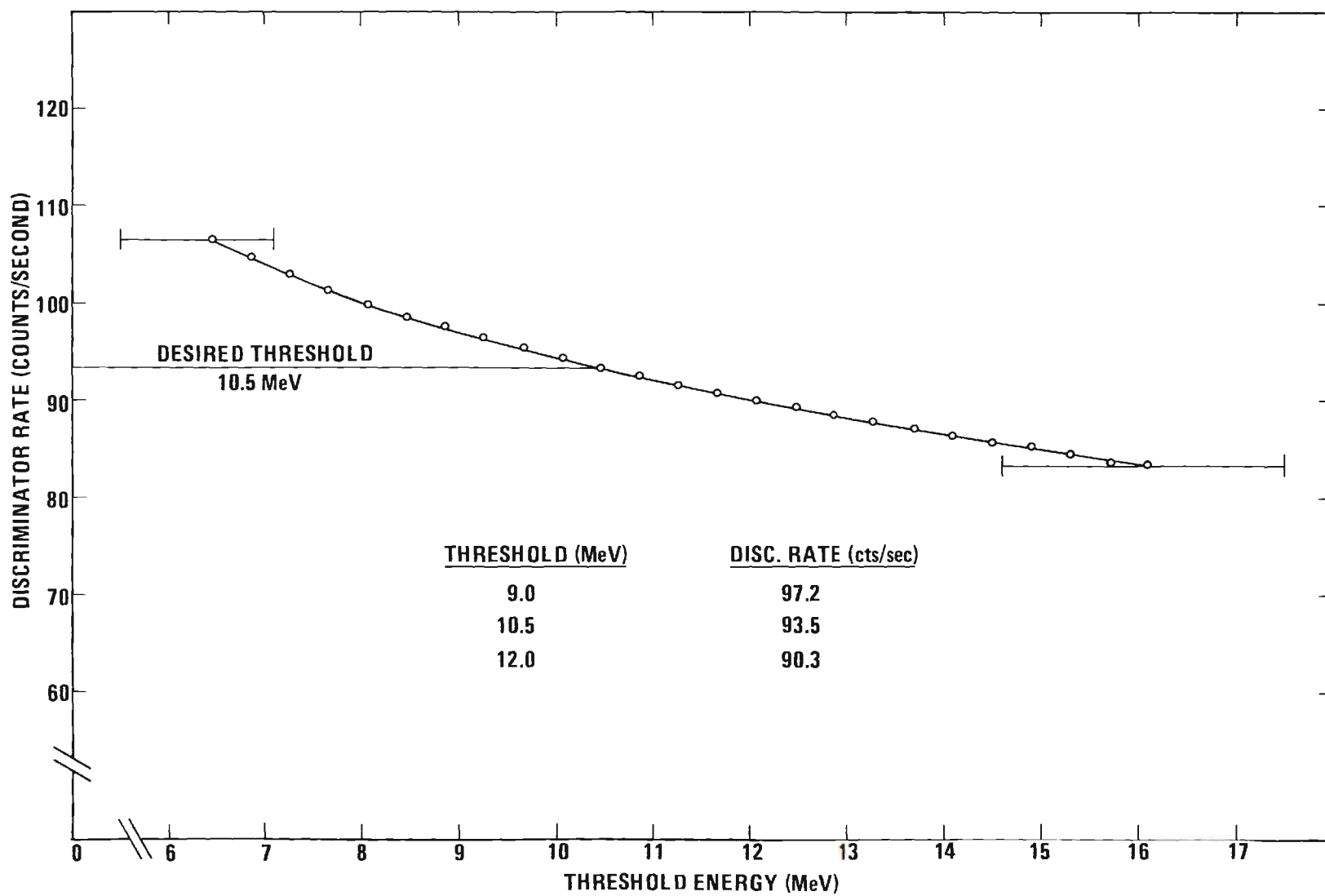


Figure 20. Discriminator count rate versus threshold energy for target cell A.

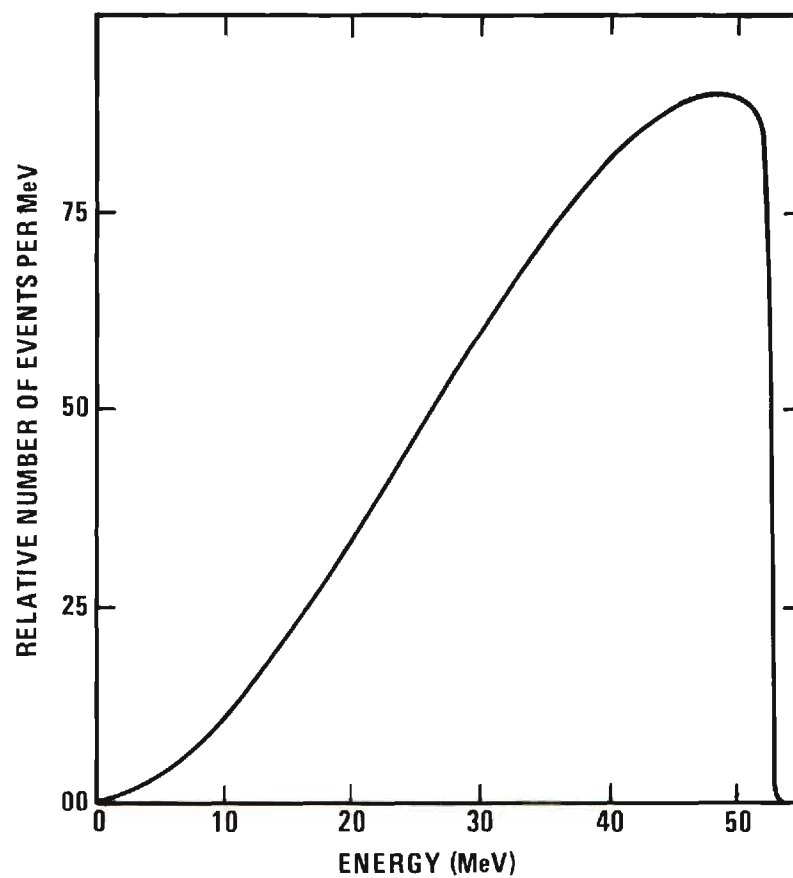


Figure 21. Electron energy distribution from μ -e decay.

An accurate knowledge of the μ -e decay electron energy distribution recorded by target cells A and C was necessary first to set an energy threshold for the detection of the decay event, and later for a determination of the μ -e decay detection efficiency of the detector.

The electron energy distribution from muon decay, as seen by the photomultiplier tubes at one end of cell A, was measured using the arrangement shown in Figure 22. An energetic muon entering cell A would initiate a delayed nine microsecond gate. This gate was delayed for a time sufficient to guarantee the decay of the initial pulse and then opened for the nine microseconds to receive the electron signal for pulse height analysis.

The same spectrum was then collected with the additional constraint that the second or electron pulse must not violate the anti-coincidence system. During the collection of neutral-particle-produced muon data such events were indistinguishable from those in which the second pulse was initiated by an outside particle passing through the detector. Thus, even though a substantial fraction of otherwise acceptable events were lost, it was necessary to veto all such events. The effect of such a veto served to lower the detection efficiency of the experiment, but improved the reliability of the remaining data.

The two muon decay electron energy distributions for cell A are shown in Figure 23 along with the "thru-muon" spectrum taken with the aid of the telescope arrangement discussed above.

As a check on the validity of the μ -e decay electron energy distribution in the detector, the above data were compared with those generated by a computer model which simulated the decay process. A

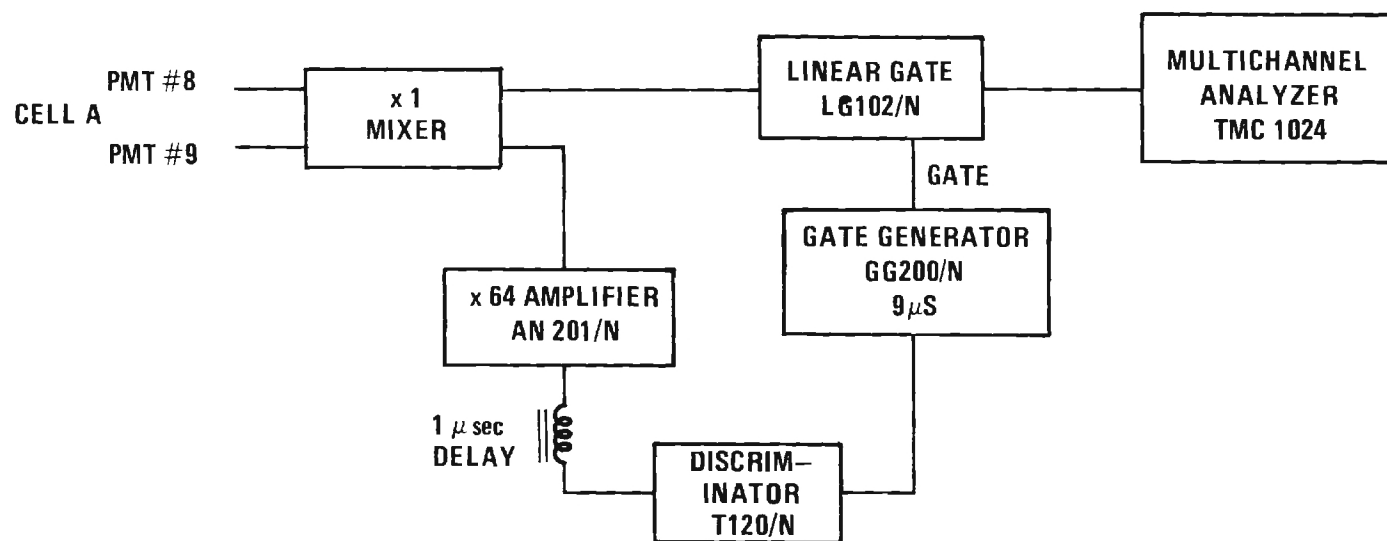


Figure 22. Electronics configuration for determining decay electron energy distribution.

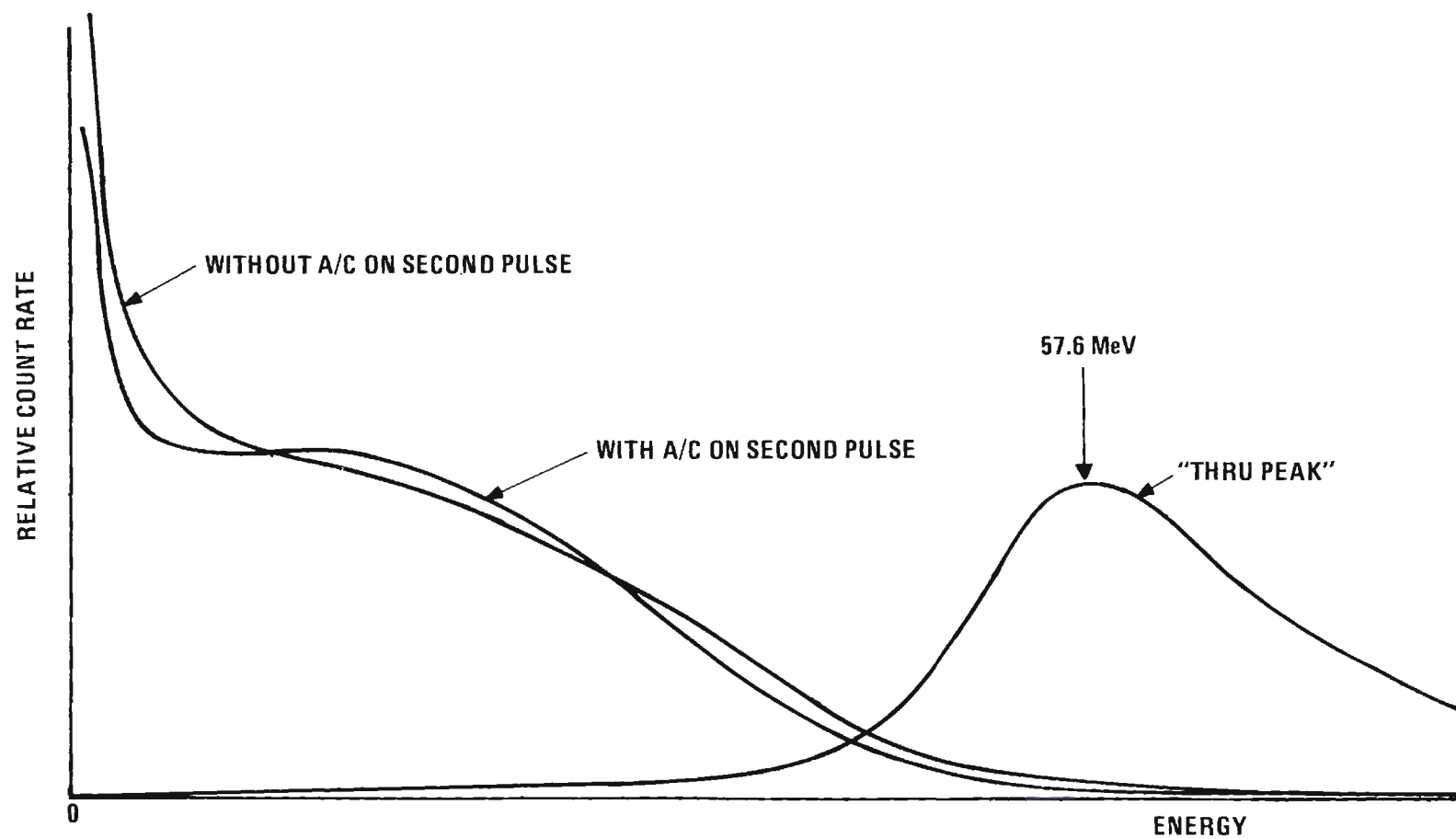


Figure 23. μ -e decay electron energy distribution with and without anticoincidence on second pulse. Muon thru-peak shown for reference. All scales linear.

detailed description of this Monte Carlo program can be found in Chapter IV in the discussion of the determination of the electron detection efficiency. Let it suffice here to say that, during the running of the program, 525,000 trials were used to build the expected electron energy distribution.

The experimentally determined electron energy distribution shown in Figure 24 was obtained by subtracting the energy dependent background (Figure 19) from the raw data (Figure 23). The smooth curve shown in the same figure is the distribution predicted by the computer model. The agreement between the experimental data and that generated from the model is quite good.

Calibration of TAC-Multichannel Analyzer System

Prior to the actual calibration of the time-to-amplitude conversion system, the differential linearity of the system was determined as a function of the various output pulse shapes available from the time-to-amplitude converter (TAC). The optimized arrangement had an integral nonlinearity of approximately 1.2 percent between channel numbers 50 and 500. Data in channels below number 50 or above 500 were discarded.

The actual calibration of the TAC-multichannel analyzer system was accomplished using a scheme developed by Hatcher and reported in EG&G's publication, Nanonotes.²⁶ A block diagram of the logic is shown in Figure 25. A 10-KHz_z signal, derived from a time mark generator, was shaped by a discriminator to form the initial, or START, member of a pulse pair. A 10-MHz_z signal also derived from the time mark generator was shaped by another discriminator to form a train of narrow pulses spaced 100 nanoseconds apart. These pulses were gated at random by

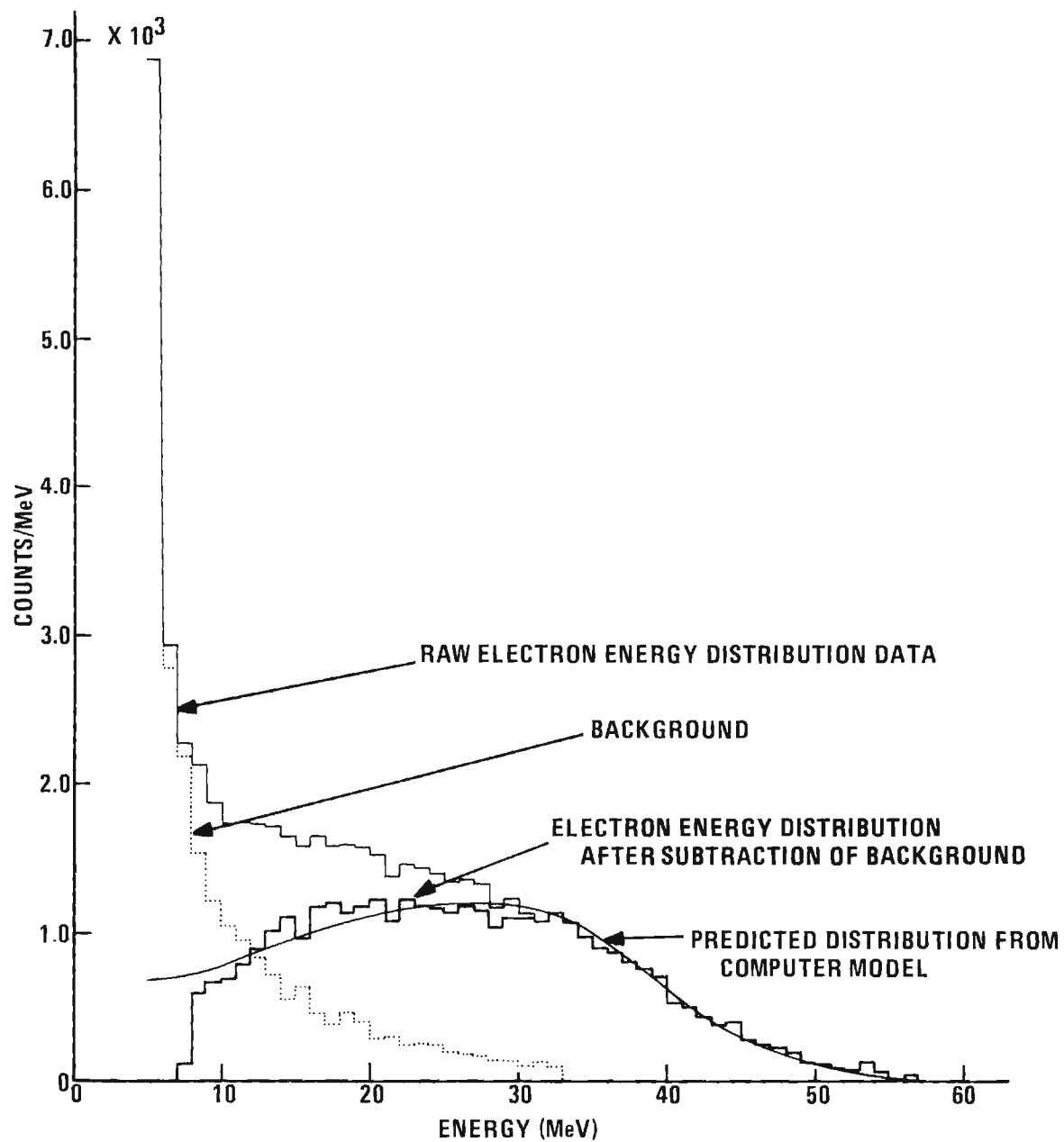


Figure 24. Comparison of experimental μ -e decay electron energy distribution with computer generated distribution.

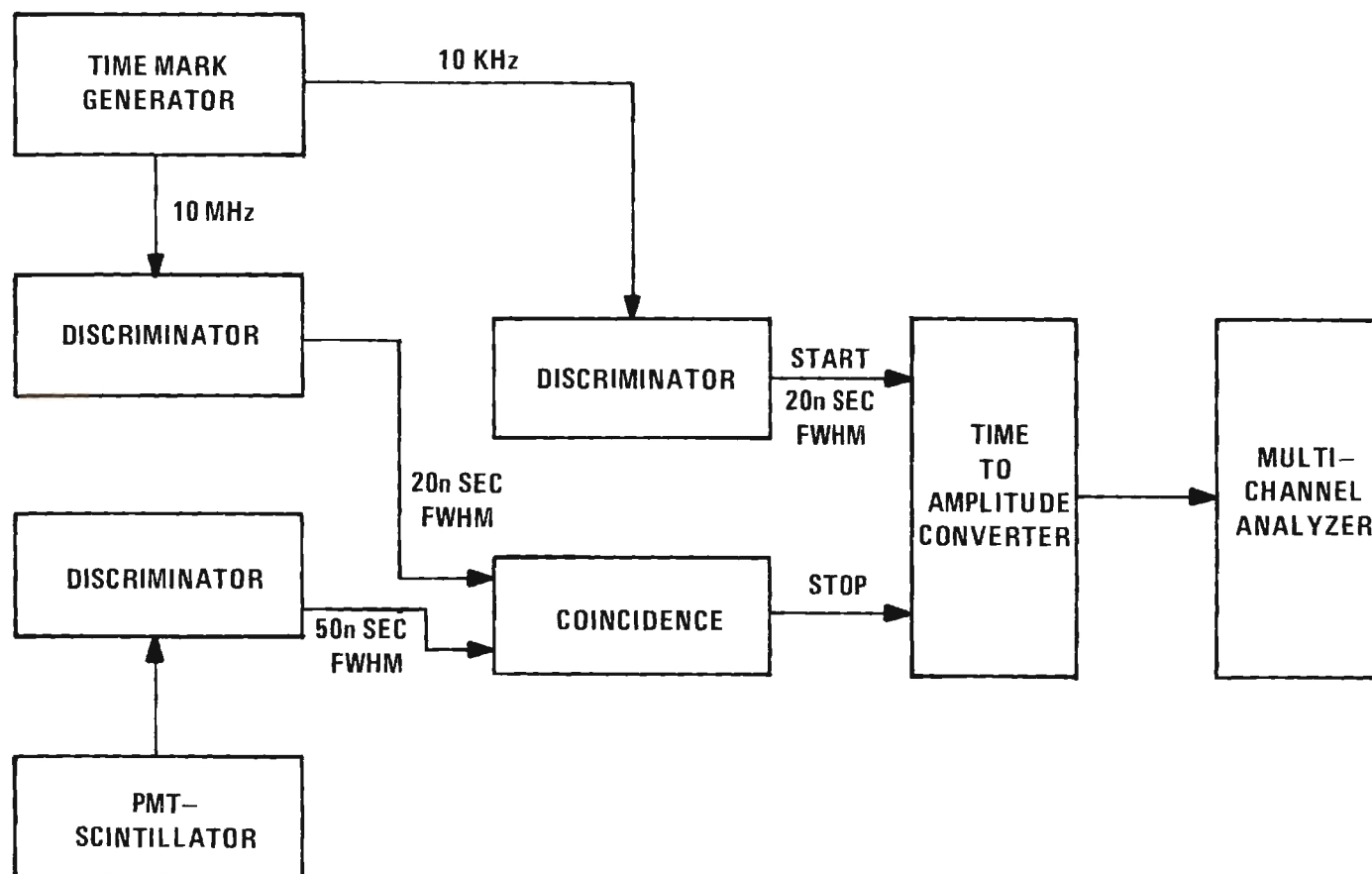


Figure 25. Calibration of the time to amplitude converter.

pulses from a third discriminator which was connected to a photomultiplier tube and scintillator. A gated 10-MHz pulse was then the second, or STOP, member of a pair and was used to stop the time-to-amplitude convertor.

The spacing between members of a pair was thus a random multiple of 100 nanoseconds and the spectrum of the time intervals appeared as a series of spikes on the pulse height analyzer. The accuracy of such a calibration is determined by the stability of the time mark generator and the number of counts in the peaks.

Effectiveness of Anticoincidence System

To determine the rate of production of neutral particle initiated events in the detector it was necessary to identify and establish rates for all processes capable of generating an artificial signature. Of particular concern was the signature generated by a muon leaking through the antineutrino system, stopping and decaying within the target region of the detector. The large muon flux near sea level made this a likely candidate for an important source of false events.

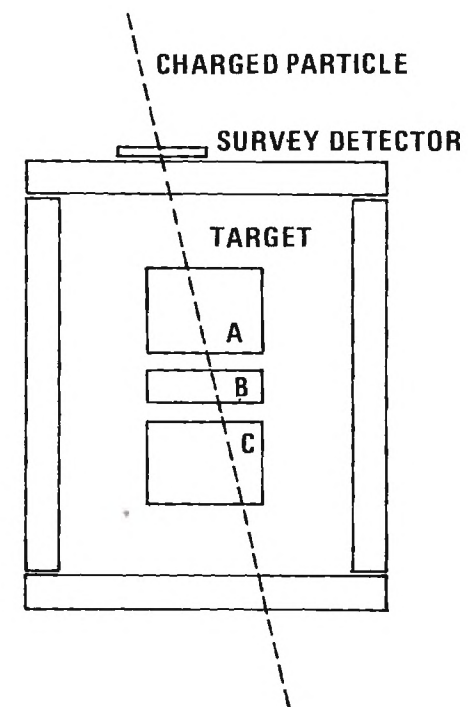
Determining the magnitude of this leak rate involved knowing the average charged particle rejection ratio of the antineutrino system, and the muon decay rate in the target for those particles satisfying the constraints imposed by the system. The determination of an averaged charged particle rejection ratio is discussed below. The application of this ratio to the muon decay rate to establish a leak rate will be treated in the chapter on the analysis of the neutral particle induced data.

As used here the charged particle rejection ratio of an anti-coincidence detector is defined as the ratio of the number of charged particles passing through a detector to the number of charged particles passing through the detector but not recorded by the detector. For example, an anticoincidence detector that is 99.9 percent efficient would have a rejection ratio of 1000:1.

The charged particle rejection ratio of the anticoincidence system as a function of position was determined with the aid of a two-element particle telescope. The target region of the detector served as one element of the telescope and a small (8" x 14" x 2" thick) plastic scintillator survey detector served as the other element (see Figure 26). Coincident pulses occurring in the telescope were used to signify the passage of charged particles through the anticoincidence system. Those events not accompanied by an output from the anti-coincidence system were considered to be leaking particles.

From these data it was possible to determine the charged particle rejection ratio at the site of the survey detector. By moving the survey detector over the anticoincidence system the rejection ratio was determined as a function of position for the entire detector. In an attempt to minimize the number of surveyed data points, advantage was taken of the symmetry inherent in each anticoincidence cell. Figure 27 summarizes the results of this survey.

To aid in the determination of the muon leak rate an average charged particle rejection ratio for the entire detector was defined. This quantity, R_A , is the average of the individual rejection ratios, each weighted by its corresponding muon flux. That is,

[illegible]

$$R_A = \frac{\sum_i C_i R_i}{\sum_i C_i} \quad (8)$$

where the R_i are the individual charged particle rejection ratios and the C_i are the corresponding relative muon flux rates. The quantity R_A when applied to the muon decay rate of the detector yields the detector's muon leak rate.

Data for the determination of the C_i 's were collected simultaneously with the charged particle rejection ratio data, and with the same experimental arrangement. The C_i 's were effectively the normalized telescope rates for the survey detection system. These data were collected for all regions of the anticoincidence system with the exception of the lower half of the sides of the detector. Due to the $\cos^2 \phi$ dependence of the incident muon flux the telescope coincidence rate in those regions was extremely small and an experimental survey was impractical.

The remaining C_i 's were determined with the aid of a computer model of the system. The $\cos^2 \phi$ muon flux incident on the detector was numerically integrated over the target region yielding rates for the flux at all points on the anticoincidence system. These rates, when normalized to the available experimental data, were used to obtain the remaining C_i 's.

As a check on the incorporation of estimated data into the calculation, it was determined that a 50-percent error in the estimated rates would yield only a 11-percent change in the calculated muon leak rate. The

actual error associated with the estimated flux is believed to be much smaller than the 50 percent, probably no more than 10 or 15 percent.

The value of R_A , the effective charged particle rejection ratio for the system, was determined to be 980:1.

Determination of Muon Lifetime

A determination of the well known muon lifetime served as a last check on the target portion of the system prior to the start of collection of neutral-particle-induced data. A 38-hour data run using cells A and C yielded 194,000 pulse pairs, each characteristic of a muon stopping and decaying within the target region. Reduction of the raw data consisted of subtracting the effect of the chance rate, and then determining the "least squares straight line" for the log of the remaining data. An analysis of the data between 350 nanoseconds and 8.9 microseconds yielded a mean muon lifetime in mineral oil of:

$$\tau = 2.13 \pm 0.05 \text{ microseconds.}$$

This compares favorably with the predicted value of 2.11 microseconds reported by Reines.²⁷ The primary source of error was that due to an approximate 40 nanosecond uncertainty in the time base. Plots of the raw and corrected lifetime data appear in Figure 28.

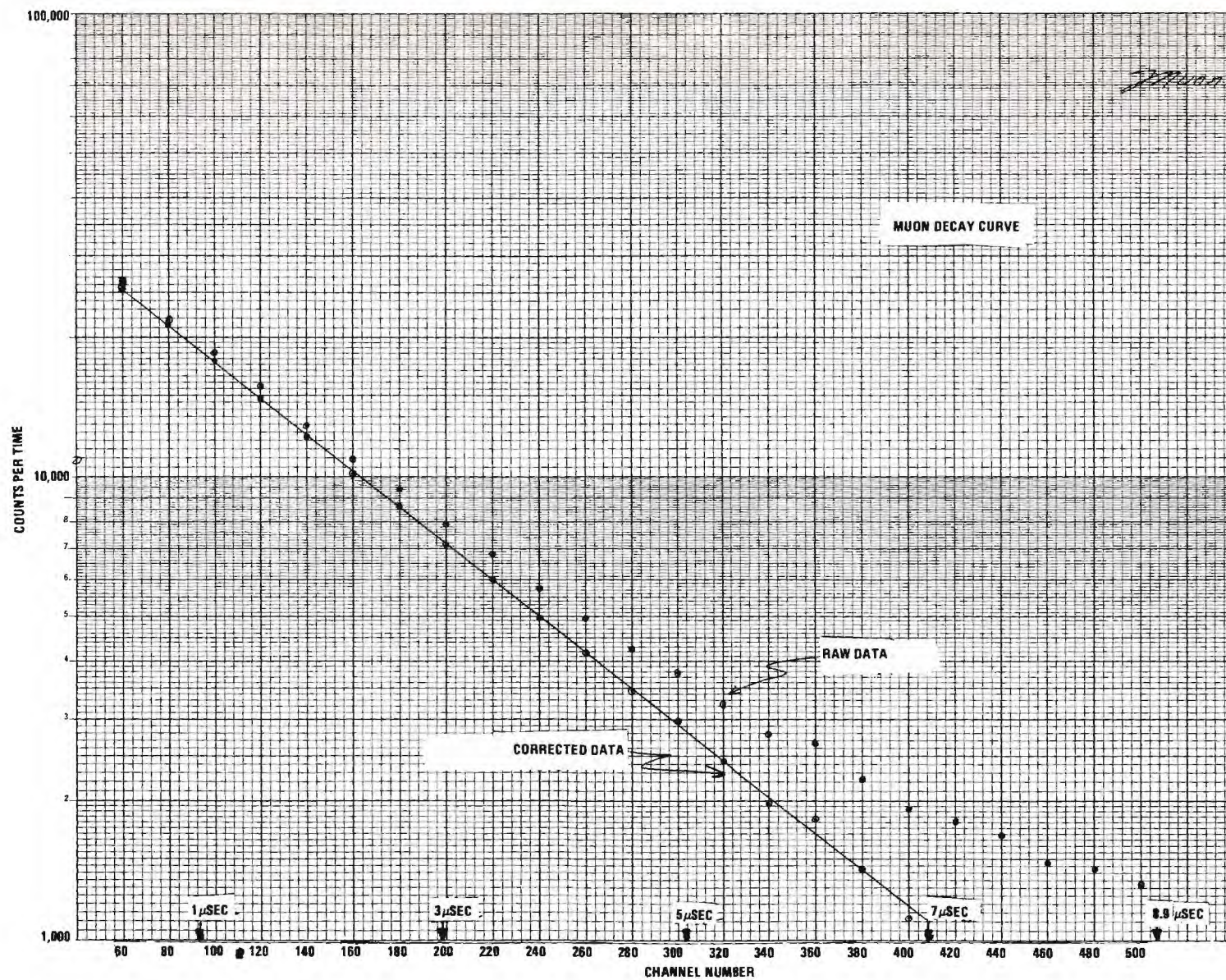


Figure 28. Muon life time curve before and after correction for background.

CHAPTER III

COLLECTION OF DATA

The design, construction, and checkout of the facility satisfied the first objective of this program. The second objective was to determine if an anomaly exists in the rate of production of low energy muons by neutral components of the cosmic radiation. The signature for such an event consists of the production of an energetic charged particle by an incident neutral cosmic ray, followed by the characteristic decay of a muon. The neutrality of the incident particle was guaranteed by the anticoincidence system and the identity of the muon was established by its characteristic lifetime. A description of the electronic system used to recognize this signature and a summary of the collected data follows.

Electronically an interesting event consisted of a "non-vetoed" pulse pair from the target region whose time separation was characteristic of muon decay. The first pulse of this pair was due to the slowing down of the neutral-produced particle or particles. The second pulse was due to the slowing down of the electron emitted by the muon decay. A veto was generated if either pulse of this pair was in time coincidence with an event in the anticoincidence system. The electronic logic shown in Figure 29 was used to obtain the desired data.

Pulse pairs occurring in cells A and/or C, when not accompanied by an output from the anticoincidence system, were used to start and

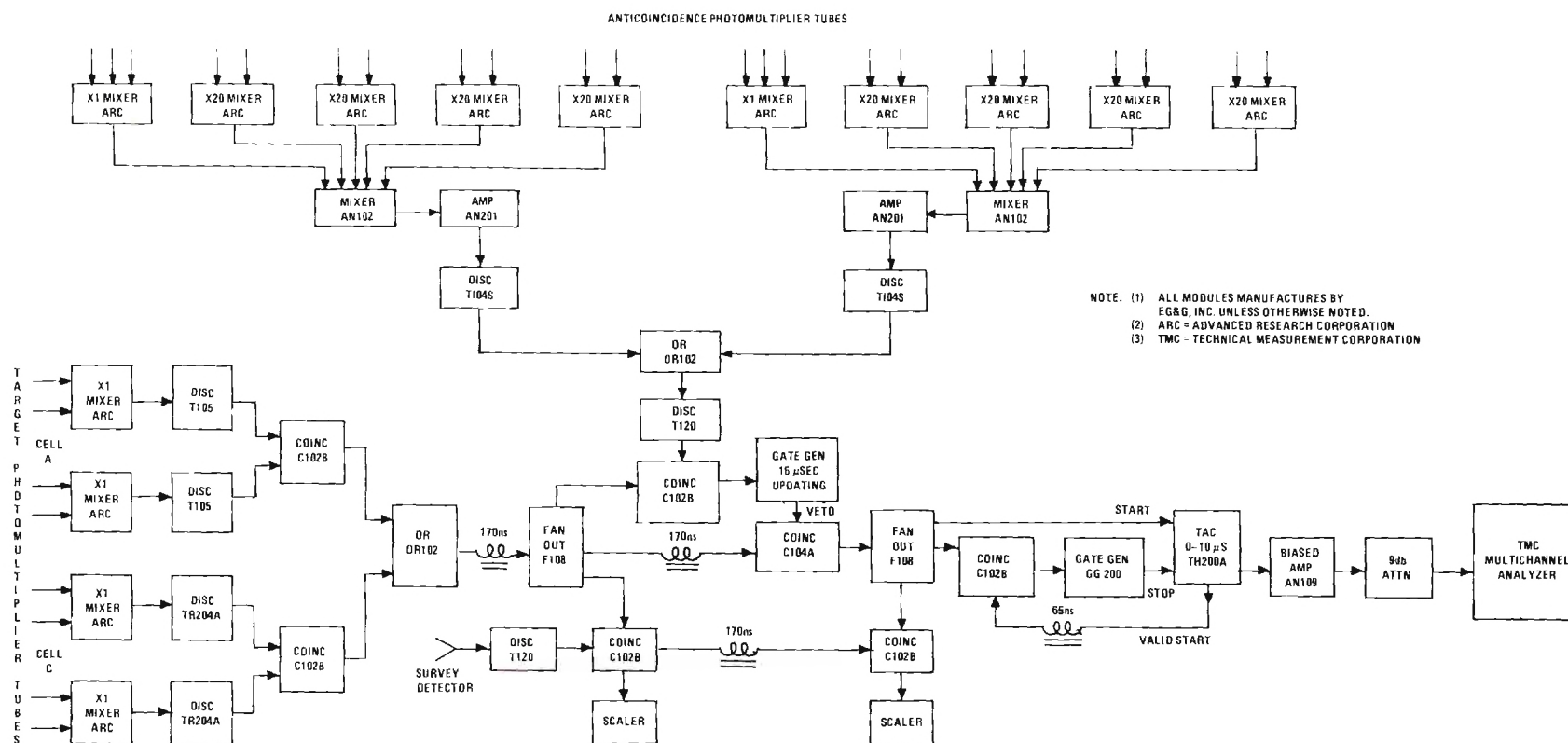


Figure 29. System logic for collection of neutral-particle-induced data.

stop a time-to-amplitude converter (TAC). The output of the TAC, a signal whose amplitude is proportional to the time separation of the inputs, was fed to a multichannel analyzer for pulse height analysis and subsequent storage of the information. The stored information was a histogram giving the frequency of occurrence of interesting events as a function of their pulse pair separation. These data were designed to provide sufficient information to verify the presence of the muon in the process and to establish a rate of occurrence for the event.

The two largest cells were each viewed by four nine-inch photomultiplier tubes, two at each end of each cell. The outputs from these pairs of tubes were linearly summed and presented to discriminators for amplitude analysis. The threshold of each discriminator was set at 10.5 MeV referenced to an event in the center of the target.

As reported by O'Sullivan¹⁵ it is possible for photomultiplier tube afterpulsing to artificially generate the μ -e decay signature. For that reason the two discriminator outputs from each target cell were operated in coincidence. This had the disadvantage of degrading the system's uniformity of response somewhat but was felt necessary to guarantee the validity of the data.

The veto pulse width from the anticoincidence system was set at 16 microseconds, the equivalent of approximately 10 muon half-lives. This was done to eliminate the possibility of a μ -e decay electron becoming the first pulse of an interesting event.

Due to the high count rate of the anticoincidence system (130,000 cps) and the necessity of a wide veto pulse width, the anticoincidence

output was gated by the output from the target region. This minimized system dead time without sacrificing the anticoincidence system's effectiveness. The neutral-particle-induced data were collected with a system dead time of approximately 17 percent.

The collection of neutral-particle-induced data started August 19, 1971, and terminated November 27, 1971. A total of 1,802.63 hours of data collection yielded 5065 events for an average raw data rate of 2.81 events/hour. With the exception of equipment failure and acts of God (lightning struck the building) data were collected approximately 22 hours a day, seven days a week. Daily performance monitoring of the equipment required approximately two hours each day.

The collected data were stored in 512 channels of a TMC multi-channel pulse height analyzer which had been calibrated in microseconds. Initially the data were outputted daily to paper and punched tape, but as confidence in the system increased the interval between readouts was shifted to three days. A total of 32 data tapes resulted, each capable of being individually corrected for system drift. A summary of the data appears in Table 3.

Table 3. Summary of Data Collected August 19 to November 27, 1971

Total Run Time	1,802.63 Hours
Total Number of	
Raw Events	5065
Average Event Rate	2.81 Hours ⁻¹
System Live Time	82.8 percent
Target Threshold	10.5 MeV*

* Referenced to center of target cell.

A detailed program of performance monitoring insured that the detector performed normally during the three-month data run. The following quantities were monitored on a regular basis: high voltage to each photomultiplier tube, low voltage to ARC built mixers, NIM voltages, count rate of each photomultiplier tube, count rate from each end of each module, total anticoincidence system count rate, cell A coincidence rate, cell C coincidence rate, $A + C$ rate, percent dead time of system, and TAC start rate. Initially these checks were performed daily but as confidence in the system increased the interval between checks increased to three days. Several times during the run the anticoincidence system was turned off and the detector was allowed to collect normal muon decay data. These data were used as an additional check on the stability of the system.

CHAPTER IV

ANALYSIS OF DATA

The objective of this investigation was to determine if an anomaly exists in the rate of production of muons by neutral components of the cosmic radiation. This involved experimentally determining the rate of production of muons in the detector and comparing this rate with that expected from known sources. Experimental data designed to satisfy this objective were collected and analyzed. The analysis yielded an observed rate for the process and proof that the observed events did involve the μ -e decay. The significance of these results will be discussed in Chapter V.

The analysis of the data was divided into three parts: (1) a verification that the observed events involved muon decay, (2) a determination, from experimental data, of the muon production rate in the target by incident neutral particles, and (3) a determination of the expected rate of production of muons in the target by the indirect π - μ process initiated by incident neutrons.

Analysis of Lifetime

The raw data collected during the neutral particle run and used to establish an event rate for the process consisted of pulse pairs supposedly generated by μ -e or π - μ -e decay events. As a check on the validity of this assumption the pulse pair data were analyzed for a meaningful half-life.

The raw lifetime data consisting of 32 printed tapes were first individually corrected for time drift in the electronic system and then summed to yield the histogram shown in Figure 30. Each bin of the histogram is approximately 191 nanoseconds wide. From performance monitoring data the time drift of the system during the three-month data collection period was determined to be less than 40 nanoseconds.

The determination of a lifetime from the corrected data involved making the assumption that the data consisted of muon decay events superimposed on a constant background. That is, it was assumed that the data could be fitted by an expression of the form

$$N(t) = N_0 e^{-\lambda t} + B, \quad (9)$$

where N_0 represents the number of observed muon decays occurring within a time Δt of $t = 0$, and $N(t)$ represents the total number of observed events occurring within a time Δt of t . The constant background rate was attributed to the chance delayed coincidence rate of the target region.

A simple least squares fit of equation 9 to the corrected lifetime data would yield values for N_0 , λ , and B by minimizing the quantity

$$F = \sum_i [N_i - (N_0 e^{-\lambda t} + B)]^2. \quad (10)$$

The assumption implicit in this fit is that the errors associated with the N_i 's are approximately equal. Considering the range of the statistical errors associated with the N_i 's in the present data, it was concluded that the simple least squares fit was inappropriate for the present analysis. A more meaningful fit to the data can be achieved by using a fitting technique that takes into account the probable errors associated with each

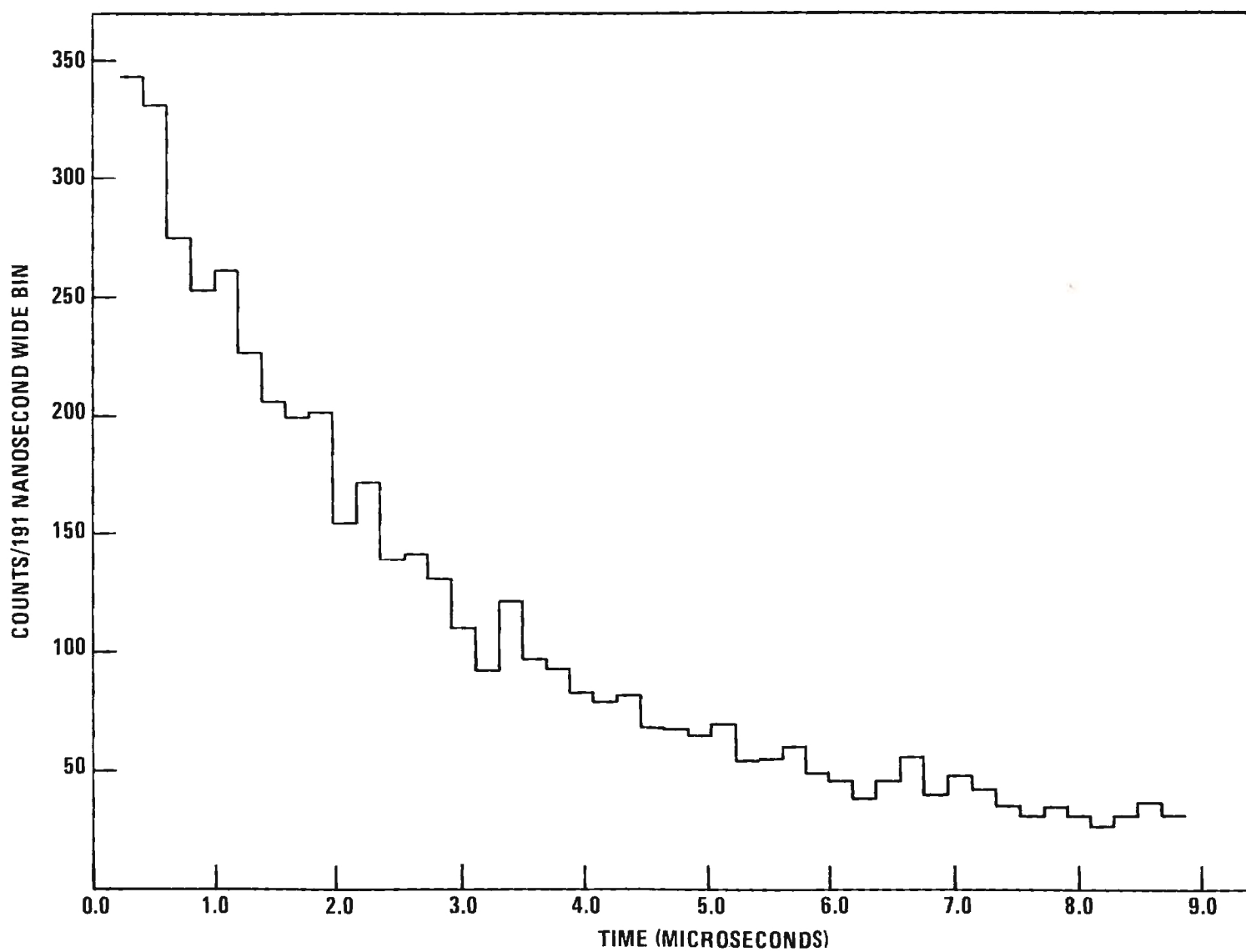


Figure 30. Raw lifetime data from neutral particle induced events.

data point.

The weighted least squares fit minimizes the sum of the squares of the differences between the experimental data and the fitting curve, but in such a manner as to give appropriate weight to each data point according to its probable error. A fit of the corrected lifetime data was achieved by minimizing the following quantity

$$\chi^2 = \sum_i \frac{[N_i - (N_o e^{-\lambda t} + B)]^2}{\sigma_i^2}, \quad (11)$$

where each squared difference is weighted by σ_i^2 , the variance associated with N_i . That is,

$$\sigma_i^2 = N_i. \quad (12)$$

The weighted least squares technique was applied to the corrected lifetime data between 256 nanoseconds and 8.855 microseconds. For the purpose of this analysis this interval was divided into 45 bins each approximately 191 nanoseconds wide. The results of the fit yielded a decay probability of

$$\lambda = 0.466 \pm 0.017 \mu\text{sec}^{-1}. \quad (13)$$

This corresponds to a mean lifetime of 2.15 ± 0.09 microseconds, in good agreement with that expected for the muon in mineral oil.²⁷ The primary source of error was that due to an approximate 40 nanosecond uncertainty in the time base. A plot of the raw data after subtraction of background and the resulting fit to these data appears in Figure 31.

In addition to the lifetime check, the above fit also yielded

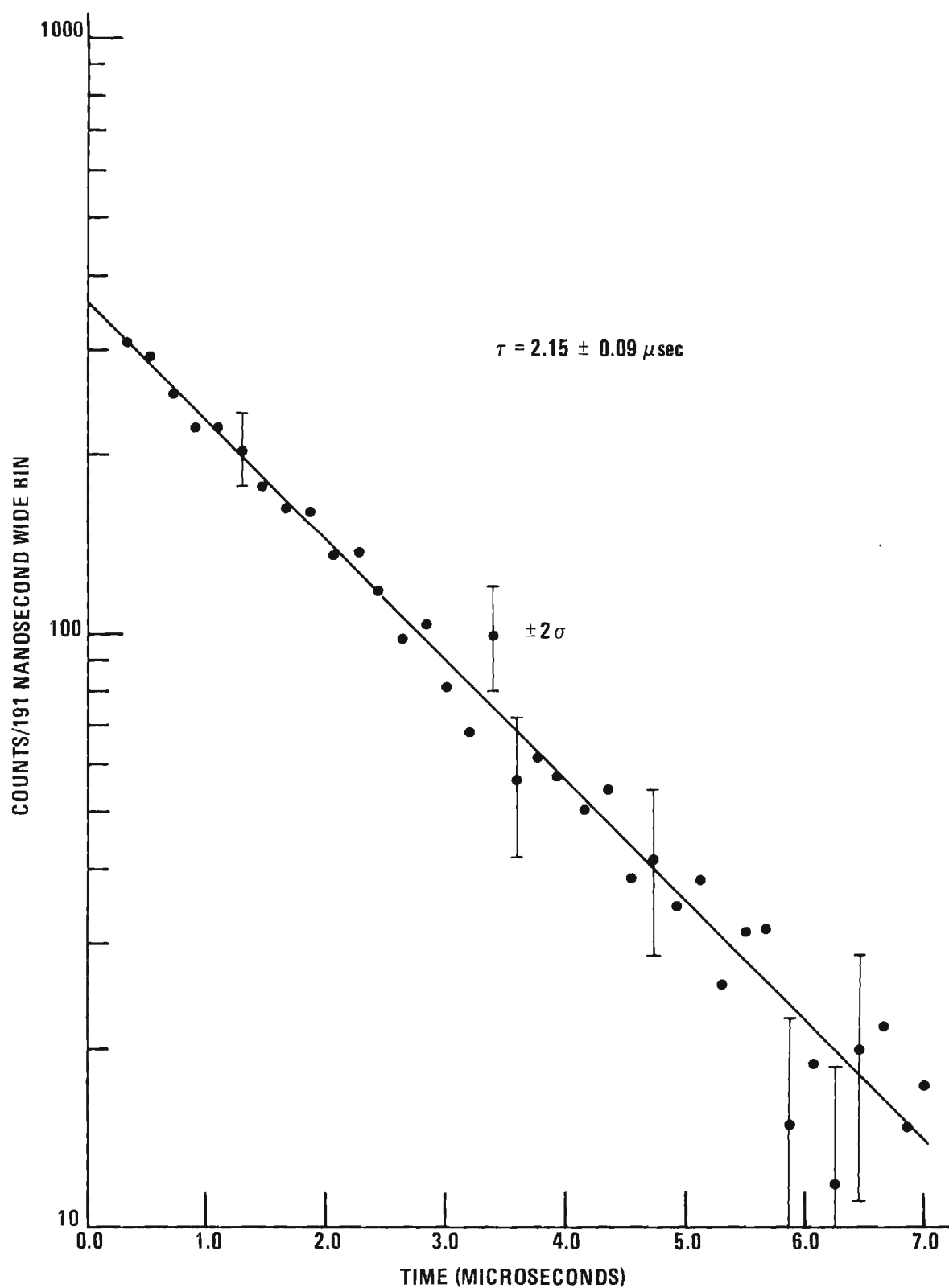


Figure 31. Muon lifetime from neutral-particle-induced data.

the background rate in the target due to uncorrelated pulse pairs. This is the rate due to random non-vetoed events starting and stopping the time-to-amplitude converter. Such events are indistinguishable from true neutral-particle-produced muon events, and thus the effect of this background on the data must be treated in a statistical manner.

Based on the above least squares fit it was determined that approximately 1,505 of the 5,065 events between 256 nanoseconds and 8.855 microseconds were due to non-correlated pulse pairs. This represents approximately 30 percent of the raw data and yields a chance event rate in the target of

$$D_c = 0.83 \pm 0.02 \text{ events/hour} . \quad (14)$$

The error represents the standard deviation associated with the 1505 events.

Observed Experimental Rate Due to Incident Neutral Particles

A determination of the rate of production of muons by incident neutral particles required knowing the rates due to all sources of false events. Although the signature used to identify an interesting event was rather unique and thus allowed the electronic logic to be very selective, it did allow for two major sources of false events. As discussed above, the chance rate background accounted for approximately 30 percent of the raw data. It will be shown below that the rate due to muons leaking through the anticoincidence system was also non-negligible.

If the anticoincidence system surrounding the target were 100 percent effective at registering the passage of muons, the only major

source of background would be that due to the chance rate. As discussed previously the anticoincidence system charged particle rejection ratio is approximately 980:1, making this detector 99.89 percent effective at rejecting incident charged particles. This rejection ratio, when applied to the rate with which incident muons stop and decay in the target, yields that portion of the "neutral" rate due to leaking muons.

A determination of the muon decay rate in the target region was made under the very special condition that the anticoincidence system was armed immediately after the entrance of a charged particle. This limited the observed muon decay rate to those muons whose decay electrons did not violate the anticoincidence system. With the exception of the lack of an anticoincidence veto on the first pulse, these data were collected under conditions identical to those used to collect the neutral-particle-induced data. The muon decay rate under these conditions was 1137 events/hour.

Applying the anticoincidence rejection ratio to this rate yielded the muon leak rate expected under neutral particle collection conditions. A value of

$$D_L = 1.16 \pm 0.14 \text{ events/hour} \quad (15)$$

was obtained. The error is the product of that associated with the uncertainty in the charged particle rejection ratio and that associated with the statistical uncertainty in the muon decay rate.

As discussed previously the observed raw data rate consisted of the true neutral-particle-induced rate plus several sources of background. That is:

$$D_o = D_N + D_L + D_c \quad (16)$$

where

D_o is the observed rate in the target;

D_N is the contribution to the observed rate due to neutral-particle-induced events;

D_L is the contribution to the observed rate due to leaking muons which stop and decay in the target; and

D_c is the contribution to the observed rate due to chance coincidences in the target.

Knowing the values for D_o , D_L , and D_c the observed rate due to neutral-particle-induced events was determined to be

$$D_N = 0.82 \pm 0.15 \text{ events/hour.} \quad (17)$$

A summary of the individual rates and their errors appears in Table 4.

Table 4. Composition of Raw Data

Source	Rate
Total Rate (D_o)	= 2.81 ± 0.04 events/hour
Muon Leak Rate (D_L)	= 1.16 ± 0.14 events/hour
Chance Coincidence Rate (D_c)	= 0.83 ± 0.02 events/hour
$D_N = D_o - D_L - D_c$	= 0.82 ± 0.15 events/hour

Determination of Expected Muon Decay Rate From Incident Neutrons

In the preceding section an observed event rate was established for the production of muons by neutral components of the cosmic radiation. Before the possibility of an anomaly in this rate can be discussed, the expected event rate in the detector must be established. The expected rate is that due to incident neutrons initiating the $\pi-\mu-e$ decay chain within the target volume. This rate was calculated using available data on the cosmic ray neutron energy spectrum and the pertinent pion production cross sections.

The Neutron Energy Spectrum

The cosmic ray neutron energy spectrum was determined by Hess, et al.²⁸ in 1959 and by Hughes and Marsden²⁹ in 1966. The Hess determination at energies above about 10 MeV was based on data from large bismuth fission chambers and from neutron-induced stars in photographic emulsions. The spectrum is given for energies to 10 GeV, but in reality is based on observations at sea level for energies only up to about 500 MeV. The extrapolation to higher energies was made by assuming the spectrum at sea level to have the same shape as the primary proton spectrum at the top of the atmosphere (Messel³²). This shape was taken from the proton spectrum of Singer, 1958.³⁰

The Hughes and Marsden neutron energy spectrum was determined from data taken with a standard IGY neutron monitor operated in coincidence with a magnetic spectrograph. The rate of interaction and the resulting multiplicity of evaporation neutrons was determined for each of the charged components of the cosmic radiation. This was compared with the total rate and multiplicity in the detector and the difference

was attributed to the incident neutron flux. Hughes and Marsden assumed the shape of the sea level neutron spectrum at higher energies to be the same as that of the sea level proton flux. Their data were fitted to the sea level proton spectrum of Brooke and Wolfendale, 1964.³¹ A plot of the Hess spectrum and the Hughes and Marsden spectrum is shown in Figure 32.

The Hughes and Marsden neutron spectrum was used in the present analysis. This decision was based on the following observations:

1. The Hughes and Marsden experiment was sensitive to neutron energies from 50 MeV to in excess of those required in the present analysis.
2. The Hess experiment was sensitive to neutron energies up to approximately 500 MeV; one half that required in the present analysis.
3. The high energy tail of the Hughes and Marsden neutron spectrum approaches that of the presently accepted proton spectrum. The Hess spectrum does not.

The data for the above neutron spectra were collected at or normalized to 44°N. latitude. These data must be corrected for the latitude effect associated with the earth's magnetic field before use in the present analysis. The following correction was indicated from the work of Simpson³³:

$$\frac{\text{Neutron Intensity at } 34^{\circ}\text{N.}}{\text{Neutron Intensity at } 44^{\circ}\text{N.}} = 0.70 \pm 0.02 .$$

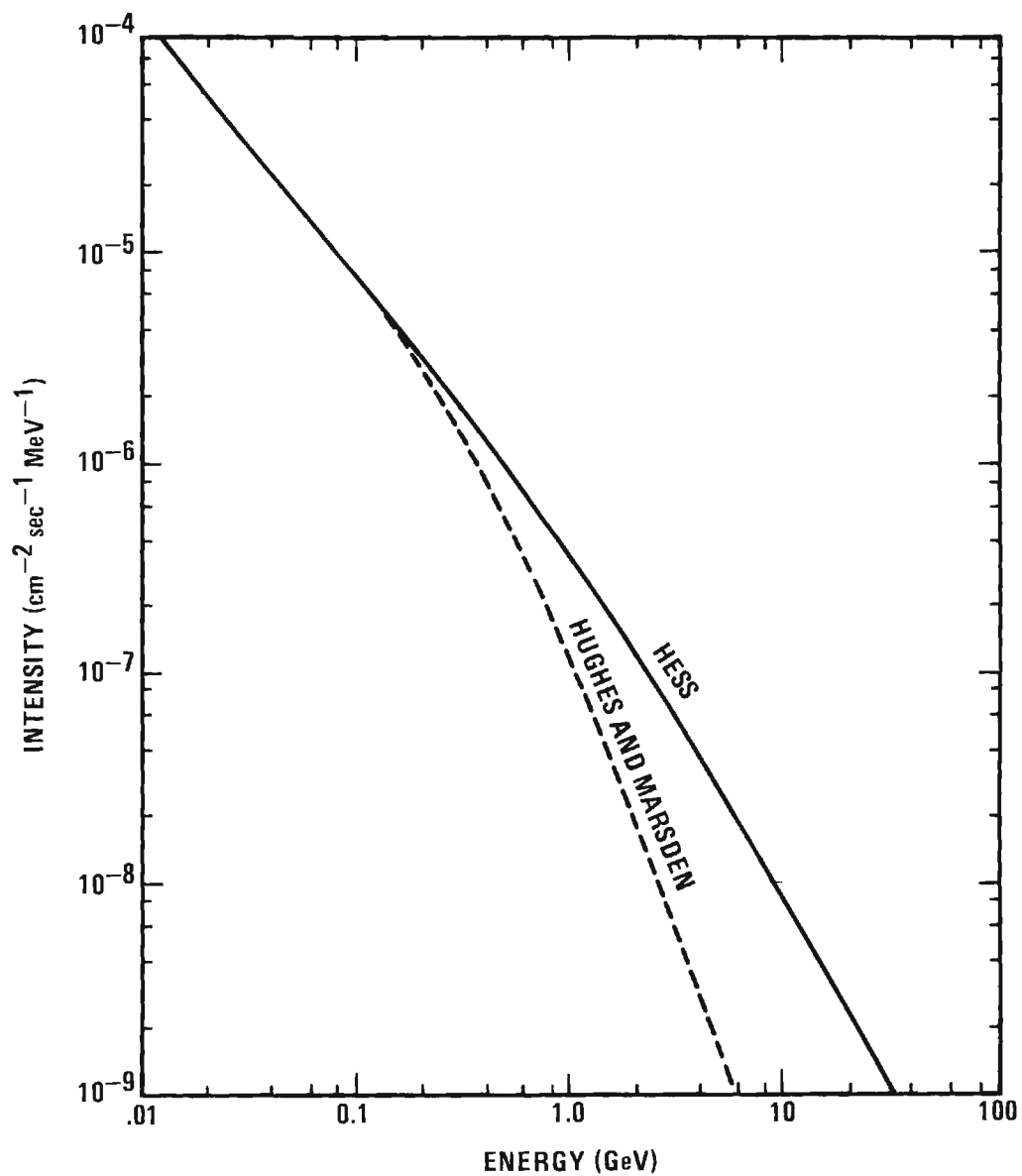


Figure 32. The differential neutron energy spectrum at sea level as given by Hess and modified by Hughes and Marsden. After Hughes and Marsden.²⁹

Pion Production Cross Sections

The source of neutron produced pions in the target region of the detector are the interactions



and



It was desired to calculate the number of pions produced per unit pion energy per unit solid angle per nucleus. Unfortunately complete $d^2\sigma/dE_{\pi}d\Omega$ cross sections for these reactions are available only at 600 MeV (Oganesyan³⁴). However, these data do indicate that the contribution due to neutron interactions with hydrogen is relatively unimportant in the present experiment.

The problem associated with the lack of detailed experimental information about the $n + C^{12} \rightarrow \pi^{\pm} + \dots$ processes was dealt with by reducing it to several smaller problems. In particular, information was independently gathered on (1) the differential cross section $d\sigma/dE_n$ for pion production as a function of incident neutron energy between 0.1 and 1.1 GeV, and (2) the energy and angular distribution of emitted pions from these processes.

Information used to construct differential cross section curves ($d\sigma/dE_n$ versus E_n) for pion production by neutrons was obtained from several sources. The only experimental $n + C^{12} \rightarrow \pi^{\pm} + \dots$ data are those of Oganesyan³⁴ at an incident neutron energy of 600 ± 100 MeV. Data points at 340 MeV were determined by using the $p + C^{12} \rightarrow \pi^{\pm} + \dots$ data of

Dudziak³⁵ and assuming that the cross sections for $p + C^{12} \rightarrow \pi^{\pm} + \dots$ can be equated with the cross sections for $n + C^{12} \rightarrow \pi^{\pm} + \dots$. This assumption was based on the results of $\{ \begin{smallmatrix} n \\ p \end{smallmatrix} \} + C^{12} \rightarrow \pi^{\pm} + \dots$ experiments performed by Bradner, et al.³⁶ in 1950. Likewise a π^{-} data point at a neutron energy of 660 MeV was determined from the $p + C^{12} \rightarrow \pi^{+} + \dots$ data of Meshkovskii.³⁷

The remaining information used in the determination was taken from the results of the intranuclear cascade calculations of Bertini.^{38,39} Differential cross sections were determined at 500, 1000, and 2000 MeV from his calculations of neutrons interacting with oxygen-16. The $A^{2/3}$ rule which has been shown to be accurate for the present range of nuclear masses^{40,41} was used to determine the carbon cross sections from those of oxygen.

The resulting differential cross sections for pion production from neutrons onto C^{12} as a function of incident neutron energy are shown in Figure 33. The curves through the data points were drawn to guide the eye and were also used for interpolation between data points. In the process of collecting the data used in this determination numerous "bits" of $n + C^{12} \rightarrow \pi^{\pm} + \dots$ and $p + C^{12} \rightarrow \pi^{\pm} + \dots$ cross section data were tabulated. This information appears in Appendix B.

To determine the expected muon production rate from the $n + C^{12} \rightarrow \pi^{\pm} + \dots$ processes requires not only a knowledge of the neutron energy dependence of the production cross sections, but also a knowledge of the energy and angular distributions of the emitted pions. The $p + Be \rightarrow \pi^{\pm} + \dots$ experiments of Yuan and Lindenbaum⁴² at 1.0 and 2.3 GeV, followed by similar experiments with carbon at 660 MeV by Meshcheriakov,

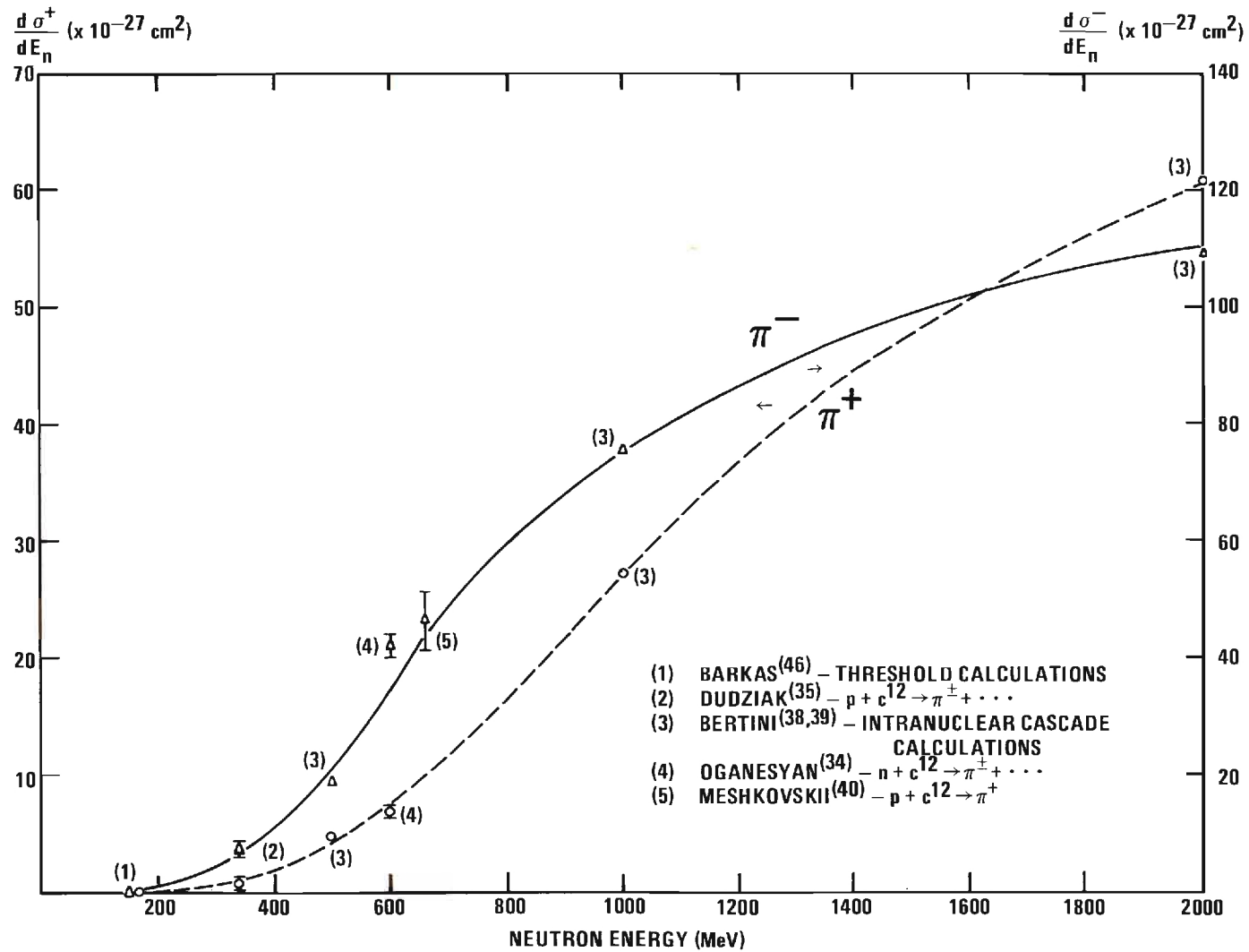


Figure 33. Differential cross sections for $n + {}^{12}\text{C} \rightarrow \pi^{\pm} + \dots$.

et al.,⁴³ and Meshkovskii, et al.,³⁷ offer strong evidence that in these processes the energy of the emitted pion in the center-of-mass system of the colliding nucleons is independent of the incident nucleon energy and the angle of pion emission. In all four experiments a strong resonance is reported in the pion energy distribution near 100 MeV. As pointed out by Yuan and Lindenbaum⁴² these data indicate that the predominate source of pions is through the excitation of one of the colliding nucleons to an excited state ($P_{3/2,3/2}$) from which the nucleon returns to the ground state by pion emission.

The center-of-mass pion energy distributions of Meshcheriakov, et al.⁴³ were used in the present analysis. These curves are shown in Figure 34. The conversion of these distributions to the lab system will be discussed later.

For the purposes of this analysis the angular distribution of the emitted pions in the center-of-mass system of the colliding nucleons was assumed to be independent of the incident nucleon energy and equal to that distribution measured by Oganessian³⁴ at a neutron energy of 600 MeV. These distributions are shown in Figure 35.

The conversion of the pion energy and angular distributions to the lab system was accomplished via the transformations derived by Hopper⁴⁴ and listed below:

$$\tan \theta_{\pi} = \frac{\beta_{\pi}^* \sin \theta_{\pi}^*}{\beta_{\pi}^* \cos \theta_{\pi}^* + \beta_c} \sqrt{1 - \beta_c^2} \quad (20)$$

and

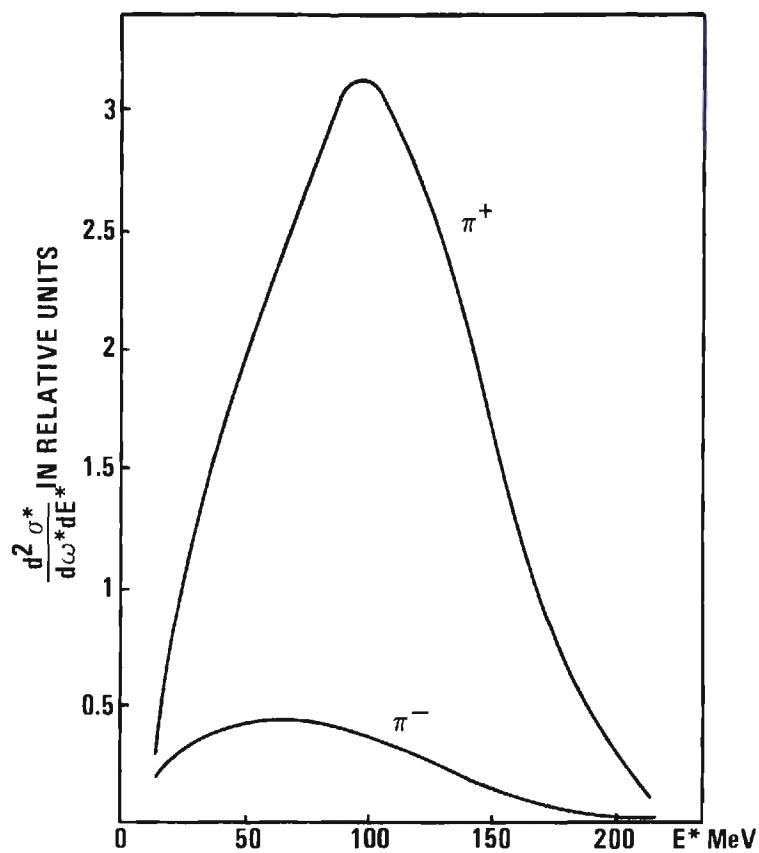


Figure 34. Pion energy distribution in center-of-mass system of colliding nucleons. Protons onto carbon target.

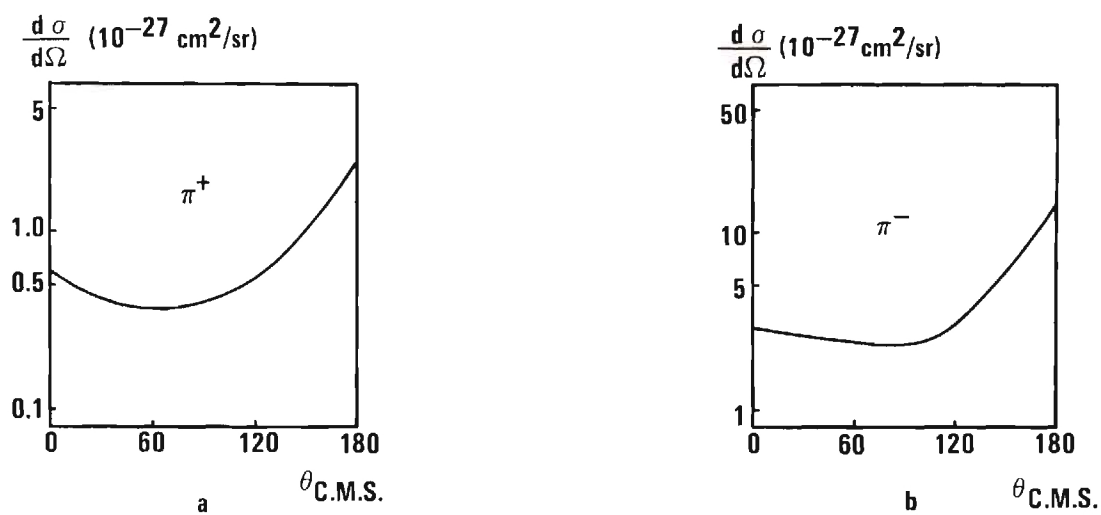


Figure 35. Pion angular distributions in center-of-mass system of colliding nucleons. Neutrons onto carbon target.

$$u_{\pi} = \frac{u_{\pi}^* + \beta_c \beta_{\pi}^* \cos \theta_{\pi} u_{\pi}^*}{\sqrt{1 - \beta_c^2}}, \quad (21)$$

where the asterick (*) implies a quantity measured in the center-of-mass coordinate system. The characters used in the above equations are defined as follows:

θ_{π} is the angle of pion emission with respect to the incident nucleon;

u_{π} is the total energy of the pion;

β_{π}^* is the velocity of the pion in the center-of-mass coordinate system; and

β_c is the velocity of the center-of-mass with respect to the lab system.

Pion Production in Target

The cosmic ray neutron flux at the detector site and the pertinent pion production cross sections for the processes $n + C^{12} \rightarrow \pi^{\pm} + \dots$ have been determined. This information will be used to calculate the pion production rate in the target region of the detector, and will, with application of pertinent detection efficiencies, yield an expected neutral-particle-produced muon rate due to incident neutrons.

Figure 36 shows the flux-cross section product for the production of pions of both signs by cosmic ray neutrons incident on carbon nuclei. The integral of these products from 0.1 to 1.1 GeV yields

$$\sigma_{\pi}^{+} = 1.15 \times 10^{-30} \text{ pions/second} \cdot \text{carbon nucleus} \quad (22)$$

for the production of positive pions, and

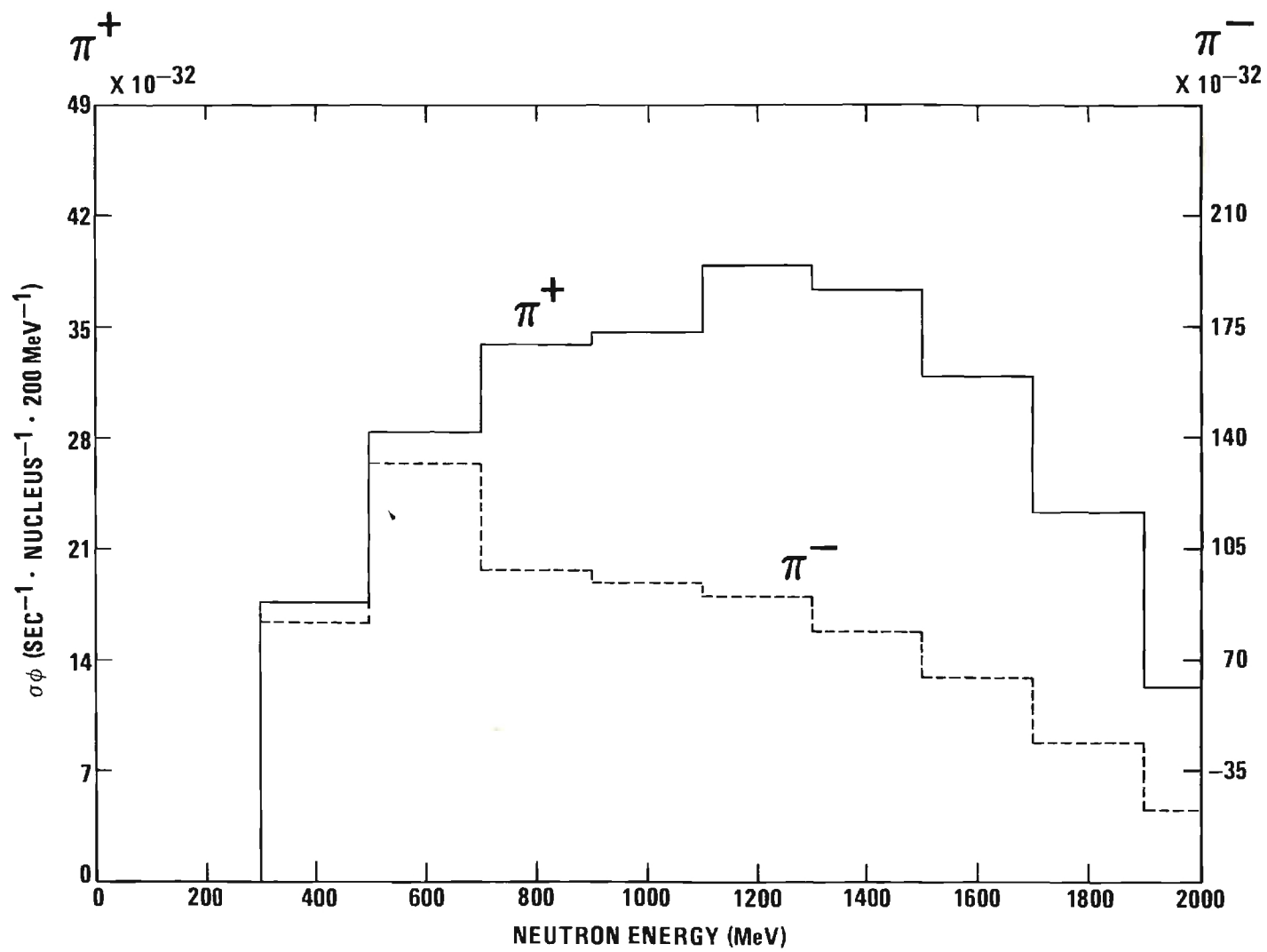


Figure 36. Flux - cross section product for $n + \text{C} \rightarrow \pi^\pm + \dots$ with cosmic ray neutron.

$$\sigma^{-}\Phi = 4.27 \times 10^{-30} \text{ pions/second} \cdot \text{carbon nucleus} \quad (23)$$

for the production of negative pions.

In the case of positive pion production the vast majority of the pions comes to rest and then decays to muons. The case of the negative pion is different since any negative pion which comes to rest will, with very high probability, undergo nuclear capture with no resulting muon. From the calculations of Shelby¹⁵ approximately two percent of the negative pions do decay in flight. Thus an effective flux-cross section product for the pi-minus event is $0.02(\sigma^{-}\Phi)$, or

$$\sigma^{-}\Phi_{\text{eff}} = 0.085 \times 10^{-30} \text{ pions/second} \cdot \text{carbon nucleus} . \quad (24)$$

A total flux-cross section product for pion production can be obtained by adding the individual products:

$$\sigma \Phi_{\text{eff}} = \sigma^{+}\Phi + \sigma^{-}\Phi_{\text{eff}} \quad (25a)$$

$$= (1.23 \pm 0.26) \times 10^{-30} \text{ pions/second} \cdot \text{carbon nucleus} . \quad (25b)$$

The error includes an eight percent uncertainty in the incident neutron flux²⁹ and an estimated 13 percent uncertainty in the pion production cross sections.

If it were not for the attenuation of the incident neutron beam by the overburden and the self-shielding characteristics of the detector, the pion production rate in the target would be equal to the above flux-cross section product multiplied by the number of carbon nuclei in the target. After measurements of Hess²⁸ the absorption length for the incident neutrons was taken to be 150 gms/cm^2 .

Assuming a vertical neutron flux, a carbon density of 3.77×10^{22}

nuclei/cm³^{20,45} and a neutron absorption length of 150 gms/cm², the pion production rate in the target was determined to be 92.1×10^{-4} events/second or (33.1 ± 8.6) per hour. A summary of the information used to make this determination appears in Table 5.

Table 5. Summary of Data Used To Determine Pion Production in Target Volume

Parameter	Value
$\sigma^+_{\Phi} (0.1 - 1.1 \text{ GeV})$	$= (1.15 \pm 0.24) \times 10^{-30} \text{ pions/second-carbon nucleus}$
$\sigma^+_{\Phi} (0.1 - 1.1 \text{ GeV})$	$= (4.27 \pm 0.89) \times 10^{-30} \text{ pions/second-carbon nucleus}$
$\sigma^-_{\Phi \text{ eff}} (0.1 - 1.1 \text{ GeV})$	$= (0.0855 \pm 0.018 \times 10^{-30} \text{ pions/second-carbon nucleus}$
$\sigma^+_{\Phi} + \sigma^-_{\Phi \text{ eff}} (0.1 - 1.1 \text{ GeV})$	$= (1.23 \pm 0.26) \times 10^{-30} \text{ pions/second-carbon nucleus}$
carbon nuclei/cm ³	$= 3.77 \times 10^{22} \text{ carbon/cm}^3$
Pion production rate in target	$= (33.1 \pm 8.6) \text{ pions/hour}$

Detection Efficiency for Pion Pulse

An absolute pion production rate by cosmic ray neutrons has been established. It is desired to know what fraction of this rate was observed during the collection of the neutral-particle-induced muon

data. This observed rate will be equal to the absolute pion production rate multiplied by the detection efficiency for the pion pulse multiplied by the detection efficiency for the μ -e decay pulse.

The efficiency for the detection of the pion pulse was determined with the aid of a computer model of the detector. A FORTRAN program modeling pertinent aspects of the incident neutron flux, the pion production cross sections, the pion energy and angular distributions, and the detector's geometry was written for the Georgia Tech Univac 1108. Using Monte Carlo techniques it was possible to integrate the incident neutron flux over the detector volume, simulating pions whose energy, angle of emission and charge distributions corresponded to those of available experimental data.

To insure statistically meaningful results 100,000 pion production histories were computed and tabulated. These histories were used to determine the pion detection efficiency by observing the fraction of events giving a satisfactory signature. To be considered satisfactory an event had to be above threshold and not violate the anti-coincidence system.

Due to the uncertainties in the target and anticoincidence thresholds the Monte Carlo program was run using five different combinations of these parameters. Based on the results of these computations a pion detection efficiency of $\epsilon_1 = 0.21 \pm 0.01$ was established. A summary of the results of these five computations appears in Table 6. The error is that associated with the uncertainty in the threshold energy of the target discriminators (see Figure 18).

Table 6. Pion Detection Efficiency As A Function of Target And Anticoincidence Threshold Energy

Target Threshold* (MeV)	Anticoincidence Threshold (MeV)	Detection Efficiency (percent)
8.32	10.0	20.3
8.32	15.0	20.7
8.32	20.0	21.1
12.00	15.0	17.6
8.32	15.0	20.7
5.00	15.0	23.7

* Referenced to scintillator-light pipe interface.

Determination of the μ -e Decay Electron Detection Efficiency

The efficiency for the detection of the emitted electron in muon decay can be considered as the product of several other efficiencies. In particular, if e_2 is the total detection efficiency, it can be represented as

$$e_2 = f_L f_1 F(f_2, f_3)$$

where

f_L is the fractional life-time of the detector,

f_1 is the fraction of muon decays falling within the specified time window,

f_2 is the fraction of muon decay electrons above threshold,

f_3 is the fraction of muon decay electrons not violating the

anticoincidence system, and

$F(f_2, f_3)$ is the fraction of muon decay electrons above threshold but not violating the anticoincidence system.

The methods used to determine each of these quantities will be summarized.

The live-time of an electronic system is that time, usually expressed as a percent, during which the system is sensitive to input. There are many possible sources for a loss of system live-time. A significant loss can occur as the result of the finite time required to process and store information. Some logic circuits have an inherent dead-time during which re-initialization of circuits must take place. The primary source of lost live-time in the present experiment was the anticoincidence system. The system's high count rate and the long veto pulse width combined to yield a non-negligible dead-time for the experiment.

The live-time of the system used to collect neutral-particle-induced muon data was determined by introducing artificially generated signals into a target discriminator of the neutral particle logic and noting what fraction of the inputs was accepted for analysis. A system live-time of (82.8 ± 3.3) percent was established.

Recall that the signature of an interesting neutral-particle-induced event consisted of the production of a charged particle by an incident neutral cosmic ray, followed by the characteristic decay of a muon. The search for the muon decay pulse was started 256 nanoseconds after the neutral-particle-induced pulse and lasted for 8.6 microseconds.

Assuming a muon lifetime of 2.15 microseconds it was determined that this time window accepted 87.2 percent of the muon decays.

The fraction of muon decays above threshold, but not violating the anticoincidence system was determined with the aid of a FORTRAN computer program written for the Georgia Tech Univac 1108. Using Monte Carlo techniques, μ -e decay electrons were generated with the proper energy and angular distribution throughout the target volume of the detector. The history of each electron was examined to determine if it represented a satisfactory decay event. To be satisfactory an event had to be above the energy threshold with respect to the photomultiplier tubes at each end of the target cell, and must not have violated the anticoincidence system. The ratio of the number of satisfactory events to the number of trials was used as a measure of the quantity $F(f_2, f_3)$. To insure statistically meaningful results the program tabulated 525,000 histories.

Due to a large uncertainty in the anticoincidence threshold energy the above program was run for five different threshold energies. From the results of these runs, which are summarized in Table 7, the quantity $F(f_2, f_3)$ was determined to be 0.29 ± 0.02 .

From the above individual efficiencies the μ -e detection efficiency was determined to be

$$e_2 = 0.19 \pm 0.03.$$

A summary of the individual efficiencies and the product efficiency appear in Table 8.

Table 7. μ -e Decay Electron Detection Efficiency as a Function of Anticoincidence Threshold

Anticoincidence Threshold Energy (MeV)	μ -e Decay Detection Efficiency (Percent)
10.0	28.86
15.0	31.04
20.0	32.92
25.0	34.46
30.0	35.61

Table 8. Individual and Product Detection Efficiencies for the μ -e Decay Electron

Factor	Efficiency
System live-time (f_2)	0.828 ± 0.033
μ -e Decay Time Window (f_1)	0.872 ± 0.009
Satisfactory Signature ($F(f_2, f_3)$)	0.29 ± 0.02
μ -e Detection Efficiency ($e_2 = f_L f_1 F(f_2, f_3)$)	0.19 ± 0.03

Observed Rate Expected From Neutron Production of Pions

The signature used to collect neutral-particle-induced muon data corresponded to the production of a charged particle by an incident neutral cosmic ray, followed by the characteristic decay of a muon. High energy neutrons can create this signature by producing energetic pions in the target volume. Due to its low energy, the muon in the π - μ decay will not be seen and the μ -e decay then becomes the second pulse of the required signature.

Applying the above determined pion and electron detection efficiencies to the absolute pion rate for the target volume yielded an expected observed event rate due to neutrons of 1.31 ± 0.59 events/hour. The data used to make this determination are summarized in Table 9.

Table 9. Data for Determination of Observed Rate Due to Neutrons

Absolute Pion Production Rate in Target By Neutrons	$= (33.1 \pm 8.6) \text{ events/hour}$
Detection Efficiency for Pion Pulse	$= 0.21 \pm 0.01$
Detection Efficiency for μ -e Decay Electron Pulse	$= 0.19 \pm 0.03$
Observed Rate Expected From Neutrons	$= 1.31 \pm 0.59 \text{ events/hour}$

CHAPTER V

CONCLUSIONS AND RECOMMENDATIONS

During the past ten years experiments performed by others have yielded results that indicate an anomaly in the rate of production of muons by neutral components of the cosmic radiation. Perhaps more exciting is the observation that the event rate fluctuates with sidereal time, and contains a significant peak at approximately 21 hours right ascension. It is worth noting that the inner arm of our galaxy is directly overhead at that time. These results raise the very interesting possibility that the detection of events having a particular signature might yield additional information about the structure and composition of our galaxy.

A versatile cosmic ray facility was designed and constructed to allow continuing studies in the field of muon production by neutral components of the cosmic radiation. This facility and the use of it to study the rate of production of single muons by incident neutral cosmic rays has been described in previous chapters. A summary of the results of this work will be given in two parts: (1) results germane to the construction of the facility, and (2) results germane to the single muon production experiment. Recommendations for future studies will be used to conclude the chapter.

Conclusions

The Facility

An efficient, high flash point, organic liquid scintillator was developed for use in the large-volume cosmic-ray detector. The scintillator consists of heavy mineral oil as primary solvent, naphthalene as secondary solvent, PPO as scintillator and Bis-MSB as wavelength shifter. The results of experimentation indicate that optimum concentrations by weight in mineral oil are: 2.5 percent naphthalene, 0.35 percent PPO, and 0.01 percent Bis-MSB.

The removal of dissolved oxygen from an organic liquid scintillator usually results in a significant improvement in the light output of that liquid. Studies with relatively small samples of the mineral oil base scintillator indicated that an improvement in response of approximately 15 percent could be obtained by bubbling the liquid with helium gas to remove dissolved oxygen. The absolute light output of the deoxygenated scintillator was determined to be 75 to 80 percent of that of Nuclear Enterprise's N.E. 213 liquid scintillator (also deoxygenated).

The decay time of the mineral oil base liquid scintillator was determined to be of the order of 25 nanoseconds, much slower than most organic scintillators.

Prior to the collection of data on neutral-particle-induced muon events, the facility was used to determine the muon lifetime in mineral oil. This determination experimentally verified the predicted muon lifetime in mineral oil and also served as a final check on the system. The obtained value of 2.13 ± 0.05 microseconds is in good agreement with the value of 2.11 microseconds predicted by Reines.²⁷

The Neutral Particle Experiment

Neutral-particle-induced muon lifetime data were collected for 1,802.63 hours at an average raw data rate of 2.81 events/hour. After corrections for background, these data were fitted to a single exponential. A mean lifetime of 2.15 ± 0.09 microseconds was obtained, indicating that the observed events did involve the decay of the muon.

The observed neutral-particle-induced event rate, after correction for the chance rate and for leaking muons, was determined to be 0.82 ± 0.15 events/hour. A predicted event rate due to incident neutrons producing the $\pi-\mu-e$ decay chain within the detector was determined by applying Monte Carlo techniques to available neutron flux and cross section data and pertinent detector parameters. A value of 1.31 ± 0.59 events/hour was predicted.

The available evidence indicates that the sea level cosmic ray neutron intensity is sufficient to account for the observed neutral-particle-induced muon event rate in the detector. Although this is by far the more palatable conclusion, it should be pointed out that the errors in the two rates allow for up to 25 percent of the events to be due to processes other than pion production by incident neutrons. In conclusion, no obvious anomaly in the rate of production of muons by neutral components of the cosmic radiation was observed.

A second problem still exists. Other researchers have reported that the neutral-produced-muon event rate fluctuates in time in such a manner as to suggest the presence of several sources on the celestial sphere. If neutrons are the sole source of events in the detector, and thus responsible for the sidereal dependence of the event rate, the origin

of these neutrons must be explained.

It is unlikely that the sidereal effect is the result of primary cosmic ray neutrons. The short lifetime of the neutron (~ 12 minutes) and the enormous distances to even our nearest celestial neighbors ($\gtrsim 4.2$ light-years) coupled with the observed detector rates would tend to rule out that possibility. A more likely explanation would be that the neutrons are secondary particles created within the earth's atmosphere by high energy primaries, or other secondaries. Any incident primary cosmic ray could initiate such an event, but due to its abundance, the proton would be a likely candidate. Statements of a more definitive nature will have to await the results of further experimentation. Potentially fruitful areas for research include anisotropy studies of the primary cosmic radiation and studies designed to identify the incident neutral particle.

An interesting result of the present work is evidence that the sea level neutron flux as determined by Hughes and Marsden is a closer approximation to the actual flux than that determined by Hess. Calculations employing the Hughes and Marsden spectrum yielded a predicted event rate for the detector in agreement with that observed. Such was not the case with the higher neutron flux of the Hess spectrum.

Recommendations

The dual objective of this work was to design and build a cosmic ray facility to allow continuing studies of muon production by neutral components of the cosmic radiation, and to use this facility to conduct a specific experiment. It is thus natural to divide recommendations and comments into those pertaining to improvements in the facility and those

pertaining to future experimentation with the facility.

In addition to the calibration of the detector and the collection of data on neutral-particle-induced events, the first year of operation of the detector was also used as a time to evaluate the system. As a result of that evaluation, the following changes are suggested:

1. Improve the charged particle rejection of the end anticoincidence detectors. This could be accomplished by replacing the existing detectors with two-inch thick sheets of plastic scintillator. An additional improvement could be gained by mounting the accompanying photomultiplier tubes at the top of the plastic sheets.

2. Replace the liquid scintillator in target cell B by a liquid with a much faster decay time, or possibly replace the entire cell with an equivalent slab of plastic scintillator. The need for a fast detector in the target region will be discussed below.

3. Elevate the entire detector to allow insertion of small survey detectors below the lower anticoincidence system.

A major difficulty associated with determining if an anomaly exists in the rate of production of muons by neutral components of the cosmic radiation results from a lack of knowledge of the incident neutron spectrum and the necessary pion production cross sections. The sea level neutron spectrum has been determined by two different research groups with the result that their distributions differ by a factor of approximately two in the energy range of interest. Furthermore, these distributions must be corrected for a latitude effect which is also not accurately known.

The problem is further compounded by the fact that there is very little cross section information concerning neutron interactions of the type: neutron + nucleus \rightarrow pion $^{\pm}$ + other. For carbon, the target nucleus in the present experiment, complete $d^2\sigma/dE_{\pi}d\Omega$ information is available only at a neutron energy of 660 MeV.

A brute force approach to a solution of the anomaly problem is possible. This approach would require determining the cosmic ray neutron energy spectrum and the necessary pion production cross sections to the desired accuracy, and repeating the type of calculations used in the present work. Such an undertaking would be a formidable task and is not likely to occur in the foreseeable future.

The question then becomes: What can be done to solve the anomaly problem short of attacking it via the brute force method? If an anomaly exists, it either involves the pion as an intermediary particle or it does not. If it does, detailed flux and cross section information is necessary. An approach will be outlined in the following paragraphs which could be used with the present facility to search for an anomaly in the rate of non-pion produced muons by incident neutral particles.

The rate of production of single non-pion produced muons by neutral components of the cosmic radiation is believed to be vanishingly small in a detector of the present size.⁵ Thus, an experimental study of the rate of production of neutral-particle-produced muons with a detector capable of distinguishing the pion-produced muon event from the non-pion-produced muon event should yield information concerning the possible existence of an anomaly in the rate of non-pion produced muons. With minor modifications, the present detector is ideally suited for such a study.

Basically, the suggested experiment is an extension of that described in earlier chapters. The signature for an interesting event remains the same: the production of a charged particle in the detector by an incident neutral cosmic ray, followed by the characteristic decay of a muon. The major difference involves the use of target cell B as a fast detector. Events occurring in this region of the detector volume would be examined for evidence of the presence of the entire π - μ -e decay chain. This would involve searching for the four MeV π - μ decay pulse on the tail of the much larger slowing-down pulse of the pion. An anomaly would be indicated if a study of such events revealed that a non-negligible fraction of the events did not involve the pion. Since the analysis would involve "fraction of events observed," detailed neutron flux and pion production cross section information would not be required.

Such an experiment would require nanosecond timing capabilities. As mentioned in the facility recommendations above, target cell B would have to be replaced by a much faster detector. A second problem of major concern would be the storage of high resolution timing information occurring in the vicinity of the first pulse while waiting for the remainder of the signature. To solve this problem, it is suggested that all non-vetoed pulses from cell B be outputted to a fast oscilloscope. The combination of the persistence of the oscilloscope phosphor and the expected event rate should allow interesting events to be photographed with very little interference from non-interesting events.

APPENDIX A

ELECTRONICS

300 MHz Low Gain Mixer

A wide band, dual output mixer was designed for the expressed purpose of linearly summing the fast anode signals for the target photomultiplier tubes of the cosmic ray detector. This mixer has the following desirable characteristics:

1. dual isolated outputs,
2. isolated test points for each input,
3. available in two input and three input versions,
4. inputs isolated from each other,
5. NIM compatible, and
6. a bandwidth of greater than 300 MHz.

A schematic of the mixer is shown in Figure 37, and the technical specifications for the unit appear below:

input D.C. offset - 1.44 volts

output D.C. offset - zero

test point D.C. offset - zero

main output noise level - <0.125 mv peak to peak

band width - >300 MHz

main output current gain - approximately 0.58

test point current gain - approximately 0.59

main output linearity - from less than 0.2 ma to greater than

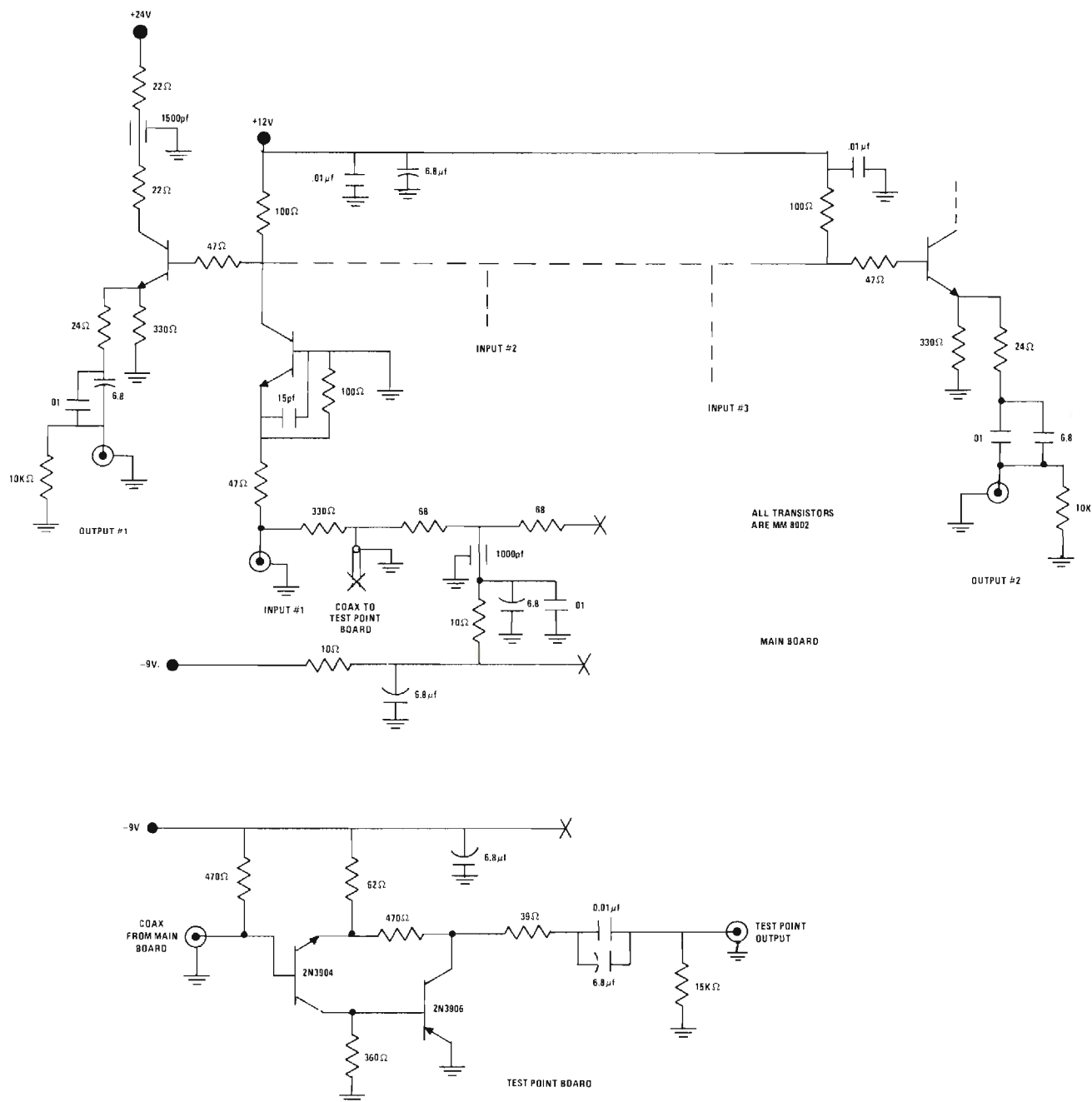


Figure 37. 300 Mhz mixer schematic and test point board.

12 ma, giving a dynamic range of greater than 60

isolation between inputs - better than 43 db for X40 overload
at input

isolation between outputs - better than 32 db.

150 MHz, X20 Mixer

A 150 MHz, X20 mixer-amplifier was designed to linearly sum and amplify negative going pulses like those from the anode of a photo-multiplier tube. The unit has dual isolated outputs, an isolated test point for each input, and can be built with an arbitrary number of inputs. A schematic of the mixer is shown in Figure 38 and the technical specifications are listed below:

1. Main output voltage gain - 21.5
2. Main output linearity - linear from below 0.2 mv to 36 mv
referenced to input.
3. Dynamic range - better than 72:1
4. Main output noise - approximately 3.5 mv peak to peak at
output.
5. Test point gain - about 0.6
6. Test point linearity - linear to 440 mv referenced to input
7. Test point noise - less than 0.5 mv peak to peak
8. Isolation between inputs - 46 db
9. Isolation between outputs - 47 db
10. Test point isolation - shorting test point produced about
0.4% change in main output
11. Isolation of adjacent wide band mixer - 50 db.

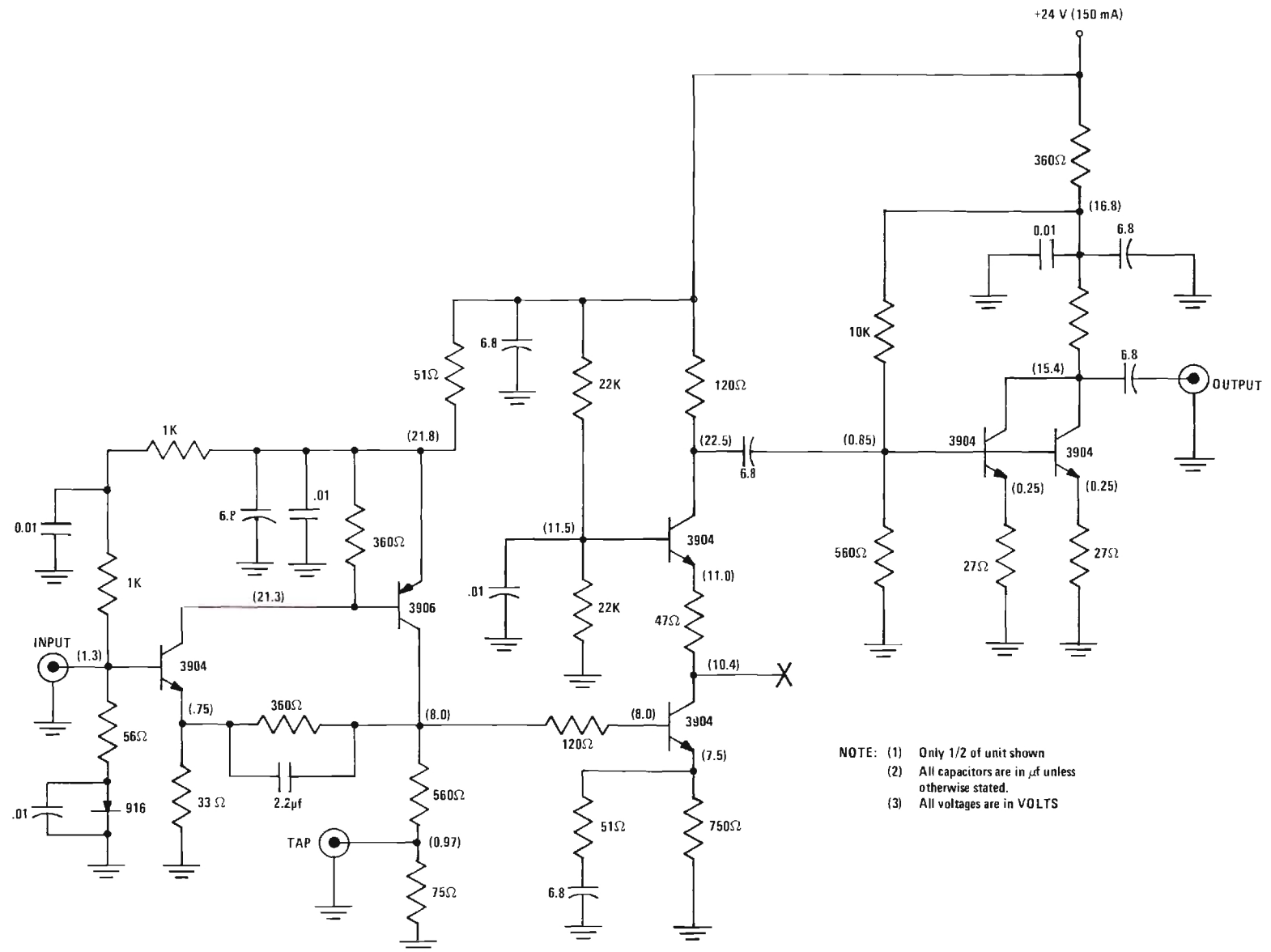


Figure 38. Schematic of X20 anticoincidence mixer.

12. D. C. offset - input - 1.35 volts
output - 0.00 volts
test point - 1.0 volts
13. Overload recovery time (to within 5 mv of base line):
X2 overload - 120 nsec
X10 overload - 190 nsec
X75 overload - 950 nsec.

15 Microsecond Updating Oneshot (AR-10)

A 15 microsecond, updating oneshot was designed and built to serve as a system veto for the cosmic ray experiment. This unit accepts a NIM fast logic input from the detector's anticoincidence system and generates a NIM fast logic output which lasts for approximately 10 muon half-lives ($T_{1/2} \sim 1.54 \mu\text{sec}$). For the unit to function properly the input pulse must be at least 50 nanoseconds wide and the output must be D.C. coupled. The NIM standard output width of this unit may be varied from 12 to 18.7 microseconds. A schematic of the AR-10 appears in Figure 39.

Electronic Instrument Inventory

A facility inventory of electronic nuclear instrumentation appears in Table 10. This inventory includes console related instruments and high voltage power supplies. Photomultiplier tubes, special test instruments, and the previously described linear mixers are not included in this inventory.

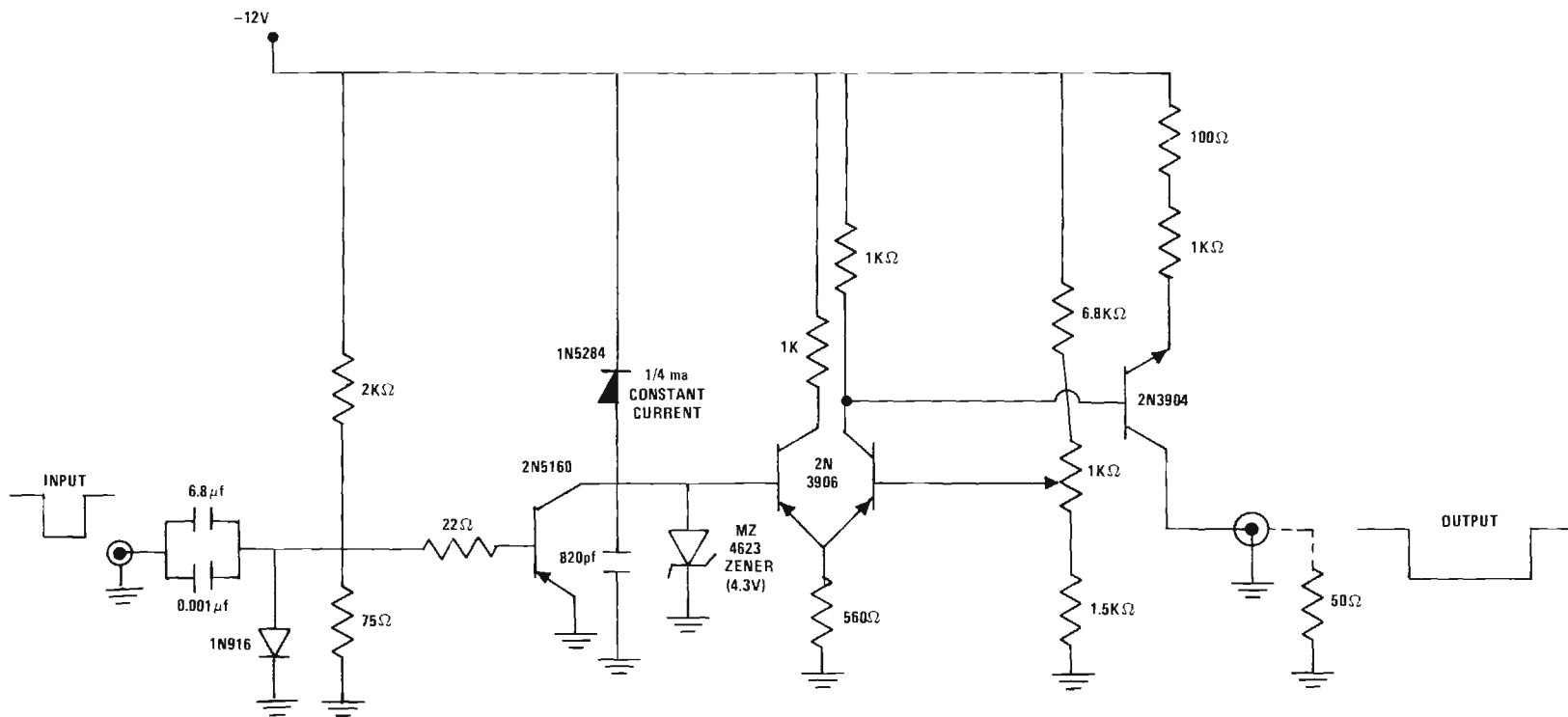


Figure 39. Schematic of 15 microsecond updating oneshot.

Table 10. Inventory of Electronic Nuclear Instruments

Quantity	Manufacturer	Model Number	Description
<u>NIM INSTRUMENTATION</u>			
1	EG & G, Inc.	AD128B/N	Analog to Digital Converter
4	"	AN102/N	6-input D.C. Mixer
1	"	AN109/N	Biased Amplifier and Linear Gate
2	"	AN201/N	Quad Amplifier
4	"	C102B/N	Dual Coincidence
1	"	C104/N	4-Fold Coincidence with Veto
1	"	C104A/N	4-Fold Coincidence with Veto
1	"	DS104/N	Quad Scaler Driver
1	"	F108/N	Dual Fanout
1	"	GG200/N	Gate Generator with Veto
2	"	LG102/N	Linear Gate & Stretcher
3	"	M127/N	NIM Fan
2	"	OR102/N	Dual OR/NOR
1	"	TH200A/N	Time-to-Amplitude Converter
2	"	T120/N	Quad Discriminator (updating)
3	"	TD101/N	Diff. Discriminator (with LLT)
1	"	TR104S/N	Dual Discriminator
1	"	TR204A/N	Dual Discriminator (updating)
2	Advanced Res. Corp.	AR-1	Dual PreAmp-Coinc.-Sum-Lin. Gate-Delay
2	"	AR-2	Diff. Discriminator
4	"	AR-3	Dual Fixed Delay
6	"	AR-4	Incremental Delay
1	"	AR-5	Nanosecond Amplifier-Coinc.
1	"	AR-6	Slow Coincidence
1	"	AR-7	Dual Pre-Amplifier

Table 10. Continued

Quantity	Manufacturer	Model Number	Description
1	Advanced Res. Corp.	AR-8	Dual Mercury Pulsers
1	"	AR-9	Dual Logic Interface
2	"	AR-10	Updating Oneshot Gate Generator
1	ORTEC, Inc.	417	Fast Discriminator
1	"	427	Delay Amplifier
2	"	425	Incremental Delay
3	EG & G, Inc.	M120A/N	Nimbin with power supply
1	Bull Run	BR-100	Nimbin with power supply
2	EG & G, Inc.	M125/N	Unpowered Nimbin
1	Bull Run	BR-100	Unpowered Nimbin

MULTICHANNEL ANALYZER COMPONENTS

1	TMC, Inc.	CN1024	Digital Computer Unit
1	"	220C	Data Output Unit
1	"	240	Display, Control Unit
1	"	210	Pulse Height Logic Unit
1	"	211	Time-of-Flight Logic Unit
1	"	216	Coincidence Pair Unit
1	"	242	Two Parameter Unit
2	"	210B	Pulse Height Logic Unit
1	"	243	Computer Program Unit
1	Hewlett-Packard	561B	Digital Recorder
1	Tally	540R	Paper Tape Punch
1	Moseley	7590B	X-Y Plotting System

POWER SUPPLIES

2	Advanced Res. Corp.	---	Dual D.C. Power Supply (NIM Voltages)
15	Hammer	N4035	High Voltage Power Supply
1	NJE	5326RM	High Voltage Power Supply

Table 10. Concluded

Quantity	Manufacturer	Model Number	Description
<u>SPECIAL TEST EQUIPMENT</u>			
1	Tektronix	555	Dual Beam Oscilloscope
1	"	RM566	Oscilloscope
1	"	581A	Oscilloscope
2	"	L	Plug-in Unit
1	"	C-12	Oscilloscope Camera
1	Advanced Res. Corp.	AR-Hg1	Mercury Pulser
1	Data Pulse	111R	Pulse Generator
<u>MISCELLANEOUS NUCLEAR INSTRUMENTS</u>			
1	Science Accessories	032	Quadruple Delay
3	Hamner	N-286	Highspeed Scaler
1	"	810	Electronic Timer

APPENDIX B

PION PRODUCTION CROSS SECTIONS FOR CARBON

During the search for cross section data for the reactions $\begin{Bmatrix} n \\ p \end{Bmatrix} + C \rightarrow \pi^{\pm} + \dots$, numerous "bits" of experimental data were tabulated. A summary of these data appears as Table 11.

Table 11. Summary of Available Experimental Cross Section Data for $\begin{Bmatrix} n \\ p \end{Bmatrix} + C \rightarrow \pi^{\pm} + \dots$
Reactions from Threshold to 1.1 GeV

Date	Principal Author	Ref.*	Reaction	Incident Energy (MeV)	Pion Lab Angle Observed (degrees)	Pion Energy Observed (MeV)	Output Pion Observed	$\frac{d\sigma^+}{d\Omega}$ x 10 ⁻²⁷	$\frac{d\sigma^-}{d\Omega}$ cm ² /Sr	Were $\frac{d^2\sigma}{dE_\pi d\Omega}$ Data Presented?	π^+	π^-	Comments
1949	Barkas	A	n + c	168	--	--	π^+	0	--	No	N.A.		mass energy calculations
1949	Barkas	A	n + c	156	--	--	π^-	--	0	N.A.	No		
1949	Jones & White	B	p + c	165-345	$\int(0-45)$	$\int(2-10)$	π^-	--	--	N.A.	No		relative yields for π^-
1953	Hamlin	C	p + c	235	90	25-120	π^+	--	--	Yes	N.A.		relative yields using
				264	90	25-120	π^+	--	--	Yes	N.A.		scintillation counter -
				294	90	25-120	π^+	--	--	Yes	N.A.		normalized to nuclear
				313	90	25-120	π^+	--	--	Yes	N.A.		emulsion data
				336	90	25-120	π^+	--	--	Yes	N.A.		
1950	Bradner	K	n + c	270	90	50-65	π^{\pm}	--	--	No	No		Film
1952	Clark	D	p + c	240	$\int(130-150)$	40	π^{\pm}	--	--	No	No		relative yields, 7 elements
1955	Merritt	B	p + c	335	0	34-147	π^+	--	--	Yes	N.A.		
1954	Dudziak	F	p + c	340	0	--	π^{\pm}	2.1	0.0714	No	No		
					90	--	π^{\pm}	0.335	0.043	No	No		
1953	Sagane	G	p + c	340	90	13,18,42	--	--	--	No	No		no cross section data
1951	Richman	H	p + c	340	90	15-115	π^{\pm}	0.23	--	Yes	Yes		π^{\pm} energy distributions
1957	Imhof	I	p + c	340	135	36,63	π^+	--	--	No	N.A.		Z dependence study
1953	Leonard	J	p + c	340	180	9-120	π^{\pm}	0.177	0.0190	Yes	Yes		good $\frac{d^2\sigma}{dE d\Omega}$ tables
1951	Henley	L	p + c	345	0 & 90	--	--	--	--	No	No		theoretical paper - formalism
1953	Tokunaga	M	p + c	345	90	30,50,60	π^{\pm}	--	--	--	--		poor data points - large spread
1950	Richman	N	p + c	345	90	15-115	π^{\pm}	0.20	0.04	No	No		
1950	Richman	O	p + c	345	90	15-115	π^{\pm}	0.20	0.04	Yes	Yes		same as #14, but in more detail
1952	Passman	P	p + c	345	90	15-120	π^+	0.47	--	Yes	N.A.		
	Passman		p + c	365	90	15-120	π^+	0.64	--	Yes	N.A.		
	Passman		p + c	380	90	15-120	π^+	0.67	--	Yes	N.A.		
1952	Block	Q	p + c	381	90	0-125	π^{\pm}	0.53	0.042	Yes	Yes		
1951	Block	R	p + c	381	90	0-120	π^{\pm}	0.52	0.046	Yes	Yes		

Table 11. Concluded

Date	Principal Author	Ref.*	Reaction	Incident Energy (MeV)	Pion Lab Angle Observed (degrees)	Pion Energy Observed (MeV)	Output Pion Observed	$d\sigma^+/d\Omega$	$d\sigma^-/d\Omega$	Were $d^2\sigma/dE_\pi d\Omega$ Data Presented?		Comments
								$\times 10^{-27}$	cm^2/Sr	π^+	π^-	
1962	Lillethum	S	p + c	450	21.5	83-236	π^+	11.1	--	Yes	N.A.	good tabulation for $d^2\sigma/d\Omega dE$
				450	60	149	π^+	3.1	--	Yes	N.A.	
				450	21.5	132-200	π^-	--	0.95	N.A.	Yes	
				450	60	99	π^-	--	0.43	N.A.	Yes	
1954	Rosenfeld	T	p + c	440	90.0		π^\pm	$0.83^{+1.11}$	$0.115^{+0.024}$	No	No	
1968	Oganessian	U	n + c	600	16	25-300	π^\pm	1.51	9.66	No	No	
				600	30	25-300	π^\pm	1.15	7.32	Yes	Yes	author notes lack of $d\sigma^2/dE_\pi d\Omega$ information in literature for $n+c^{12} \rightarrow \pi + \dots$ reactions concludes that π^+ meson energy independent of angle of emission and equal to ~ 100 MeV in cms of colliding nucleons
				600	60	25-300	π^\pm	0.60	3.56	No	No	
				600	90	25-300	π^\pm	0.40	2.40	Yes	Yes	
				600	123	25-300	π^\pm	0.35	2.02	No	No	
1957	Meshkovskii	V	p + c	600	45	79-320	π^\pm	6.77	1.00	No	Yes	
1958	Meshkovskii	W	p + c	660	19.5	102-356	π^+	12.34	--	Yes	N.A.	energy independent of angle of emission and equal to ~ 100 MeV in cms of colliding nucleons
				660	29	80-324	π^+	10.22	--	Yes	N.A.	
				660	38	80-313	π^+	7.13	--	Yes	N.A.	
				660	56	75-278	π^+	4.62	--	Yes	N.A.	
				660	65	44-268	π^+	3.70	--	Yes	N.A.	
1957	Meshcheriakov	X	p + c	660	24	60-400	π^\pm	--	--	Yes	Yes	
1957	Meshkovskii	Y	p + c	660	45	75-285	π^+	--	--	Yes	N.A.	tables of $d^2\sigma/dE d\Omega$
1958	Azhgfrez	Z	p + c	670	56	30-394	π	5.1 0.8	1.0 0.2	No	No	
1966	Heer	AA	p + c	600	0.8	all	π	--	--	Yes	Yes	
				600	21.5	all	π	--	--	Yes	Yes	
				725	0	all	π	--	--	Yes	Yes	

NOTE: Dashes indicate that information was not available.

*Reference refers to Cross Section Bibliography on following pages.

Cross Section Bibliography

- A. W. H. Barkas, Phys. Rev., 75, 1109 (1949).
- B. S. B. Jones and R. S. White, Phys. Rev., 78, 12 (1950).
- C. D. A. Hamlin, USACE Report UCRL-2414 (1953).
- D. D. L. Clark, Phys. Rev., 87, 157 (1952).
- E. J. Merritt and D. A. Hamlin, Phys. Rev., 99, 1523 (1955)
- F. W. F. Dudziak, USAEC Report UCRL-2564 (1954).
- G. R. Sagane, Phys. Rev., 90, 1003 (1953).
- H. C. Richman, M. Weissbluth, and H. A. Wilcox, Phys. Rev., 85, 161 (1952).
- I. W. Imhof, H. T. Easterday, V. Perez-Mendez, Phys. Rev., 105, 1859 (1957).
- J. S. L. Leonard, Phys. Rev., 93, 1380 (1954).
- K. H. Bradner, D. J. O'Connell, and B. Rankin, Phys. Rev., 79, 720 (1950).
- L. E. M. Henley, Phys. Rev., 85, 204 (1952).
- M. S. Tokunaga, K. Yuasa, K. Nishikawa, T. Isii, J. Phys. Soc. Japan, 8, 571 (1953).
- N. C. Richman and H. A. Wilcox, Phys. Rev., 78, 496 (1950).
- O. C. Richman, H. A. Wilcox, USAEC Report UCRL-592 (1950).
- P. S. Passman, M. M. Block, and W. W. Havens, Jr., Phys. Rev., 88, 1247 (1952).
- Q. M. M. Block, S. Passman, and W. W. Havens, Jr., Phys. Rev., 88, 1239 (1952).

Cross Section Bibliography (Concluded)

- R. M. M. Block, S. Passman, and W. W. Havens, Jr., Phys. Rev., 83, 1967 (1951).
- S. E. Lillethun, Phys. Rev., 125, 665 (1962).
- T. A. H. Rosenfeld, Phys. Rev., 96, 130 (1954).
- U. K. O. Oganesyan, Sov. Phys.-JETP, 27, 679 (1968).
- V. A. G. Meshkovskii, Iu. S. Pligin, Ia. Ia. Shalamov, and V. A. Shebanov, Sov. Phys.-JETP, 5, 1085 (1957).
- W. A. G. Meshkovskii, Ia. Ia. Shalamov, and V. A. Shebanov, Sov. Phys.-JETP, 34, 987 (1958).
- X. M. G. Meshcheriakov, I. K. Vzorov, V. P. Zrelov, B. S. Neganov, and A. F. Shabudin, Sov. Phys.-JETP, 4, 79 (1957).
- Y. A. G. Meshkovskii, Iu. S. Pligin, Ia. Ia. Shalamov, and V. A. Shebanov, Sov. Phys.-JETP, 4, 842 (1957).
- Z. L. S. Azhgirei, I. K. Vzorov, V. P. Zrelov, M. G. Meshcheriakov, and V. I. Petrukhin, Sov. Phys.-JETP, 34, 939 (1958).
- AA. E. Heer, W. Hirt, M. Martin, E. G. Michaelis, C. Serre, P. Skarek, and B. T. Wright, Proceedings of the 1966 Williamsburg Conference on Intermediate Energy Physics, Williamsburg, Virginia, 1, 277 (1966).

LITERATURE CITED

1. V. F. Hess, *Physikalische Zeitschrift*, 14, 610 (1913).
2. W. Kohlhörster and G. V. Salis, *Naturwiss*, 14, 936 (1923).
3. A. E. Sandstrom, *Cosmic Ray Physics*, John Wiley and Sons, New York, 1965, Chapter 1, p. 58.
4. A. E. Sandstrom, *Cosmic Ray Physics*, John Wiley and Sons, New York, 1965, Chapter 1, p. 2.
5. E. Segrè, *Nuclei and Particles, An Introduction to Nuclear and Subnuclear Physics*, W. A. Benjamin, Inc., New York, 1964, p. 340.
6. C. L. Cowan and D. F. Ryan, "Experimental Evidence for an Observable Cosmic Neutrino Signal," unpublished report, Physics Department, Catholic University of America, Washington, D. C. (1964).
7. C. L. Cowan, "The Production of Muons," Proceedings of Informal Conference on Experimental Neutrino Physics, CERN-65-32 (1965).
8. C. Cowan, D. Ryan, and G. Buckwalter, Proceedings of the Ninth International Conference on Cosmic Rays, Paper MU-NU-44 (London, 1965).
9. D. F. Ryan, V. Acosta, G. L. Buckwalter, W. M. Carey, Jr., C. L. Cowan, and D. J. Curtin, *Physics Letters*, 21, 475 (1966).
10. T. B. Novey, "Cosmic Ray Induced ' μ -e' Events," Proceedings of Informal Conference on Experimental Neutrino Physics, CERN-65-32 (1965).
11. G. L. Buckwalter, C. L. Cowan, and D. F. Ryan, *Physics Letters*, 21, 478 (1966).
12. P. W. Hess, F. L. Talbott, and C. L. Cowan, *The Astrophysical Journal*, 148, L73 (1967).
13. S. Standil and R. P. Bukata, *Physical Review Letters*, 12, 487 (1964); *Canadian Journal of Physics*, 42, 1834 (1964); *Can. J. Phys.*, 43, 883 (1964).
14. C. Malboux, P. Mosrin, and M. Scherer, *C. R. Acad. Sc. Paris*, 5262 (20 Juin 1966).

LITERATURE CITED (Continued)

15. G. L. Buckwalter, G. Steffy, and D. D. Steffy, 1969 Spring Meeting of the American Physical Society, Paper AJ11 (Washington, D. C.).
16. C. T. O'Sullivan, "Some Properties of a Neutral Component of the Cosmic Radiation," Ph.D. Thesis, Catholic University of America, Washington, D. C. (1969).
17. R. N. Shelby, "A Background to the Observation of Direct Muon Production by Neutral Cosmic Rays Near Sea Level," Ph.D. Thesis, Catholic University of America, Washington, D. C. (1970).
18. J. B. Birks, The Theory and Practice of Scintillation Counting, The MacMillan Company, New York, 1964, p. 99.
19. J. C. Barton, A. Crispin, and M. Slade, Journal of Scientific Instruments, 41, 736 (1964).
20. Witco Chemical Company, Sonneborn Refined Petroleum Products, New York.
21. T. P. Lang, Jr., private communications, Advanced Research Corporation, Atlanta.
22. R. W. Pringle, L. D. Black, B. L. Funt, and S. Sobering, Phys. Rev., 92, 1582 (1953).
23. C. A. Ziegler, H. H. Seliger, and I. Jaffe, Phys. Rev., 99, 663 (1955).
24. B. L. Funt and E. Neparko, Journal of Physical Chemistry, 60, 276 (1956).
25. A. O. Weissenberg, Muons, North-Holland Publishing Company, Amsterdam, 1967, p. 59.
26. "Time-To-Amplitude Conversion Calibration," Nanonotes, 1, January 1964, publication of EG & G, Inc., Salem, Massachusetts.
27. F. Reines, "Progress Report for A Research Program in Neutrino Physics, Cosmic Rays and Elementary Particles, 1 October 1969 to 30 September 1970," University of California, Irvine (1970).
28. W. N. Hess, H. W. Patterson, and R. Wallace, Phys. Rev., 116, 445 (1959).
29. E. B. Hughes and P. L. Marsden, Journal of Geophysical Research, 71, 1435 (1966).

LITERATURE CITED (Continued)

30. S. F. Singer, "The Primary Cosmic Radiation and Its Variations," *Progress in Cosmic Ray Physics*, 4, 261 (1958).
31. G. Brooke and A. W. Wolfendale, "The Momentum Spectrum of Cosmic Ray Protons Near Sea Level in the Momentum Range 0.6-150 GeV/C," *Proceedings of the Physical Society (London)*, A83, 843 (1964).
32. H. Messel, "The Development of a Nucleon Cascade," *Progress in Cosmic Ray Physics*, 2, 132 (1954).
33. J. A. Simpson, *Phys. Rev.*, 83, 1175 (1951).
34. K. O. Oganesyan, *Soviet Physics-JETP*, 27, 679 (1968).
35. W. F. Dudziak, *Phys. Rev.*, 95, 866 (1954) and "Production Cross Section for Positive and Negative Pions from Carbon Initiated by 340 MeV Protons," UCRL-2564 (1954).
36. H. Bradner, D. J. O'Connell, and B. Rankin, *Phys. Rev.*, 79, 720 (1950).
37. A. G. Meshkovskii, Ia. Ia. Shalamov, and V. A. Shebanov, *Soviet Physics-JETP*, 34, 987 (1958).
38. H. W. Bertini, "Preliminary Data from Intranuclear-Cascade Calculations of 0.75, 1-, and 2-GeV Protons on Oxygen, Aluminum, and Lead, and 1-GeV Neutrons on the Same Elements," ORNL-TM-1996 (1967).
39. H. W. Bertini, private communication (1972).
40. A. G. Meshkovskii, Iu. S. Pligin, Ia. Ia. Shalamov, and V. A. Shebanov, *Soviet Physics-JETP*, 4, 842 (1957).
41. S. Passman, M. M. Block, and W. W. Havens, Jr., *Phys. Rev.*, 88, 1239 (1952).
42. Luke C. L. Yuan and S. J. Lindenbaum, *Phys. Rev.*, 103, 404 (1956).
43. M. G. Meshcheriakov, I. K. Vzorov, V. P. Zrelov, B. S. Neganov, and A. F. Shabudin, *Soviet Phys.-JETP*, 4, 79 (1957).
44. V. D. Hopper, Cosmic Radiation and High Energy Interactions, Prentice-Hall, Inc., Englewood Cliffs, 1964, pp. 19-27.

LITERATURE CITED (Concluded)

45. E. Meyer, White Mineral Oil and Petrolatum and Their Related Products Petroleum Sulfonates and Microcrystalline Waxes, Chemical Publishing Company, Inc., New York, 1968, 2nd ed., p. 10.
46. W. H. Barkas, Phys. Rev., 75, 1109 (1949).

VITA

Charles Thomas Brown was born December 21, 1941 in Montgomery, Alabama. He is the oldest of the three children of James Wiley and Jane Barber Brown. On June 17, 1966, he was married to Donna Edna Evans of Atlanta, Georgia. They have two daughters, Michele Leigh Brown and Yvonne Marie Brown.

Mr. Brown attended Robert E. Lee High School in Montgomery, and entered Georgia Institute of Technology as a freshman in 1960. He received the degrees of Bachelor of Science in Physics in 1964 and Master of Science in Physics in 1966. He is a member of Tau Kappa Epsilon, Tau Beta Pi, and Sigma Xi.

Mr. Brown has been associated with the Georgia Tech Engineering Experiment Station as a Graduate Research Assistant since 1966. His activities during this period included developmental work related to neutron detecting liquid scintillators, the design and construction of a parallel plate spark chamber, the development of new organic liquid scintillators, and various contract related support activities for Advanced Research Corporation, an Atlanta based company. Several unpublished reports have resulted from these activities.